

**Untersuchungen zur Belagsbildung  
kontinuierlich betriebener Polymerisationen**

**Investigations on the formation of fouling in  
continuously operated polymerisations**

Dissertation

With the aim of achieving the doctoral degree at the Faculty of Mathematics,  
Informatics and Natural Science

Submitted to the  
Department of Chemistry  
University of Hamburg

Submitted by  
**Rolf Sören Rust**  
from Hamburg, Germany  
Hamburg, 2024

Date of approval for publication: July 12, 2024

The following evaluators recommend the admission of the dissertation:

1. Evaluator: Dr. Werner Pauer
2. Evaluator: Prof. Dr. Gerrit. A. Luinstra

The Date of the disputation: July 12, 2024

Members of examination committee:

1. Dr. Christoph Wutz
2. Prof. Dr. Volkmar Vill
3. Dr. Werner Pauer

The work mentioned in this thesis was conducted under the supervision of Dr. Werner Pauer from November 2020 to December 2023 at the Institute of Technical and Macromolecular Chemistry of the University of Hamburg.

## I. List of Publications

1. **Sören Rust**, Werner Pauer\*. “Determination of inline-particle sizes by turbidity measurement in high solid content emulsion polymerisations” *Journal of Polymer Research* 29, 307 (2022). <https://doi.org/10.1007/s10965-022-03141-z> (**Impact factor 2022: 3.097**)
2. **Sören Rust**, Werner Pauer\*. “Formulation and process determined fouling prediction for the continuous emulsion co polymerisation of vinyl acetate” *Journal of Polymer Research* 30, 242 (2023). <https://doi.org/10.1007/s10965-023-03588-8> (**Impact factor 2023: 3.061**)
3. **Sören Rust**, Marco Osenberg, Thomas Musch, Werner Pauer\*. “Ultrasonic and conversion-based inline fouling measurements for continuous emulsion copolymerisation of vinyl acetate in tubular reactors” *Scientific Reports* 14, 4077 (2024). <https://doi.org/10.1038/s41598-024-54321-4> (**Impact factor 2024: 4.379**)
4. Jan Förster, Thomas Fritsch, Jan Tebrügge, Thomas Musch, Marco Osenberg, Dominik Haspel, Werner Pauer, **Sören Rust**, Annika Klinkert, Wolfgang Augustin, Stephan Scholl, Timo Melchin, Bernhard Eckl. “KoPPonA 2.0 – Continuous polymerization in modular, intelligent, fouling resistant reactors – Subproject: Process development and implementation for emulsion polymerization“, project report, Technische Informationsbibliothek (TIB), Hannover (2022) p. 56 - 74.

My contribution to this section of the report, describing the work contributed at the University of Hamburg, is 70 %. The specific contributions were the design and performing of the experiments regarding emulsion polymerisation and fouling measurement as well as evaluation of the chemical data.

5. Marco Osenberg, Jan Förster, **Sören Rust**, Thomas Fritsch, Jan Tebrügge, Werner Pauer, Thomas Musch. “Ultrasound Sensor for Process and Fouling Monitoring in Emulsion Polymerization Processes” *IEEE Sensors*, Dallas, TX, USA, pp. 1-4 (2022) <https://doi.org/10.1109/SENSORS52175.2022.9967228> (**Impact factor 2022: 4.729**)

My contribution to this paper is 20%, the specific contributions were the design of the investigated formulation and the realisation and evaluation of the chemical experiments.

6. Vanessa Neßlinger, **Sören Rust**, Jan Atlanov, Werner Pauer, Guido Grundmeier. “Monitoring Polymeric Fouling in a Continuous Reactor by Electrochemical Impedance Spectroscopy” *Chemie Ingenieur Technik* XX, XXX (2023). <https://doi.org/10.1002/cite.202300032> (**Impact factor 2023: 1.716**)

My contribution to this paper is 15%, the specific contributions were the design of the investigated formulation and the realisation and evaluation of the chemical experiments.

## II. List of Figures

Figure 1: Mechanism of emulsion polymerisation. (a) initiation and formation of oligoradicals in continuous phase, (b) nucleation of particles and (c) particle growth and termination. <sup>[9]</sup> ...	18
Figure 2: Nucleation in emulsion polymerisation. The different pathways for homogeneous and heterogeneous nucleation are shown. <sup>[11]</sup> .....	19
Figure 3: Developments in polymerisation rate during emulsion polymerisation. The polymerisation is divided into three phases, in the first phase nucleation occurs and the reaction rate is increasing. In the second phase nucleation and termination are in equilibrium and reaction rates are constant and in the third phase the monomer depletion occurs and termination increases so that reaction rate is decreasing. <sup>[25]</sup> .....	19
Figure 4: The appearance of polymer and polymerisation fouling on reactor surfaces. <sup>[38]</sup> .....	26
Figure 5: Images of fouling layers taken with an optical microscope of polymerisation fouling (a) and polymer fouling (b). <sup>[38]</sup> .....	26
Figure 6: Residence time measurements for the tubular reactor without fouling using colour-markers in water. The intensities of colouration were measured at the inlet and outlet of the reactor photometrically and the mean residence time was determined as time between the mean inlet signal and mean outlet signal. ....	85
Figure 7: Residence time measurements for fouling detection in the reactor. A reactor containing fouling produced by the standard recipe was used and after rinsing with water the residence time was measured using water and colour-marker. ....	86
Figure 8: sample plates hydrophilic coated with titanium dioxide a) directly after 45 min polymerisation in the measurement cell and b) after rinsing with water showing the thin, remaining fouling layer. ....	90
Figure 9: Development of particle sizes of polymer dispersion samples of the standard recipe with 8 wt.% emulsifier <sup>[84]</sup> over time to detect agglomeration. As the time intervals were wide, a logarithmic scale was chosen. ....	93
Figure 10: Visualisation of the composition of the deposits depending on the extraction method a) Soxhlet and b) boiling for 24 h. ....	94
Figure 11: Monomer conversion of the polymerisation depending on the comonomer composition. ....	95
Figure 12: Correlation between glass transition temperature and comonomer composition given as weight fraction of vinyl neodecanoate. ....	96

## Table of contents

I. List of Publications .....	5
II. List of Figures .....	7
Table of contents .....	8
1. Zusammenfassung.....	10
2. Summary .....	14
3. Introduction.....	17
3.1 Emulsion polymerisation.....	18
3.2 Emulsion polymerisation of vinyl acetate .....	21
3.3 Fouling .....	23
3.4 Fouling during emulsion polymerisation .....	25
3.5 Fouling Detection .....	28
4. Aim of Work .....	30
5. Cumulative part of the dissertation .....	32
5.1 Determination of inline-particle sizes by turbidity measurement in high solid content emulsion polymerisations.....	32
5.2 Formulation and process determined fouling prediction for the continuous emulsion copolymerisation of vinyl acetate .....	39
5.3 Ultrasonic and conversion-based inline fouling measurements for continuous emulsion copolymerisation of vinyl acetate.....	51
5.4 KoPPonA 2.0 – Continuous polymerisation in modular, intelligent, fouling resistant reactors – Subproject: Process development and implementation for emulsion polymerisation.....	64



6. Unpublished Work .....	84
6.1 Residence time characterisation of the tubular reactor .....	84
6.2 Cleaning procedures for polymerisation reactors.....	87
6.3 Influences of reactor coating on fouling masses .....	89
6.4 Chemical properties of polyvinyl acetate dispersions.....	91
6.5 Chemical properties of polyvinyl acetate deposits.....	94
6.6 Influences of comonomer composition on polymerisation and product properties .....	95
7. Discussion .....	97
8. References.....	102
9. Appendix.....	108
9.1 Table of Chemicals.....	108
9.2 Supporting information “Formulation and process determined fouling prediction for the continuous emulsion co polymerisation of vinyl acetate” .....	110
9.3 Supporting information “Ultrasonic and conversion-based inline fouling measurements for continuous emulsion copolymerisation of vinyl acetate” .....	113
10. Acknowledgement .....	129
11. Declaration on oath .....	130

## 1. Zusammenfassung

Im Vergleich zur Masse- oder Lösungspolymerisation gewährleisten Emulsionspolymerisationen eine gute Wärmeabfuhr und damit einhergehend Prozesssicherheit. Vinylacetat ist ein häufig verwendetes Monomer in der Emulsionspolymerisation. Polyvinylacetat und seine Copolymere finden Anwendung als Betonzuschlag sowie in Klebstoffen, Bindemitteln für die Lackindustrie und Beschichtungen. Emulsionspolymerisationen werden großtechnisch bisher weitgehend in einer *semibatch* Fahrweise durchgeführt. Eine kontinuierliche Betriebsweise wäre von Seiten der Effizienz hinsichtlich Kosten und Raum-Zeit-Ausbeute deutlich bevorzugt, allerdings stellt die Belagsbildung eine große Herausforderung dar. Die an den Reaktorwänden anhaftenden Beläge resultieren in einem Verlust an Reaktionsvolumen und setzen die Wärmeabfuhrleistung deutlich herab. Dies reduziert die Prozesssicherheit und führt zu veränderten Produkteigenschaften und einer verringerten Kosteneffizienz aufgrund erhöhter Totzeiten. Es treten vor allem zwei Belagsbildungsmechanismen in Erscheinung. Das Polymerfouling durch Agglomeration von Latices und anschließende Sedimentation. Dem gegenüber steht das Polymerisationsfouling, bei welchem die Polymerisation in Filmen auf der Reaktoroberfläche abläuft und somit Polymere auf den Flächen aufwachsen.

Diese Arbeit liefert Beiträge zum Verständnis der Belagsbildung während der kontinuierlichen Emulsionspolymerisation von Vinylacetat-Copolymeren. Hierfür wurde eine reproduzierbare und belagsintensive Rezeptur im Rohrreaktor entwickelt sowie die Belagsbildung und die Einflüsse auf diese untersucht. Darüber hinaus wurden Sensorkonzepte zur *inline*-Quantifizierung von Reaktionsbelägen im Rohrreaktor entwickelt und die Polymerisation sowie die Eigenschaften der Polymere charakterisiert.

Die Partikelgröße ist eine der wesentlichen Größen zur Charakterisierung von Polymerdispersionen und damit relevant für die Kontrolle der Produkteigenschaften. Partikelgrößen werden zumeist *offline* mittels Lichtstreuanalytik von verdünnten Polymerdispersionen gemessen. Diese Verfahren sind zeit- und kostenaufwendig und würden insbesondere bei einem kontinuierlichen Polymerisationsprozess zu erheblich verzögerten Anpassungen auf Veränderungen im Produkt führen. Daher ist die Etablierung einer *inline*-Methode zur simultanen Messung der Partikelgrößen im Prozess ein wichtiger Schritt für die Steigerung der Prozesseffizienz. Hierzu wurde eine Methode entwickelt, die ausgehend von der Trübung der Dispersion die zahlenmittleren hydrodynamischen Partikelgrößen der Latices mit

Abweichungen zu Referenzmethoden unter 5 % bestimmen kann. Grundlage der Methode ist eine Kalibrierung der Trübungswerte mit den entsprechenden zahlenmittleren hydrodynamischen Partikelgrößen und die Annahme, dass die Teilchenanzahl während der Messung nahezu konstant bleibt, welche nach der Nukleationsphase für Emulsionspolymerisationen erfüllt ist. Die Methode ermöglicht bei Polymergehalten von bis zu 50 wt.% eine schnelle und präzise Verfolgung der zahlenmittleren hydrodynamischen Partikelgröße.

Die Einflüsse der Rezeptur auf die Belagsbildung wurden für der Emulsionscopolymerisation von Vinylacetat und Vinylneodecanoat untersucht und auf Basis der experimentellen Befunde ein Modell entwickelt, welches es ermöglicht Belagsmassen für unbekannte Rezepturen vorherzusagen. Es wurden direkte Einflüsse des Monomerumsatzes und der Monomerzusammensetzung auf die Belagsmenge gefunden. Der Monomerumsatz wird dabei maßgeblich von der Reaktionstemperatur, dem Initiatorgehalt und dem Emulgatorgehalt beeinflusst. Folglich kann die Belagsmenge durch eine Verringerung des Umsatzes oder Veränderung der Monomerzusammensetzung reduziert werden. Beides ist industriell wenig attraktiv, da eine Verringerung des Umsatzes die Ausbeuten schmälert und die Aufarbeitung des Produkts komplizierter macht und eine Veränderung der Monomerzusammensetzung zu anderen Produkteigenschaften führt. Zusammenfassend ist es möglich, die Einflüsse des Prozesses auf die Belagsmasse zu quantifizieren und sogar vorherzusagen. Die Vorhersagen lassen eine industrielle Umsetzung jedoch nicht wahrscheinlicher erscheinen, da die belagsarmen Rezepturen wenig vorteilhaft erscheinen. Hierfür wäre der Einsatz von Beschichtungen im Reaktor vielversprechender, da sowohl für hydrophobe als auch hydrophile Beschichtungen im Reaktor zwar keine reproduzierbare Reduktion der Belagsmasse beobachtet werden konnte, jedoch die Reinigung deutlich erleichterten. Dies würde zu gesteigerten Effizienzen durch kürzere Reinigungszeiten führen.

Sensoren basierend auf Umsatz, Verweilzeit sowie Ultraschall-Messtechnik zur Belagsdetektion wurde entwickelt und implementiert. Diese Methoden zur direkten und indirekten quantitativen Belagsdetektion wurden hinsichtlich ihrer Robustheit, der Messgrenzen und der Skalenabhängigkeit evaluiert. Vielversprechende Ergebnisse konnten durch Messung des Verweilzeitverhaltens des Rohrreaktors erzielt werden. Die gemessene Verweilzeit wird durch Beläge im Rohrreaktor signifikant reduziert und das Marker-Signal verbreitert. Dies deutet auf erhöhte Totzonen im Reaktor durch die Belagsaufwüchse. Die Detektionsgrenze der Verweilzeitmethode Methode ist hoch, da erst eine deutliche Volumenveränderung im Reaktor vorliegen muss, damit Beläge erkannt werden können. Ein

weiteres Konzept zur Belagsdetektion kann durch die Ermittlung des Umsatzrückgangs während der Reaktion erhalten werden. Hierfür muss die Verweilzeit im Rohrreaktor ungefähr der Reaktionszeit entsprechen, denn dann führt eine Reduktion des Reaktorvolumens durch Beläge zu einer verkürzten Reaktionszeit und folglich zu einem Umsatzrückgang. Der Vorteil dieser Methode ist, dass eine Umsatzanalytik oft bereits existiert, da der Reaktionsumsatz eine wichtige Zielgröße ist. Somit sind Einsparungen durch die Verwendung einer bestehenden Analytik möglich und es werden präzise Ergebnisse erhalten. Geringe Belagsmengen sind nur mit Verzögerung zu detektieren, da auch hierbei eine signifikante Volumenänderung vorliegen muss.

Es wurde nachgewiesen, dass die Messung von Polymerbelägen mittels einer Ultraschall-Messzelle gut geeignet ist, um bereits frühe Stadien der Belagsbildung präzise zu erfassen. Die Schallgeschwindigkeit der Ultraschallwellen ist stark medienabhängig, sodass es zu einer Verschiebung der Schallgeschwindigkeit in einer Messzelle kommt, wenn Beläge entstehen. Durch eine Kalibrierung gegenüber den Belagsmassen im Reaktor wurde eine robuste und präzise analytische Methode zur Detektion von Belägen entwickelt. Diese kann das Belagswachstum sowie auch den Belagsabbau durch Reinigung verfolgen und ist in der Lage einen autonomen Betrieb zu ermöglichen.

Neben der Untersuchung der Belagsbildung im kontinuierlichen Betrieb, spielen die Produkteigenschaften der Polymere eine wesentliche Rolle für die spätere Anwendung des Polymers. Daher wurden die chemischen Eigenschaften von Polymeren aus *batch* Prozessen, mit denen aus dem Rohrreaktor verglichen. Bei den Molmassen, Partikelgrößen und Emulsionsstabilitäten wurden keine Unterschiede festgestellt. Der Reaktionsumsatz ist vom Herstellungsverfahren abhängig, da im kontinuierlichen Betrieb die Verweilzeit eine wesentliche Rolle spielt. Durch Anpassung der Verweilzeit kann der Reaktionsumsatz angeglichen werden, sodass beide Prozesse Produkte mit vergleichbaren polymeren Eigenschaften liefern. Unabhängig vom Prozess weisen die Beläge ein signifikant höhere Molmassen auf als die Polymerdispersion, sodass auf Polymerisationsfouling als wesentlichen Mechanismus geschlossen werden kann, da die Konzentrationsverhältnisse in polymerisierenden Filmen entlang der Reaktorwände von der dispersen Phase abweichen und somit Verschiebungen in der Molmasse zu erwarten sind. Eine Vernetzung der Beläge konnte mittels Messung der Gelgehalte ausgeschlossen werden.

Zusammenfassend wurden viele Aspekte der kontinuierlichen Emulsionspolymerisation sowie der Belagsbildung dieser Polymerisation untersucht und Erkenntnisse gewonnen, wie diese auftritt und über welche Messverfahren sie zugänglich ist. Damit wurden wesentliche Beiträge zur Umsetzung von kontinuierlichen Emulsionspolymerisationen auf großtechnischer Skala erbracht und Grundlagen zum Verständnis der Belagsbildung und für Belagsvermeidungsstrategien erarbeitet.

## 2. Summary

In comparison to bulk or solution polymerisation, emulsion polymerisation ensures good heat dissipation and therefore process reliability. Vinyl acetate is a frequently used monomer in emulsion polymerisation. Polyvinyl acetate and its copolymers are used as a concrete aggregate and in adhesives, binders for the paint industry and coatings. To date, emulsion polymerisation has largely been carried out on an industrial scale in a semi-batch process. A continuous mode of operation would be clearly preferable in terms of efficiency, costs and space-time yield, but the formation of deposits poses a major challenge. The deposits adhering to the reactor walls result in a loss of reaction volume and significantly reduce the heat dissipation capacity. This reduces process reliability and leads to altered product properties and reduced cost efficiency due to increased dead times. There are two main fouling mechanisms. Polymer fouling due to agglomeration of latices and subsequent sedimentation. On the other hand, there is polymerisation fouling, in which polymerisation takes place in films on the reactor surface and polymers grow on the surfaces.

This work contributes to the understanding of fouling during the continuous emulsion polymerisation of vinyl acetate copolymers. For this purpose, a reproducible and fouling-intensive formulation was developed in the tubular reactor and the fouling formation and the influences on it were investigated. In addition, sensor concepts for the inline quantification of fouling in the tubular reactor were developed and the polymerisation and properties of the polymers were characterised.

Particle size is one of the key parameters for characterising polymer dispersions and is therefore relevant for controlling product properties. Particle sizes are usually measured offline using light scattering analysis of diluted polymer dispersions. These methods are time-consuming and costly and would lead to considerably delayed adjustments to changes in the product, especially in a continuous polymerisation process. Therefore, the establishment of an inline method for the simultaneous measurement of particle sizes in the process is an important step towards increasing process efficiency. For this purpose, a method was developed that can determine the number-average hydrodynamic particle sizes of the latices with deviations of less than 5 % from reference methods based on the turbidity of the dispersion. The method is based on a calibration of the turbidity values with the corresponding number-average hydrodynamic particle sizes and the assumption that the number of particles remains almost constant during the measurement, which is fulfilled after the nucleation phase for emulsion polymerisations. The method enables

fast and precise tracking of the number-average hydrodynamic particle size for polymer contents of up to 50 wt.%.

The influences of the formulation on fouling formation were investigated for the emulsion copolymerisation of vinyl acetate and vinyl neodecanoate and a model was developed on the basis of the experimental findings, which makes it possible to predict fouling masses for unknown formulations. Direct influences of the monomer conversion and the monomer composition on the fouling mass were found. The monomer conversion is significantly influenced by the reaction temperature, the initiator content and the emulsifier content. Consequently, the fouling mass can be reduced by reducing the conversion or changing the monomer composition. Both are not very attractive industrially, as a reduction in the conversion reduces the yields and makes the processing of the product more complicated and a change in the monomer composition leads to different product properties. In summary, it is possible to quantify and even predict the influences of the process on the fouling mass. However, the predictions do not make industrial realisation appear any more likely, as the low fouling formulations appear to be less advantageous. The use of coatings in the reactor would be more promising for this purpose, as no reproducible reduction in the fouling mass could be observed for either hydrophobic or hydrophilic coatings in the reactor, but cleaning was significantly easier. This would lead to increased efficiency through shorter cleaning times.

Sensors based on conversion, residence time and ultrasonic measurement technology for fouling detection were developed and implemented. These methods for direct and indirect quantitative fouling detection were evaluated in terms of their robustness, measurement limits and scale dependency. Promising results were obtained by measuring the residence time behaviour of the tubular reactor. The measured residence time is significantly reduced by deposits in the tubular reactor and the marker signal is broadened. This indicates increased dead zones in the reactor due to the fouling. The detection limit of the residence time method is high, as there must first be a significant change in volume in the reactor for deposits to be recognised. Another concept for fouling detection can be obtained by determining the decrease in conversion during the reaction. For this, the residence time in the tubular reactor must correspond approximately to the reaction time, as a reduction in the reactor volume due to fouling then leads to a shortened reaction time and consequently to a decrease in conversion. The advantage of this method is that a conversion analysis often already exists, as the reaction conversion is an important target variable. This means that savings can be made by using an existing analysis and precise results are obtained. Small amounts of fouling can only be detected with a delay, as a significant change in volume must also be present here.

The measurement of polymer deposits using an ultrasonic measuring cell is well suited to the precise detection of early stages of fouling. The sonic velocity of ultrasonic waves is strongly dependent on the medium, so that there is a shift in the sonic velocity in a measuring cell when deposits form. A robust and precise analytical method for detecting fouling has been developed by calibrating against the fouling masses in the reactor. This can track the growth of fouling as well as their degradation through cleaning and enables autonomous operation.

In addition to investigating the fouling in continuous operation, the product properties of the polymers play a key role in the subsequent application of the polymer. Therefore, the chemical properties of polymers from batch processes were compared with those from the tubular reactor. No differences were found in the molar masses, particle sizes and emulsion stabilities. The reaction conversion depends on the production process, as the residence time plays a significant role in continuous operation. By adjusting the residence time, the reaction conversion can be equalised so that both processes deliver products with comparable polymer properties. Regardless of the process, the deposits have a significantly higher molar mass than the polymer dispersion, so that polymerisation fouling can be concluded as the main mechanism, as the concentration ratios in polymerising films along the reactor walls deviate from the disperse phase and therefore shifts in the molar mass are to be expected. Cross-linking of the deposits could be ruled out by measuring the gel content.

In summary, many aspects of continuous emulsion polymerisation and the fouling of this polymerisation were investigated and insights were gained into how this occurs and which measurement methods can be used to access it. This has made significant contributions to the implementation of continuous emulsion polymerisation on an industrial scale and provided a basis for understanding the formation of deposits and for fouling prevention strategies.



### 3. Introduction

Polymerisation reactions are an important part of industrial chemistry as polymers are used for various applications in daily life. More than 390 Mt of plastics were produced in 2021<sup>[1]</sup> with an increasing trend for the future. Polymers are products by process, so the manufacturing process is important for the resulting product properties. The emulsion polymerisation is one of these processes which is of industrial interest as it is high process safety and easy accessibility. The market for emulsion polymers is with USD 28.8 billion in 2021 an important share of the global polymer market which is with an annual growth rate about 10 % increasing.<sup>[2]</sup> Emulsion polymerisation combines high molecular weights of the polymers with process safety aspects and environmental benefits. The use of water as continuous phase with a high heat capacity and lower viscosities compared to solution or bulk polymerisation increase heat transfer rates and with that the process safety for exothermic processes. Moreover, emulsion polymerisations are free of toxic or hazardous solvents, which otherwise must be separated afterwards. Thus, the product is free of volatile organic compounds (VOC). Water-based polymer dispersions can be used often directly as obtained by the process for coatings, adhesives and additives. Dried dispersions are used for powder applications for example in construction work. Emulsion polymers are used for synthetic rubbers or plastic applications as well.<sup>[1,3,4]</sup> Most emulsion polymerisation processes are performed in batch or semi-batch operation mode as a continuous process is challenging. The challenges are mostly given by reaching comparable product properties and fouling during the reaction, which causes high cleaning times and costs especially in continuous operation. Therefore, to increase the efficiency of the process the fouling mechanism must be investigated to obtain knowledge about the processes and reasons that cause the formation of deposits in the reactor.

Polyvinyl acetate is one of the common polymers produced by emulsion polymerisation. The global production of vinyl acetate is about 7.2 Mt in 2023 and is mainly used for polymerisation and production of polyvinyl alcohol as emulsifier for the production of polyvinyl acetate.<sup>[3]</sup> The largest part is used for the production of the homopolymer polyvinyl acetate followed by the production of copolymers e.g. polyethylene-co-vinyl acetate which contains 10 – 20% of ethylene for lower glass transition temperatures and better product properties.<sup>[3]</sup> Polyvinyl acetate and its copolymers are used for construction materials, automotive applications, adhesives, paints and coatings for moisture barriers and electric insulation.<sup>[3]</sup> The production processes are all in batch or semi-batch operation mode as fouling is an important challenge which requires cleaning between the batches and prevents continuous operation.

### 3.1 Emulsion polymerisation

In emulsion polymerisation, a hydrophobic monomer is emulsified in an aqueous phase using an emulsifier. Most of the monomer is in the monomer droplets or micelles and only small amounts of monomer are solved in the continuous water phase (Fig. 1). Anionic (e.g. SDS, SDBS) or neutral surfactants (e.g. Mowiol) are usually used as emulsifiers.<sup>[5-7]</sup> The initiation is carried out by a hydrophilic initiator in aqueous phase. For initiation thermal (e.g. AIBN, BPO) or redox initiator systems (Ascorbic acid/*tert*-butyl hydroperoxide/iron catalyst)<sup>[8]</sup> can be used. Subsequently, the radicals formed react in the aqueous phase with the monomer molecules present there to form oligoradicals (Fig. 1a). The hydrophilicity of these oligoradicals decreases with increasing chain length, so that the oligoradicals are no longer water-soluble and nucleation occurs (Fig. 1b).<sup>[5-7]</sup>

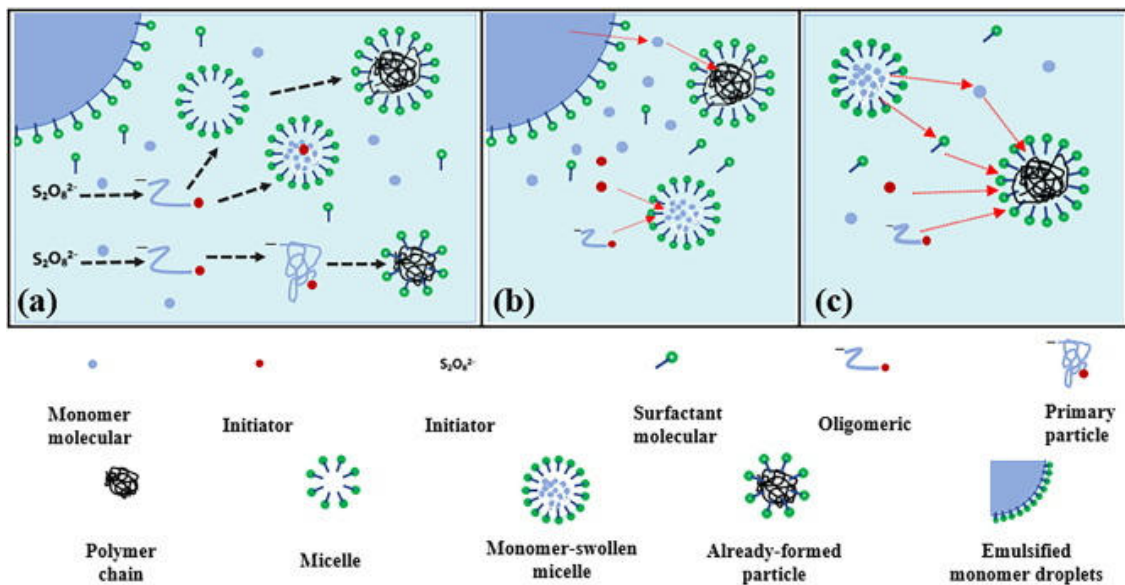


Figure 1: Mechanism of emulsion polymerisation. (a) initiation and formation of oligoradicals in continuous phase, (b) nucleation of particles and (c) particle growth and termination.<sup>[9]</sup>

Two relevant mechanisms are known for nucleation (Fig. 2). Depending on the monomer, homogeneous or heterogeneous nucleation predominates. In the case of heterogeneous nucleation, the hydrophobic oligoradicals diffuse into the monomer-swollen micelles in which growth begins. This mechanism is particularly relevant with a high emulsifier concentration and a hydrophobic monomer.<sup>[5]</sup> More hydrophilic monomers or emulsifier concentrations below the critical micelle concentration (CMC) favour homogeneous nucleation as predominant mechanism. The oligoradicals continue to grow due to the higher concentration of monomer in the aqueous phase until they are too hydrophobic and therefore precipitate. The precipitating oligoradicals are stabilised by the emulsifier and thus latex particles are formed.<sup>[5,10,11]</sup>

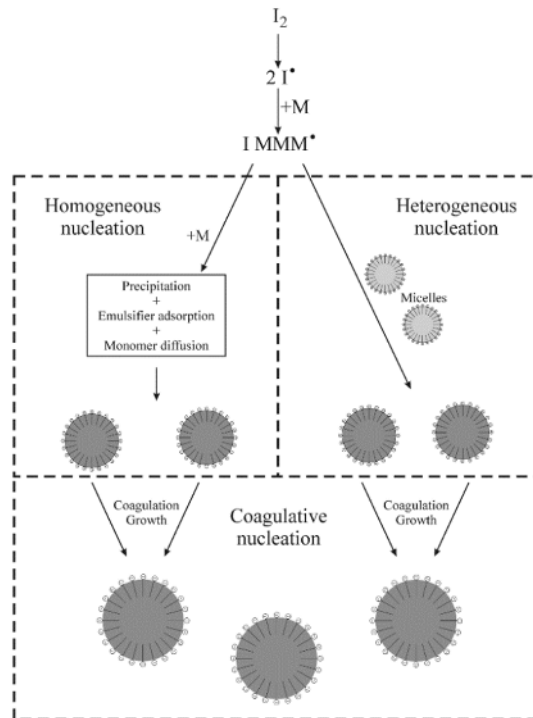


Figure 2: Nucleation in emulsion polymerisation. The different pathways for homogeneous and heterogeneous nucleation are shown.<sup>[11]</sup>

The polymerisation rate of the emulsion polymerisation can be divided into three phases. During nucleation the reaction rate in the latex particles increases significantly due to the higher concentration of monomer. After nucleation (phase I) is complete, the polymerisation rate remains constant caused by constant monomer feed from the monomer droplets (phase II) until all monomer is in the micelles and monomer depletion occurs (phase III). Subsequently, the polymerisation rate decreases until all chains are terminated (Fig. 3).<sup>[5,10,19–24,11–18]</sup>

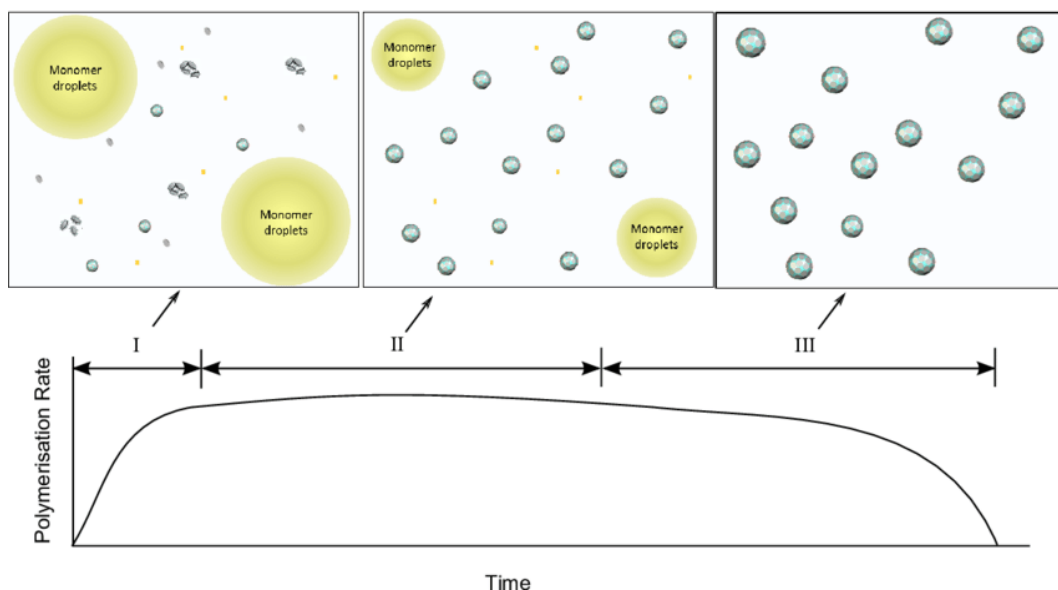


Figure 3: Developments in polymerisation rate during emulsion polymerisation. The polymerisation is divided into three phases, in the first phase nucleation occurs and the reaction rate is increasing. In the second phase nucleation and termination are in equilibrium and reaction rates are constant and in the third phase the monomer depletion occurs and termination increases so that reaction rate is decreasing.<sup>[25]</sup>

The classical assumption of NOMURA et al.<sup>[26]</sup> determines the number of radicals per micelle to be 0 or 1. This assumption applies well to very fine-particle latices, as termination is significantly faster than possible desorption. For real emulsion polymerisation micelles with more radicals can also be observed especially with larger particle sizes of the latices. Hydrophilic monomers, such as vinyl acetate, show another difference to ideal kinetics as chain transfer of the oligoradical to a monomer occurs. Subsequent desorption of this monomer radical is much more likely than termination by recombination of both radicals. With increasing hydrophobicity of the monomers and increasing size of the latex particles, the probability of desorption decreases compared to termination.<sup>[27]</sup>

### 3.2 Emulsion polymerisation of vinyl acetate

With an annual production volume of 7.2 Mt, polyvinyl acetate is one of the polymers of industrial relevance.<sup>[3]</sup> The large-scale polymerisation of vinyl acetate is generally carried out as free radical polymerisation using a thermal initiator.

Emulsion polymerisation is often preferred, as dispersions or powders are the favoured form for most applications in adhesives or coating industry. In addition, the reaction enthalpy of the polymerisation of vinyl acetate is very high at  $\Delta H_R = -88.8 \text{ kJ mol}^{-1}$ , meaning that good heat dissipation is necessary for reliable polymerisation and process safety. An anionic emulsifier is not sufficient for the formation of a stable emulsion; instead, partially hydrolysed vinyl alcohol polymers are used in the processes, which are surface-active as hydrophilic polymers.<sup>[13,28]</sup>

Pure homopolymerisation of vinyl acetate is of minor importance, as the homopolymer has a glass transition temperature  $T_g$  of 30 °C which is too high for many applications and the polymer therefore too brittle.<sup>[29]</sup> However, the pure homopolymer is used for hydrolysis to polyvinyl alcohol.

Copolymers or terpolymers are used for most applications. In the usual case, monomers of the VeoVa family or ethylene are added. This lowers the glass transition temperature and also increases resistance to hydrolysis and UV radiation.<sup>[30]</sup> Both comonomers serve as internal plasticisers and ensure that no additional additives are required. The advantage of the VeoVa system lies in the simple polymerisation process at normal pressure and the low mass fraction required to achieve the polymer properties. The side chain of the comonomer increases the free volume of the polymer, which lowers the glass transition temperature  $T_g$  of the polymer. This is particularly important for the production of thin polymer films, as the minimum film formation temperature (MFT) correlates directly with the glass transition temperature. For the homopolymer, the MFT is around 15 – 20 °C, making film formation at room temperature more difficult.<sup>[29]</sup> The addition of a small amount of long-chain vinyl esters significantly reduces the MFT so that film formation can be improved. The addition of long-chain vinyl esters increases the hydrolysis resistance of the polymer, so that the material properties are improved with regard to environmental influences. This effect is caused by steric shielding of the hydrolysis-sensitive bonds by the highly branched side chains of the long-chain vinyl esters.<sup>[31,32]</sup> However, the higher price of the monomers is a disadvantage.

In contrast, vinyl acetate-ethylene copolymers (VAE) offer a favourable comonomer, but the polymerisation must be carried out under increased pressure so that sufficient ethylene is soluble in the vinyl acetate. The reaction is carried out at pressures between 20 and 60 bar ethylene.<sup>[33]</sup> The process is usually carried out as a semi-batch with a redox initiator system as a starter, but continuous processes are also known from the literature.<sup>[34]</sup> Typically, the ethylene content is 5 – 40 %. This increases the process costs, but the raw material costs are lower than using vinyl esters, making this process more economical for large production volumes. Polymerisation is often carried out in batch or semi-batch autoclave reactors.<sup>[35,36]</sup>

### 3.3 Fouling

Fouling describes the deposition of solid material on the surface of reactors or internals. A distinction is made between different forms of fouling. Fouling can be formed in water treatment as salts (e.g., limescale deposits) or bioorganic layers (biofilms, bacteria, algae) may occur in the pipes or vessels. For chemical processes, the formation of deposits during the reaction caused by reduced inertness of the reactor surface is usually decisive.<sup>[37]</sup> The problems of deposit formation are primarily the formation of an additional barrier for heat dissipation due to the new boundary layer and the poor thermal conductivity of the deposit. Both reduce the effect of heat dissipation, so that the reactor design must take this into account. In addition, the reactor volume, and the resulting residence time change, meaning that the product specifications can deviate. In the worst case, clogging of the reactor or mixing elements would be possible.<sup>[38]</sup> Cleaning procedures for large-scale industrial plants are time and cost intensive, so it is advantageous to avoid fouling for obtaining an efficient process. Fouling mechanisms are often very complex as multiple factors e.g., surface temperatures, electrostatics, are influencing. The full understanding of these processes is very challenging and needs a lot of research. For wastewater treatment the fouling mechanisms are published by Ekowati et al.<sup>[39]</sup> who found out that cationic polymers cause fouling on reverse osmose membranes. In the publication the prediction of time dependent fouling masses was achieved and they distinguished between reversible fouling which could be removed by chemical cleaning and irreversible fouling that influenced the efficiency of the membranes permanently.<sup>[39]</sup> For heat exchangers, the fouling in dependence of heating or cooling operations can be predicted by the usage of learning algorithms.<sup>[40]</sup> For most other applications there are no detailed mechanisms described and only empirical correlations are known. Most of the established strategies are patented as they are important improvements for process efficiency.

One strategy is to use additives to reduce or avoid fouling.<sup>[41–47]</sup> Some examples are alkylphosphonate esters which reduce the fouling during polymerisation of ethylene dichloride.<sup>[43]</sup> Polyoxyalkenes are reported to reduce fouling in solution polymerisation of ethylene co- and homopolymers.<sup>[46]</sup> Alkyl and aryl phthalates prevent polymer fouling during monomer synthesis and solution polymerisation of acrylates, methacrylate or acrylic acid.<sup>[47]</sup> Moreover, the addition of comonomers to the recipe can reduce fouling which is described for kinetic hydrate-inhibitor formulations.<sup>[48]</sup> As the lack of inertness of reactor surfaces is one reason for chemical fouling. There are different applications that describe coatings of the equipment as solution for fouling reduction.<sup>[49–52]</sup> The fouling-free polymerisation of vinyl halides or vinylidene monomers is possible with monolayer coatings of polyvinyl alcohol and

the disodium salt of bisphenol A on reactor surfaces.<sup>[49]</sup> For the polymerisation of vinyl chloride coatings of alumina oxalyl bis(benzylidene)hydrazide<sup>[50]</sup> respectively aqueous selenous acid<sup>[51]</sup> can be used for fouling reduction.

Special reactor concepts can be another approach to reduce or prevent fouling.<sup>[53-58]</sup> McFadden et al.<sup>[54]</sup> reported that highly precise control of monomer streams and process parameters reduced fouling during continuous polymerisation. Side reactions are mainly responsible for fouling and these can be reduced by precision in process control.<sup>[54]</sup> Lowell et al.<sup>[55]</sup> optimised the geometry of the reactors for gas phase polymerisation to eliminate fouling-rich zones and reduce fouling therefor.

The optimisation of cleaning concepts for the reactors is another approach. The efficiency of the process could be increased by efficient cleaning. Deposits of olefinic polymers can be removed efficiently by circulating aromatic hydrocarbon solvents at high temperature in the reactor and recovering them by flash separation.<sup>[59]</sup> Haruyama<sup>[60]</sup> developed a mechanical cleaning strategy which removes polymeric fouling by displacement through expansion or contraction of the reactor parts.<sup>[60]</sup> Saikhwan et al.<sup>[61]</sup> investigated temperature and pH conditions where non-cross-linked acrylate-styrene copolymers are easily cleaned by taking advantage of their swelling behaviour.



### 3.4 Fouling during emulsion polymerisation

The mechanism and kinetics of emulsion polymerisation for various monomers and process conditions are described in multiple publications but there are less publications discussing the kinetics or mechanisms for fouling. For bulk or solution polymerisation there are some detailed publications.<sup>[62–64]</sup> Deglmann et al.<sup>[62]</sup> reported fouling processes during free radical polymerisation of N-vinyl pyrrolidone are caused by radical transfer reactions. This is leading to terminal double bonds which can be crosslinked. The crosslinked polymers show increased molecular weights and are not sufficiently dissolvable which leads to deposition.<sup>[62]</sup> Neßlinger et al.<sup>[65]</sup> investigated fouling during solvent polymerisation of vinyl pyrrolidone. They discussed the fouling reduction of coated reactor surfaces and their long-term suitability.<sup>[65]</sup>

Fouling formation for the emulsion polymerisation of vinyl acetate is described in literature as well.<sup>[58,66–68]</sup> Carvalho et al.<sup>[58]</sup> investigated continuous emulsion copolymerisation of vinyl acetate and n-butyl acrylate in a tubular reactor and reported problems in operation caused by fouling. With an oscillating pulsed flow control and internal sieve plates in the reactor the fouling could be reduced. The oscillating flow causes short periods of turbulent flow control with high shear rates which suppress the deposition of fouling while the internal sieve plates improve radial mixing and reduce side reactions.<sup>[58]</sup> The fouling behaviour on heated and cooled surfaces was investigated for emulsion copolymerisation of vinyl acetate and vinyl esters. They reported that higher temperatures increase fouling masses. A general trend for surface modifications was not observable as it is dependent on the other process parameters.<sup>[66–68]</sup> Hohlen et al.<sup>[67]</sup> compared fouling of non-reactive polymer dispersions with the fouling during emulsion polymerisation processes. Reactive polymerisation systems cause increased fouling masses so the polymerisation process is an important part for fouling.<sup>[67]</sup> During emulsion polymerisation two main mechanism for fouling can occur, polymerisation and polymer fouling. Polymerisation fouling describes the formation of deposit during the polymerisation reaction. Due to positive interactions, growing polymer chains are deposited homogeneously on the reactor surface, forming a uniform polymer film that covers the entire surface.<sup>[67]</sup> This is caused by the reduction of the surface energy, so fouling should be material dependent. In addition, dependent on the reactor material unpaired electrons in the reactor walls can also lead to initiation on the wall and thus to the formation of polymer layers. On the other hand, there is polymer fouling, which is caused by stabilisation problems in the polymer latex. If the polymer dispersion is not stable, agglomeration of latex particles into larger particles will occur,<sup>[69]</sup> which tend to sediment. This is resulting in non-stabilised solids that accumulate, particularly in dead zones of the reactor. As a result, polymer fouling forms selectively at reactor edges and

imperfections in the surface. This creates an uneven appearance, and the fouling structure is not a homogeneous film but have a drop-like structure. The appearance of the two types of fouling is shown in Figure 4.<sup>[38]</sup>

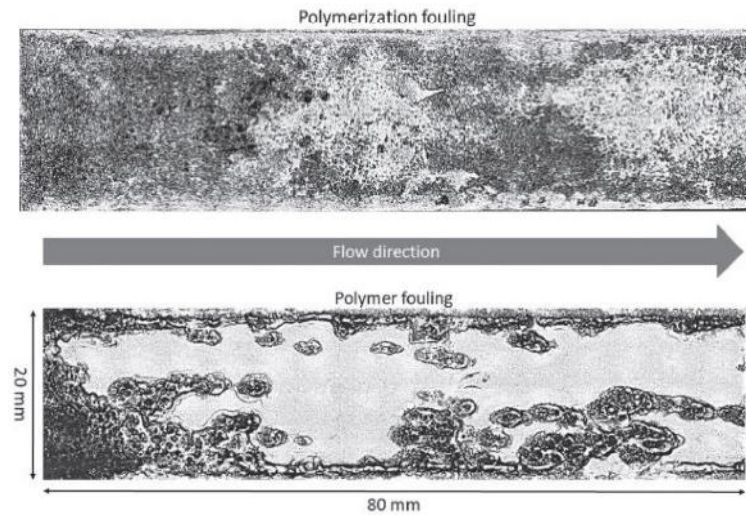


Figure 4: The appearance of polymer and polymerisation fouling on reactor surfaces.<sup>[38]</sup>

The structural differences in fouling can be seen in the images; the homogeneous film formation in the case of polymerisation fouling produces an even surface, while the polymer fouling surface is macroscopically structured. The fouling structures also differ on microscopically scale, as Figure 5 illustrates.

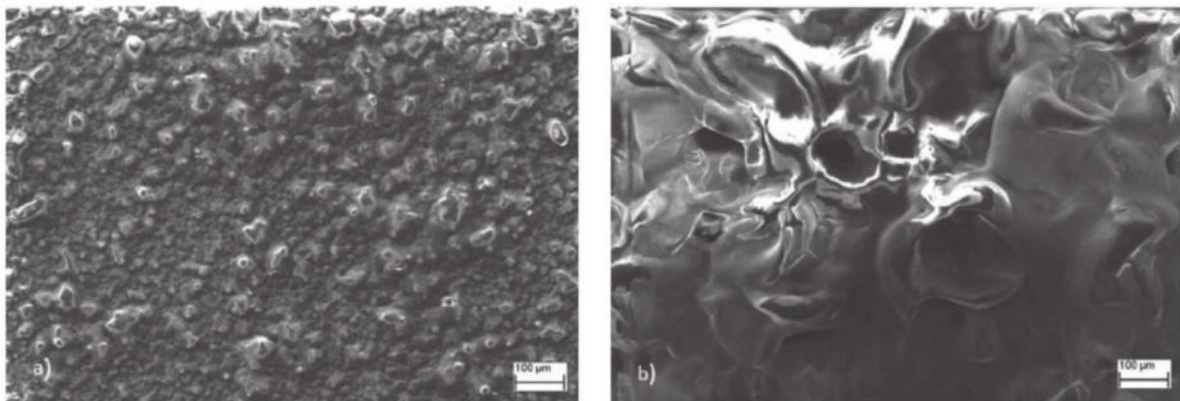


Figure 5: Images of fouling layers taken with an optical microscope of polymerisation fouling (a) and polymer fouling (b).<sup>[38]</sup>

The surface structure in the case of polymerisation fouling (Fig. 5 a) is much more finely structured, the structuring of the surface is in lower micrometre range, as there is no significant agglomeration of the latex particles. With polymer fouling, the surface is more structured, as the latex particles agglomerate to form particles many micrometres in size, which are deposited (Fig. 5 b).<sup>[38]</sup>

The fouling depends on some reaction parameters independent of the mechanism. An increase in the reactor wall temperature leads to increased fouling, while increased Reynolds numbers, cause a reduction in fouling.<sup>[38]</sup> The shear rate is indirectly correlated with fouling processes, as high shear tends to detach growing deposits and thus the fouling is inhibited. The polymer content has no influence on the tendency to fouling if the stability of the emulsion is guaranteed. This theoretical understanding is difficult to realise in practice, as ideal conditions are hard to achieve and a high polymer content increases the tendency to agglomerate, which in turn accelerates the polymer fouling.<sup>[38,66,70]</sup> The choice of emulsifier and the quantity used also influences the stability of the emulsion. Electrostatic and steric stabilisation of the latex particles are relevant mechanisms. Electrostatic stabilisation of dispersions is particularly dominant with hydrophobic monomers, as the micellar structure of an ionic surfactant is favourable here and a high density of emulsifier molecules can be achieved on the surface. These are thus sufficiently stabilised, while more hydrophilic monomers do not cause sufficient alignment of the ionic emulsifiers, so that the density on the particle surface is insufficient. Steric stabilisation is the more important mechanism here, in which non-ionic protective colloids are used to make the surfaces compatible. The use of sterically stabilising protective colloids, such as polyvinyl alcohol, improves the stability of the emulsion against electrolyte addition and higher solid contents,<sup>[71]</sup> although the dependence on the concentration of the emulsifier is high. Polyvinyl acetate does not form a stable emulsion by ionic emulsifiers alone. Non-ionic surfactants such as polyvinyl alcohol are usually added for this purpose.<sup>[70]</sup>

### 3.5 Fouling Detection

Fouling detection is another important field of research as the knowledge about possibly occurring fouling is necessary for process safety on industrial scale. If fouling is detectable inline it is possible to react and start cleaning procedures in order to keep the process safe and the product specifications constant. Besides optical detection methods like inspection glasses there are different technical approaches described.<sup>[72-78]</sup> For non-reactive systems polymer fouling can be measured using emulsion stability. This is accessible via particle size measurement as coagulation causes an increasing particle size which can be detected by e.g., dynamic light scattering (DLS) or nephelometry. The resulting particle size data can be used to develop models that enable predictions for fouling behaviour. The limitation is given as reactive systems and polymerisation fouling cannot be described as the fouling is mainly caused by reaction and not emulsion stability.<sup>[78]</sup> For inline detection of reactive systems most approaches are only established on lab-scale so far. The implementation of conductivity sensors to detect the formation of fouling is one way of fouling detection as fouling layers often show different conductivity than liquid phase.<sup>[77]</sup> Böttcher et al.<sup>[72]</sup> reported an inline measurement technique for monitoring fouling masses during emulsion copolymerisation of butyl acrylate and methyl methacrylate using a quartz crystal microbalance with dissipation monitoring. The frequency of the quartz crystal resonator is dependent on the mass adsorbed at the surface of the quartz crystal. So thin fouling layers can be monitored in frequency shifts. For fouling intense processes this method reaches saturation quickly and no longer information about fouling deposition can be obtained.<sup>[72]</sup> In this case on lab-scale it is established to detect the changes in the reactor weight.<sup>[73,74]</sup> At low fouling masses this method is not as precise as a quartz crystal microbalance but for stronger fouling differential weighting of the whole reactor or parts of it is more suitable. This method is mostly used on lab- or pilot plant scale but would be possible on industrial scale as well.<sup>[73,74]</sup>

The development of inline or atline measurement cells for scale-independent real-time fouling detection during polymerisation process are another field of research. An advantage would be that the same measurement cell and technology can be used on lab-scale and in industrial applications. There are different sensor technologies which are addressing this field. Neßlinger et al.<sup>[65,79]</sup> investigated the application of electrochemical impedance spectroscopy (EIS) for fouling detection during different polymerisation processes and were able to detect early stages of fouling growth in the measurement cell. The saturation of this measurement technology is reached in an early stages of polymerisation, so that it is only possible for detecting thin fouling layers.<sup>[79]</sup> Osenberg et al.<sup>[75,76]</sup> reported the suitability of ultrasonic fouling detection for polymerisation processes, such as solvent polymerisation and emulsion polymerisation.<sup>[75,76,80]</sup> For solvent polymerisation of polyurethanes the fouling mass in the measurement cell could be measured by analysing the average sound velocity (ASV), which is media-dependent and changes with growing fouling.<sup>[75,76]</sup> For emulsion polymerisation of vinyl acetate the average sound velocity (ASV) or the signal attenuation of the coupling reflection are possible measured variables.<sup>[80]</sup> Concluding, there are different approaches for fouling detection on lab-scale but no universal solution for wide applications is present.

## 4. Aim of Work

The goal of this work was to investigate fouling processes in continuously operated reactors. For that purpose, an emulsion copolymerisation was chosen as an industrial relevant system with strong tendency to deposit formation. Vinyl acetate and vinyl neodecanoate were chosen as comonomers as it is a commonly used industrial copolymer. The reactions were carried out in a continuous plug flow reactor (PFR) with static mixers because it is a favourable reactor concept for large scale industrial purposes and for continuous emulsion polymerisation there are less investigations and publications.

The polymerisation was carried out as redox-initiated polymerisation with ascorbic acid, *tert*-butyl hydroperoxide and ammonium iron(III) sulphate dodecahydrate as initiator system. This initiator system enables fast emulsion polymerisations at low temperatures and the kinetics are well known.<sup>[8,81,82]</sup> Monomer concentrations between 10 wt.% and 50 wt.% have been investigated. Monomer and emulsifier solution were pre-emulsified using a continuously stirred tank reactor (CSTR) and combined with the initiator at the entrance of the reactor. The reactor setup was characterised regarding residence times and mixing of components.

A standard operation procedure and recipe were developed and the reproducibility of polymer properties and fouling behaviour investigated. Afterwards the recipe and process parameters were varied to investigate the influences on dispersion and polymer properties as well as on the fouling masses. The changes in recipe included monomer content, comonomer composition and emulsifier and initiator concentration. The investigated process parameters were temperature and mass flow, which change the mean residence time. Moreover, the initial mixing situation and their influences on fouling were considered. The goal was to achieve an experiment-based model for fouling prediction in that process which helps to find suitable formulations for reducing fouling and reaching the product properties.

The polymer properties of the deposits and emulsion were analysed. For that purpose, molecular weights, solubility and swelling behaviour were measured. The chemical properties of fouling and dispersion were compared and samples from different spots in the reactor taken to obtain knowledge about fouling processes.

Moreover, an inline measurement technology for determining particle sizes was established as the particle size is one of the key specifications for dispersion properties and sampling followed by offline analysis of the dispersion is time-consuming. A calibrated inline measurement using nephelometry was investigated and the precision and deviation evaluated.

The development of inline or atline sensor concepts for real-time fouling detection was another goal of this work. Different approaches were investigated and their suitability was evaluated. These technologies were a conversion-based fouling detection, an ultrasonic measurement technique and electrochemical impedance spectroscopy (EIS). Besides the suitability for detecting fouling growth, the robustness, reproducibility, and precision were examined.

Different approaches for increasing the efficiency of the polymerisation process were investigated as well. This includes possible fouling reduction strategies as well as efficient cleaning concepts. For that purpose, coatings of reactor parts were tested and their influence on fouling masses determined. Chemical cleaning concepts were developed that should reduce cleaning time and effort. Optimally this cleaning concepts do not need hazardous or expensive substances so that a scale-up to industrial scale is possible.

## 5. Cumulative part of the dissertation

### 5.1 Determination of inline-particle sizes by turbidity measurement in high solid content emulsion polymerisations

Sören Rust, Werner Pauer

#### **Synopsis**

The particle size of a dispersion is one of the key specifications for product properties as it influences the chemical properties as well as the processability for the applications. The established methods for determining particle sizes require high effort as samples must be taken, diluted and measured. Typically, polymer emulsions are showing particle sizes between 100 nm and 1000 nm, a size range that is accessible via dynamic light scattering (DLS) or disc centrifugation. Both methods lead only to reliable results with highly diluted samples. For high solid content polymer emulsions one or more dilution steps are necessary. The dilution of polymer dispersions can affect their stability as the concentration of the emulsifier is changed and agglomeration may occur. So measured particle sizes can be falsified due to the preparation of the samples. An inline measurement technology which is able to handle high solid contents up to 50 wt.%.

% would be a great improvement for fast analysis of the dispersion properties. Following a process probe measuring the turbidity of the dispersion was integrated and the turbidity-values were correlated with the particle sizes of the dispersion analysed by dynamic light scattering. A recipe-dependent correlation between particle size and turbidity was obtained which allowed to measure particle sizes inline during emulsion polymerisation. This achievement significantly reduces the time for analysing the particle sizes. Process monitoring can be improved, and process efficiency increased.<sup>[83]</sup>





# Determination of inline-particle sizes by turbidity measurement in high solid content emulsion polymerisations

Sören Rust<sup>1</sup> · Werner Pauer<sup>1</sup>

Received: 16 March 2022 / Accepted: 14 June 2022 / Published online: 1 July 2022  
© The Author(s) 2022

## Abstract

Particle size determination in optically dense systems requires costly techniques or dilution of collected samples. Against this background, turbidimetry was investigated as a potentially robust as well as inexpensive alternative. Emulsion copolymerisations of vinyl acetate and VeoVa10® with solid contents up to 48 wt% were examined time resolved with respect to mean particle size at different temperatures, solid contents and with different co-monomer ratios and emulsifier concentrations. The mean hydrodynamic diameters were validated by dynamic light scattering (DLS). Precise number mean hydrodynamic diameters in the range from 100 to 250 nm were obtained in-line for polyvinyl acetate dispersions with deviations in particle sizes below  $\pm 5\%$ . In addition, the turbidity values were recorded by means of a nephelometry process probe and thus a robust, system-related calibration was created, which was subsequently able to reliably track the number mean hydrodynamic diameter inline time-resolved.

**Keywords** Emulsion polymerization · High solid contents · Turbidity measurement · Particle size determination · Inline analytics · Vinyl acetate

## Introduction

In emulsion polymerisation an inline or online analytical measurement procedure for the determination of the mean particle size would be advantageous over established offline procedures [1]. Several approaches can be found in literature for inline measurement of the mean particle size, but very few of them are commercially available and established. Moreover, most methods are not related to polymer dispersions, but rather to dusts, powders and aerosols with different particle size ranges [1]. Typical analytical methods for this are dynamic light scattering (DLS) or photon density wave spectroscopy (PDW) light scattering methods or measurements via the disc centrifuge.

Swithenbank et al. reported a laser diffractometric method that detect particles and droplets in liquid phase inline. Due to the used wavelength of the laser, their method is limited to the micrometre range and cannot detect particles below one micrometre [2]. For crystallisation processes, several

methods of inline particle size measurement were also investigated and compared, whereby the shape of the particles as well as their influence on the measured size are of interest, since crystallisation processes do not usually produce spherical particles. Here, both ultrasound techniques and laser scattering methods (3D-object-relational mapping and Focused Beam Reflectance Measurement) were successfully used for inline particle size determination in the range between 80–200  $\mu\text{m}$ , whereby the sensitivity of the method to the particle shape varied. However, use of the measurement methods for particles in the submicrometric range has not been described [3].

Regarding to the submicron-range a frequently described solution is the use of an at line analysis, in which a sample is taken continuously and automatically diluted, prepared and fed to a light scattering analysis via an autosampler. The dilution step is essential to eliminate multiple scattering, to which dynamic light scattering reacts very sensitively [4–6]. Therefore, different particle sizing methods were compared in the nanometre range with regard to their suitability for mapping polydisperse as well as multimodal distributions of polymer latices. It was shown that all the methods investigated (Tunable Resistive Pulse Sensing (TRPS), disk centrifuge (CPS) and dynamic light scattering (DLS)) can correctly determine the

✉ Werner Pauer

<sup>1</sup> Institute for Technical and Macromolecular Chemistry,  
University of Hamburg, Bundesstraße 45, 20146 Hamburg,  
Germany

particle size for monomodal distributions, but that DLS fails for multimodal distributions. Referenced studies were carried out against an electron microscopy evaluation [7]. One method for the inline measurement of submicron mean particle sizes is the photon density wave spectroscopy, which is suitable to measure hydrodynamic diameters even in high solid dispersions. Unfortunately, the method is expensive [8, 9].

The usage of turbidity measurement in emulsion polymerisation was investigated as well. Bloch et al. investigated the changes in turbidity during the emulsion polymerisation of styrene, especially during the early phases of emulsion polymerisation to obtain nucleation and inhibition times of the polymerisation. Moreover he showed the sensitivity of the method to changes in the polymerisation system, which goes along with differences in particle sizes [10]. Houben et al. reported that a Raman spectroscopy could be used to monitor particle sizes during emulsion polymerisation of styrene copolymers by computer-based partial least-squares (PLS) models basing on changes in chain-expansion vibrations [11]. Gao et al. showed a dependence of the turbidity values of N-isopropylacrylamide dispersions on the concentration of the particles as well as the particle size [12]. Moreover Tauer et al. performed numerous studies on the changes in characteristic properties during emulsion polymerisation, including the change in turbidity values of the system during particle growth but never used this data to predict particle sizes by turbidity measurement [13, 14]. Kiparissides et al. [15] have also shown that the particle size of polyvinyl acetate emulsions can be mathematically derived from the turbidity and thus inline turbidity measurement could be a suitable method for tracking particle size in the polymerisation process. They never proved this mathematical approach by experiment or determined the limitations and deviations of the method [15]. The general methodological suitability of a turbidity probe was also shown by Liu et al. [16] who used turbidity to track the adsorption of polymer particles on modified cellulose. Here, the suspension's content of 40 nm polymer particles could be quantitatively tracked up to 0.2% solid content [16].

All these works have in common that industrially relevant solid contents are not investigated.

Turbidity in polymer dispersions could be described by Mie scattering theory or Rayleigh scattering, because the particle sizes are in range of  $0.1 \lambda \leq d \leq 0.3 \lambda$ , so it is the transition area of both theories. Both theories describe that at a constant concentration of particles  $c$ , the scattering intensity  $I$  is directly proportional to the particle volume  $V$  and consequently correlates cubically proportional with the particle diameter (Eq. 1) [17].

$$I = c \cdot F_1$$

$$F_1 = \frac{24\pi^3}{\lambda^4} \cdot V \cdot \left| \frac{m^2 - 1}{m^2 + 2} \right| \quad (1)$$

With scattering intensity  $I$ , particle concentration  $c$ , a concentration independent term  $F_1$ , the wavelength of the irradiated light  $\lambda$ , the particle volume  $V$  and the refractive exponent  $m$ .

Following to previous work this paper uses turbidity measurement as analytical approach for inline measurements in high solid content polyvinyl acetate copolymer dispersions. In contrast to previous work, this paper takes a lab-based approach to develop a cheap and experimentally easy-to-implement method for in-line measurement of mean hydrodynamic diameter in polyvinyl acetate dispersions with a large formulation window up to more than 48 wt% solids content. Moreover, the polymer system related calibration reduces the effects of additives to the obtained data, so that the method could also be used for industrial processes. Even differences in formulation could be easily implemented in this method by calibrating the system to the new formulation within hours.

## Exp. section

All reactions were carried out in a cylindrical jacket-tempered 500 mL batch reactor produced by Colaver (type: 49CL4005), which was stirred at 250 rpm using an elliptical magnetic stirrer bar ( $d = 50$  mm). The precise setup is shown in Fig. 1. Turbidity was measured using a Mettler Toledo InPro 8200 process probe and Trb 8300 transmitter and recorded via LabView. The internal reactor temperature was recorded using a type K temperature probe via NuDam boxes and LabView software. The final turbidity was determined after the polymerisation was complete and the temperature had stabilised back to the initial value.

A comonomer stock system containing vinyl acetate and vinyl neodecanoate (trade name VeoVa10®) was used for emulsion polymerisation, with 10 wt% VeoVa10® based on total monomer content. Polymerisation was carried out with a monomer content of 23.8 wt%, unless otherwise stated. Polyvinyl alcohol was used as emulsifier in different weight proportions (Mowiol 4-88®, 2 – 20 wt% based on monomer). The initiation was carried out by a redox initiator system consisting of tert-butyl hydroperoxide, ascorbic acid and ammonium iron(III) sulphate dodecahydrate in a molar ratio of 1:1:0.03 [18].

## Results

### Calibration of the turbidity probe against DLS

To establish the calibration between turbidity and particle size, a series of tests was carried out in which the emulsifier content was changed in order to be able to set variable particle sizes. All other parameters, especially the solids content, were left the same so that the tests could be compared. The

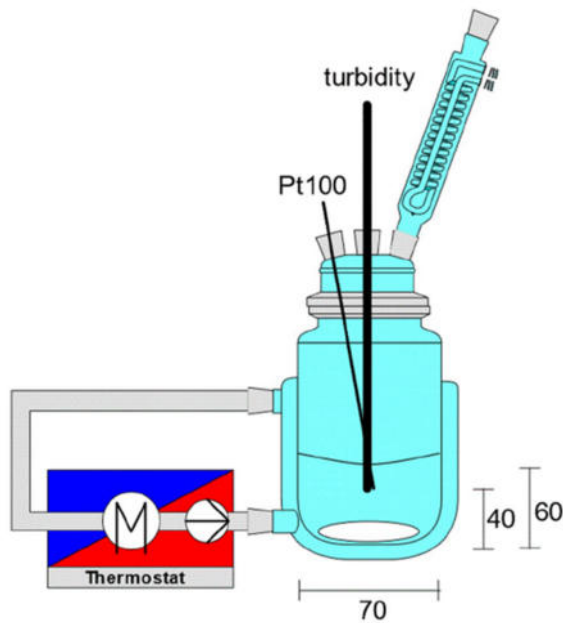


Fig. 1 Schematic structure of the reactor including the position of the measuring instruments

mean particle size was described by the mean hydrodynamic diameter, which could be determined by dynamic light scattering (DLS) of the diluted final sample. In addition, the turbidity values measured inline by the process probe were averaged and the particle size was plotted against the turbidity value (Fig. 2).

The particle size correlates with the turbidity and can be described by a cubic function, which shows high agreement ( $R^2=0.97$ ). The cubic calibration function shows a high agreement as well as a good accordance to the Mie scattering functions, which expects a cubic dependency (Eq. 1). The precision amounts to  $\pm 5$  nm deviation between calibration function and measured samples for particle sizes in the range between 120 and 250 nm. For particle sizes above 250 nm the turbidity values are close to the detector saturation and fluctuations around the mean value can be distorted as a result.

The influence of the solids content was investigated, as this is a parameter that, according to the underlying Lorenz-Mie scattering theory, has a strong influence. For this purpose, emulsion polymerisations were carried out with solids contents between 10 wt% and 48 wt% and the measured data were plotted as a function of this (Fig. 3).

From the Fig. 3, the influence of the solids content on the turbidity can be confirmed, so that it is important that the calibration used was measured for the same solids content. For deviations in the solids content, up to approx. 5%, the calibration can still be used with a deviation between

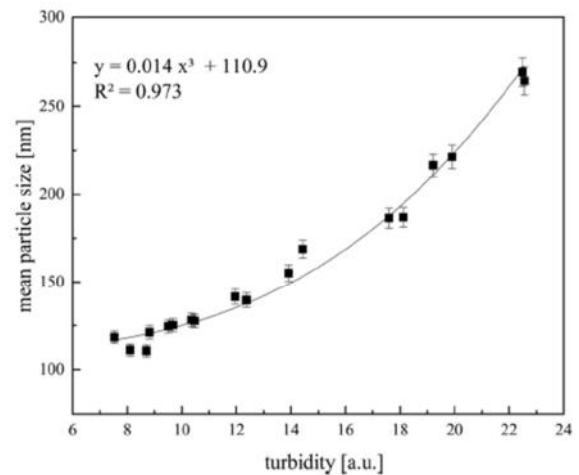


Fig. 2 Plot of the mean particle sizes measured by DLS including device-specific error against the turbidity values determined inline for the reactions with solid contents about 23.8 wt% at 20 °C. A cubic fit was chosen as the calibration function. Calibration functions for other solid contents are shown in Fig. 3

measured sample particle sizes and calibration of  $\pm 15$  nm. For larger deviations above 5% solid content deviation an adjustment of the calibration to the new system is essential to obtain valid particle sizes.

To validate the calibration function obtained by a different experimenter with 23.8 wt% solid content new polymerisations were carried out. A new calibration curve was determined and compared with those of Fig. 2.

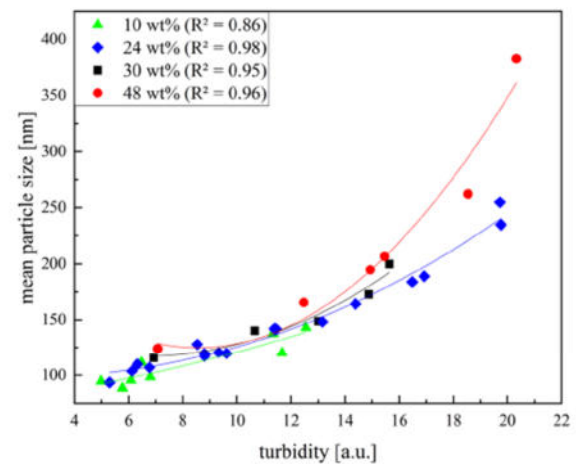


Fig. 3 Plot of the mean particle sizes measured by DLS against the turbidity values determined inline for the reactions with different solid contents between 10 wt% and 48 wt% at a reaction temperature of 20 °C. Fluctuations in the data may be because the real solids content deviates in part

The independent set of reactions has a high agreement with the calibration function obtained above (Fig. 4) ( $R^2 = 0.96$ ). Deviations between the determined mean particle size by the originally calibration function (red) and fit of validation experiments (black) are below 3%, which is in range of the errors set by experiment. The mean hydrodynamic diameter could be measured inline in the measurement range between 120 and 250 nm with a deviation of less than  $\pm 10$  nm to the calibration function.

### Influence of various process and recipe parameters on the validity of the calibration

The impact of the temperature on the turbidity values obtained was also investigated as a potentially relevant influencing variable that could falsify correlated particle sizes (Fig. 5).

The temperature has a subordinate influence on the average turbidity. Although the temporal fluctuation of the turbidity values increases somewhat with increasing temperature, the average remains the same for the same solids content and particle size, so that a change in the process temperature does not necessarily require a new calibration, as long as no other changes occur in the material system that could influence the product properties.

The influence of the co-monomer composition on the turbidity of the emulsion was also investigated. (Fig. 6) The vinyl acetate content was varied between 80 and 100% by weight.

In the window of the ratio Vac:Veova10 from 10:0 to 8:2, the differences in particle size caused by co-monomer composition changes of  $\pm 10\%$ , so that the same calibration could be used for a similar formulation with deviations in

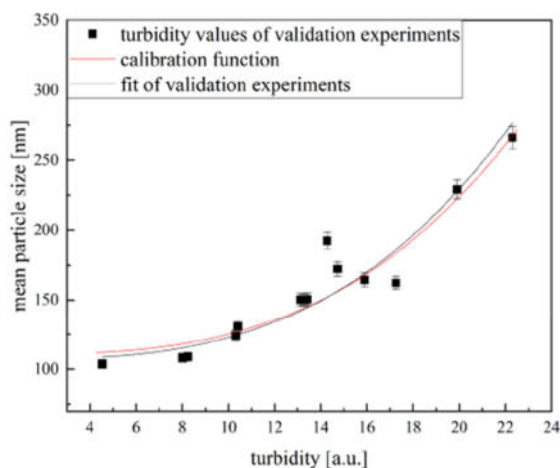


**Fig. 4** Measured particle sizes by DLS vs turbidity for independent experiments at 24 wt% at 20 °C temperature. The calibration function (Fig. 2) is compared with a fit function of the validation experiments

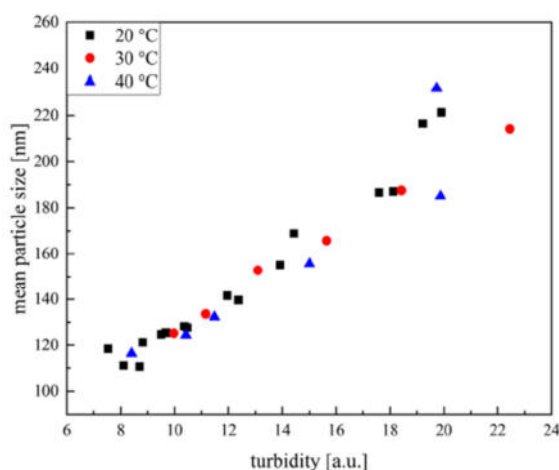


**Fig. 5** Plot of turbidity against mean particle size of the tests carried out at different temperatures, the fluctuations within the test series are greater than between the test series

predicted particle sizes smaller than 5%. Thus, individual screening experiments can be evaluated with the universal calibration, but for a longer-term use it is worthwhile to prepare a calibration specially for the system.

### Measurement limits

The measurement limits of the method were previously established by the particle sizes achieved in the formulation window used and no precise limit values were determined. Therefore, in the following, these measurement limit values for the mean particle size at 23.8 wt% were determined

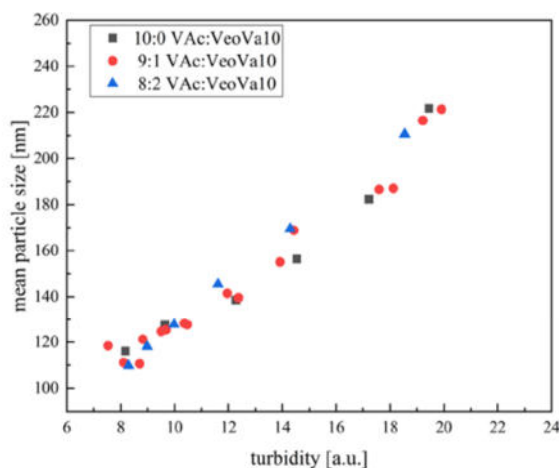


**Fig. 6** Plot of turbidity against particle size of the tests carried out with different vinyl acetate contents at 20 °C, the fluctuations within the test series are greater than between the test series

mathematically from the calibration and the measuring range of the detector as well as confirmed by experiments. The lower measurement limit of the detectable particle size results mathematically from the calibration function and the background value of the turbidity (4.22 a.u. for clear water) at around 110 nm. This agrees with the experimental findings where particle sizes of 98 nm could not yet be reliably distinguished from the background noise, but at a mean hydrodynamic diameter of 105 nm detection was possible due to a small increase in turbidity. Consequently, in practice, the detection of particles from a particle size of approx. 110 nm is possible.

The upper measurement limit of the measurable hydrodynamic diameter also has a technical limitation, which is given by the detector saturation of the turbidity probe. This is at an absolute turbidity of 22.6 a.u., which corresponds to a mean hydrodynamic diameter of about 270 nm. This also corresponds to experiments in which particles with a particle size of around 250 nm or more reach the detector saturation. However, the upper measurement limit can be determined less precisely, since the temporal turbidity fluctuations are greater there than in the range of small particles due to the substance system. Above 250 nm, no statement can be obtained with the detector used; with another detector, the range could most likely be extended. The lower measurement limit could be lowered by a shorter wavelength of the light used. Due to different calibration functions for other solid contents the measurement limits will be dependent from the solid content and cannot be determined universally.

### Application in practice

The created calibration was used to follow emulsion polymerisations with different solid contents about 24 wt% and 48 wt% inline. For this purpose, the turbidity course during the reaction was recorded and converted into a particle size course by means of the calibration. In parallel, samples were taken from the reaction solution and measured using DLS and disc centrifuge. The course and the obtained particle sizes of the offline methods are plotted in Figs. 7 and 8.

The particle sizes calculated by means of calibration agree within  $\pm 10$  nm with the particle sizes of the samples taken at the time points. Even for dispersions with high solids contents of over 48 wt%, the particle sizes can be determined in real time. Small deviations can be explained by the fact that intermediate samples continued to react despite the immediate addition of inhibitor solution and thus falsified the particle size at the time of sampling.

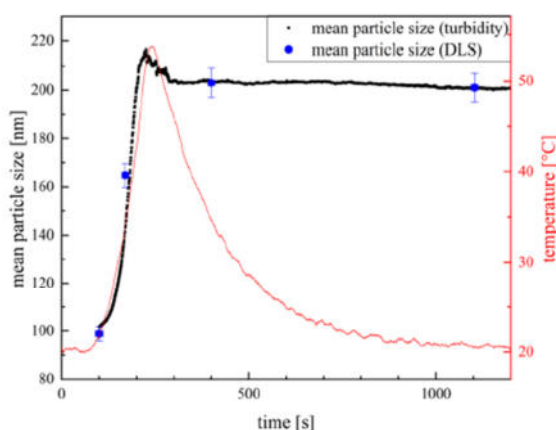


**Fig. 7** Plot of the calculated temporal particle size course of the inline turbidity measurement and the particle sizes determined offline from intermediate samples taken, including error bars. Especially during the fast reaction in the beginning, differences between DLS and turbidity may be caused by delays in sampling and stopping the reaction. The reaction was carried out at 24 wt% solid content

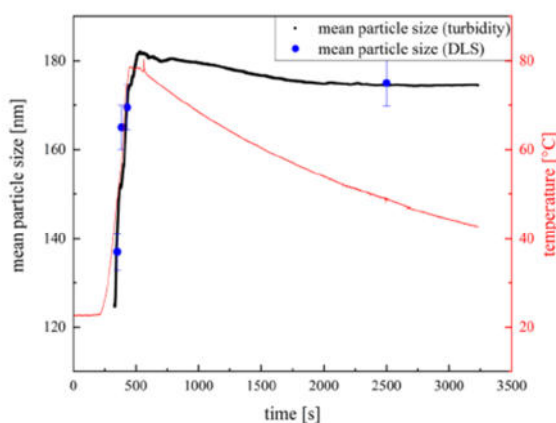


**Fig. 8** Plot of the calculated temporal particle size course of the inline turbidity measurement and the particle sizes determined offline from intermediate samples taken, including error bars. Especially during the fast reaction in the beginning, differences between DLS and turbidity may be caused by delays in sampling and stopping the reaction. The reaction was carried out at 48 wt% solid content

## Summary

Turbidity measurement for polymer dispersions with solid contents between 10 and 48 wt% is a suitable method for in-line measurement of mean hydrodynamic diameters in polymer dispersions in the range between 100 and 250 nm. For this purpose, a universal calibration related to the system is necessary, which is robust against common variances in a procedure. The calibration shows significant dependencies on the solids content of the system, while no significant dependency on temperature or stirrer speed/flow or minor recipe changes could be found. The tracking of the particle size development of a complete emulsion polymerisation could also be successfully established for solid contents up to 48 wt%.

**Author contribution** All authors conceived the experiments, Sören Rust performed the experiments and analysed the data. The first draft of the manuscript was written by Sören Rust and all authors commented on previous versions of the manuscript. All authors read and approved the final manuscript.

**Funding** Open Access funding enabled and organized by Projekt DEAL. The work has been funded by the German Federal Ministry for Economic Affairs and Climate Action as part of the ENPRO Initiative (KoPPonA 2.0, FKZ: 03EN2004M).

## Declarations

**Conflict of interest** The authors declare that they have no conflicts of interest for the submitted work.

**Open Access** This article is licensed under a Creative Commons Attribution 4.0 International License, which permits use, sharing, adaptation, distribution and reproduction in any medium or format, as long as you give appropriate credit to the original author(s) and the source, provide a link to the Creative Commons licence, and indicate if changes were made. The images or other third party material in this article are included in the article's Creative Commons licence, unless indicated otherwise in a credit line to the material. If material is not included in the article's Creative Commons licence and your intended use is not permitted by statutory regulation or exceeds the permitted use, you will need to obtain permission directly from the copyright holder. To view a copy of this licence, visit <http://creativecommons.org/licenses/by/4.0/>.

## References

- Merkus HG (2009) Particle Size Measurements. Springer
- Swithenbank J, Beer J, Taylor D, Abbot D, McCreath G (1976). A laser diagnostic technique for the measurement of droplet and particle size distribution. <https://doi.org/10.2514/6.1976-69>
- Mostafavi M, Petersen S, Ulrich J (2014) Effect of particle shape on in-line particle size measurement techniques. *Chem Eng Technol* 37:1721–1728. <https://doi.org/10.1002/ceat.201400212>
- Sacoto P, Lanza F, Suarez H, Garcia-Rubio LH (1998) A Novel Automatic Dilution System for On-Line Particle Size Analysis. *ACS Symp Ser* 693:23–29. <https://doi.org/10.1021/bk-1998-0693.ch003>
- AI Z (2018) et: United States Patent : 5861366 United States Patent : 5861366. N Y 2:1–29
- Celis M-T, Garcia-Rubio LH (2002) Continuous Spectroscopy Characterization of Emulsions. *J Dispers Sci Technol* 23:293–299. <https://doi.org/10.1080/01932690208984205>
- Anderson W, Kozak D, Coleman VA, Jämting ÅK, Trau M (2013) A comparative study of submicron particle sizing platforms: Accuracy, precision and resolution analysis of polydisperse particle size distributions. *J Colloid Interface Sci* 405:322–330. <https://doi.org/10.1016/j.jcis.2013.02.030>
- Jacob LI, Pauer W (2020) In-line monitoring of latex-particle size during emulsion polymerizations with a high polymer content of more than 60%. *RSC Adv* 10:26528–26534. <https://doi.org/10.1039/d0ra02523b>
- Bressel L, Hass R, Reich O (2013) Particle sizing in highly turbid dispersions by Photon Density Wave spectroscopy. *J Quant Spectrosc Radiat Transf* 126:122–129. <https://doi.org/10.1016/j.jqsrt.2012.11.031>
- Bloch D (2017) Etablierung der In-line-Trübungsmessung zur Prozessüberwachung von Emulsionspolymerisationen
- Houben C, Nurumbetov G, Haddleton D, Lapkin AA (2015) Feasibility of the Simultaneous Determination of Monomer Concentrations and Particle Size in Emulsion Polymerization Using in Situ Raman Spectroscopy. *Ind Eng Chem Res* 54:12867–12876. <https://doi.org/10.1021/acs.iecr.5b02759>
- Gao J, Hu Z (2002) Optical properties of N-isopropylacrylamide microgel spheres in water. *Langmuir* 18:1360–1367. <https://doi.org/10.1021/la011405f>
- Tauer K, Padtberg K, Dessy C (2002) On-line monitoring of emulsion polymerization. *ACS Symp Ser* 801:93–112. <https://doi.org/10.1002/cite.202055476>
- Tauer K, Deckwer R, Kühn I, Schellenberg C (1999) A comprehensive experimental study of surfactant-free emulsion polymerization of styrene. *Colloid Polym Sci* 277:607–626. <https://doi.org/10.1007/s003960050433>
- Kiparissides C, Macgregor JF, Singh S, Hamielec AE (1980) Continuous emulsion polymerization of vinyl acetate. Part III: Detection of reactor performance by turbidity-spectra and liquid exclusion chromatography. *Can J Chem Eng* 58:65–71. <https://doi.org/10.1002/cjce.5450580110>
- Liu D, Hao L, Fang K (2014) Adsorption of cationic copolymer nanospheres onto cotton fibers investigated by a facile nephelometry. *Colloids Surfaces A Physicochem Eng Asp* 452:82–88. <https://doi.org/10.1016/j.colsurfa.2014.03.079>
- Mie G (1908) Beiträge zur Optik trüber Medien, speziell kolloidaler Metallösungen. *Ann Phys* 330:377–445. <https://doi.org/10.1002/andp.19083300302>
- Schroeter BL (2018) Kinetik von Redoxinitiatoren für die Emulsionspolymerisation. University Hamburg, Hamburg

**Publisher's Note** Springer Nature remains neutral with regard to jurisdictional claims in published maps and institutional affiliations.

## 5.2 Formulation and process determined fouling prediction for the continuous emulsion co polymerisation of vinyl acetate

Sören Rust, Werner Pauer

### **Synopsis**

Fouling is a major challenge in industrial chemistry as it influences both, product properties and process safety. Especially emulsion polymerisations are fouling intense processes which lead to challenges in process optimisation and intensification. A mechanistic knowledge about the fouling processes and influencing variables could improve this situation. The influencing parameters for fouling growth are not fully known. Some publications report influences of the temperature<sup>[66,67]</sup> or emulsion stability<sup>[69]</sup> but no publication investigates the influences of all process and recipe parameter. A standard procedure for fouling quantification was established and the process and recipe influences of the fouling behaviour during continuous emulsion polymerisation were investigated to obtain deeper knowledge about the fouling pathways. Influences of temperature, comonomer composition, emulsifier and initiator concentration were investigated. Firstly, a single factor approach was chosen to determine the influences of the parameters on fouling mass and conversion. Then a multivariate approach was followed, and the results compared for validation of the single factor approach. Both approaches agree very well with small deviations in reproduction experiments. All parameters influenced the fouling formation, but most of them indirectly by influencing the conversion of the reaction. Only the comonomer composition directly influences the fouling deposition. The experimental correlations between these process parameters and the fouling mass enabled the development of a model to predict the expected fouling masses for different recipes and process conditions of vinyl acetate copolymers. The obtained model was able to predict conversion and fouling mass for unknown recipes with a precision of 15 %. For a different polymerisation or reactor system the model must be adjusted by performing a few experiments, but the general procedure can be transferred. With these achievements the experimental effort can be reduced, and promising recipes and process conditions can be found using the model and then controlled in an experiment.



# Formulation and process determined fouling prediction for the continuous emulsion co polymerisation of vinyl acetate

Sören Rust<sup>1</sup> · Werner Pauer<sup>1</sup>

Received: 23 February 2023 / Accepted: 4 May 2023 / Published online: 30 May 2023  
© The Author(s) 2023

## Abstract

Fouling is challenging for the industrial implementation of continuous emulsion polymerisations. A requirement for the development of successful anti-fouling concepts is an in-depth understanding of the processes involved in fouling and the knowledge of the main influencing factors. In this work, an experiment-based strategy was developed for the quantification of fouling trends and in order to calculate the expected fouling intensities during the continuous emulsion polymerisation of vinyl acetate copolymers. These, then, can be correlated with the direct process parameters temperature, initiator and emulsifier content and comonomer ratio. The expected fouling tendency for formulations could be determined in the investigated range with an accuracy of  $\pm 15\%$  referred to experimental validations.

**Keywords** Emulsion polymerization · Fouling · Fouling prediction · Continuous emulsion polymerisation · Vinyl acetate · Fouling model

## Introduction

As fouling is an important challenge for the chemical industry there are lots of patents regarding fouling reduction for different industrial polymerization systems or reaction processes. One widely used strategy is the fouling prevention by using additives during the process [1–7]. For example alkylphosphonate esters reduce the fouling during polymerisation of ethylene dichloride [3], polyoxyalkenes could be used for fouling reduction in solution polymerisation of ethylene co- and homopolymers [6] or alkyl and aryl phthalates could be used for the polymerisation of acrylates, methacrylate or acrylic acid. [7]. Another commonly used strategy in different fields of application is the coating of reactor surfaces [8–11]. Examples for this are monolayer coatings with polyvinyl alcohol and the disodium salt of bisphenol A for the polymerisation of vinyl halides, vinylidene halides or vinylidene monomers [8] or coatings with a water dispersion of alumina oxalyl bis(benzylidene)hydrazide [9] respectively aqueous selenous acid [10] for vinyl chloride

polymerisation. Moreover there are some ideas for reducing fouling by special reactor concepts [12–17]. For example McFadden et al. [13] reported that fouling during continuous polymerization could be reduced by highly precise control of monomer streams and process parameters. Lowell et al. [14] investigated that special geometry changes could reduce fouling for gas phase polymerisation. Carvalho et al. [17] used at lab scale an oscillatory flow reactor for a fouling free continuous emulsion polymerization. For specialized applications there are ideas of adding comonomers to reduce fouling like for Kinetic Hydrate Inhibitor Formulations [18].

Besides fouling reduction or prevention there are some patents and publications regarding the optimized cleaning procedures for fouling intensive processes. For olefinic polymer deposits a cleaning procedure by circulating high boiling aromatic hydrocarbon solvents in the reactor and afterwards recovering them by flash separation is described [19]. Haruyama [20] published a cleaning strategy for mechanical cleaning of polymeric fouling. The polymerization is carried out in the gap between two tempered tubes built into each other, which can be tempered independently of each other for cleaning, so that the reaction gap is closed by material expansion or contraction and removes polymer residues [20]. Saikhwan et al. [21] investigated the swelling and cleaning behavior of non-cross-linked acrylate-styrene copolymers

✉ Werner Pauer  
werner.pauer@chemie.uni-hamburg.de

<sup>1</sup> Institute for Technical and Macromolecular Chemistry,  
University of Hamburg, Bundesstraße 45, 20146 Hamburg,  
Germany



and reported temperature and pH conditions where cleaning is easily done.

In dependence of heating or cooling operations the prediction of heat exchanger fouling can be realized by the usage of learning algorithms [22].

Besides multiple publications on emulsion polymerization kinetics e.g. by Schork and Lu Fujun [23–27] and the influences of oxygen and process parameters on the nucleation and particle formation by Krishnan et al. [28] there are less publications discussing the mechanisms or reasons for fouling. Deglmann et al. [29] reported that the fouling processes in the radical polymerisation of N-vinyl pyrrolidone are mainly caused by transfer reactions leading to terminal double bonds which are crosslinked afterwards. This crosslinking leads to a significant increase in the molecular weight and is an important reason for deposit formation [29]. Neßlinger et al. [30] have investigated the fouling during solvent polymerisation of vinyl pyrrolidone. They discussed the influences of coatings of reactor surfaces on fouling masses and their possibility of fouling prevention [30]. Ekowati et al. [31] investigated the fouling on membranes during waste water treatment and reported that cationic polymers are causing fouling on reverse osmosis membranes. They were able to predict the time dependent fouling masses and could distinguish between reversible fouling that could be removed by chemical cleaning and irreversible fouling that couldn't be removed and influenced the efficiency of the membranes permanently [31].

Fouling processes during emulsion polymerisation of vinyl acetate are investigated in literature as well. There are different publications discussing this topic [17, 32–34]. Carvalho et al. [17] investigated the continuous emulsion copolymerisation of vinyl acetate and n-butyl acrylate in a tubular reactor. They reported that fouling during reaction caused problems and that could be solved by oscillating pulsed flow control and internal sieve plates in the reactor. The oscillating flow leads to short periods of turbulent flow control and prevents fouling while the internal sieve plates optimize radial mixing and reduce side reactions [17]. Moreover the fouling during emulsion copolymerisation of vinyl acetate and vinyl esters on heat-exchangers is investigated and compared to the fouling of commercial polyvinyl acetate dispersions on heated or cooled surfaces. In these publications the influences of temperature and surface modifications on fouling masses are discussed and it could be shown that higher temperatures lead to higher fouling masses. For surface modifications a general trend could not be observed as it is highly dependent on the other process parameters [32–34]. Hohlen et al. [33] investigated the differences between fouling of reactive emulsion polymerisation systems compared to the fouling of non-reactive polymer dispersions. Reactive systems cause more fouling than non-reactive so polymerisation fouling is the major part. The

morphology of the deposits has its origin in the fouling process. Thus the dominant fouling process can be concluded from the fouling morphology [33].

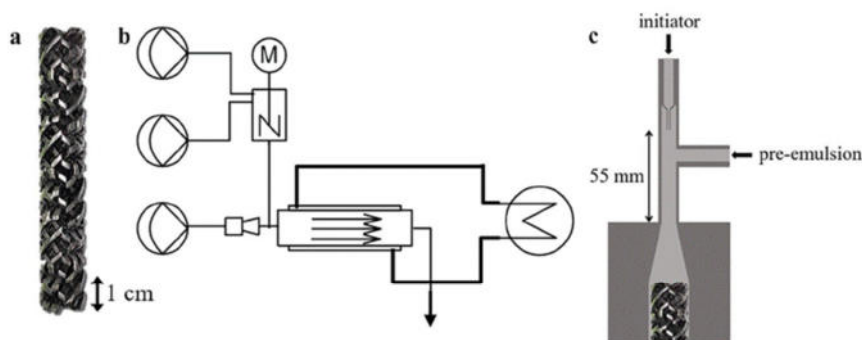
For fouling quantification there are different strategies described in literature. Böttcher et al. [35] presented an inline measurement technique for monitoring heat-transfer fouling masses during emulsion copolymerisation of butyl acrylate and methyl methacrylate using a quartz crystal microbalance with dissipation monitoring. They showed that there are two different pathways for heat-transfer fouling, one leading to thin fouling films which don't grow further after being formed and the other leading to thick fouling which grows over time [35]. For fouling quantification in fouling intense processes it is commonly used practice to detect the changes in the weight of the reactor [36, 37]. In early stages of fouling this method is not as precise as a quartz crystal microbalance for example. For stronger fouling a quartz crystal microbalance does not work. The weight detection of the whole reactor or parts of them is more robust.

Concluding all these publications there are lots of patents which optimize fouling behaviour in small, specialized applications but less literature which discusses scientific approaches to fouling processes. Most of the scientific publications are focussed on mechanistic influences or temperature effects so there are no publications addressing fouling behaviour to the set of process parameters that could be changed for the continuous emulsion polymerisation process of vinyl acetate copolymers. This work presents a strategy for evaluating the process and recipe dependent fouling behaviour in emulsion polymerisations and results in an experiment-based model for fouling prediction in the investigated system.

## Experimental section

For the stirred tank in series concept the continuous production of polybutadiene and polyvinyl acetate derived latices is well established. In contrast tubular reactors are not well established in continuous emulsion polymerisation although the specific heat transfer capacity and thus the theoretic space time yield is much higher at lower costs than that of continuous stirred tank reactors. The main reason is the challenging fouling tendency of these products. In order to come forward with continuous emulsion polymerization experiments were carried out in a Fluitec ContiPlant LAB<sup>®</sup> tubular reactor with CSE-X static mixing elements (Fig. 1a). The half-shell reactor has a channel diameter of  $d = 12$  mm filled with CSE-X static mixing elements and resulting volume of  $V = 45.5$  mL. Temperature control was achieved by a cryostat of the type Julabo FP50 tempering the double jacket to a constant inlet temperature, closed loop temperature controlled at the jacket inlet (Fig. 1b).

**Fig. 1** **a** picture of the static mixers type CSE-X, **b** Schematic structure of the reactor plant, **c** detailed plan of the initiator nozzle



Three solenoid-driven diaphragm metering pumps ProMinent® Gamma were used to deliver the dosing flows. The monomers (ProMinent gamma/4-1, stroke volume 0.13 mL/stroke, dosing flow 0.05 g/s) and the emulsifier solution containing poly(vinyl alcohol), Ascorbic acid and ammonium iron(III)sulphate (ProMinent gamma/5, stroke volume 0.16 mL/stroke, dosing flow 0.15 g/s) were pre-emulsified in a cylindrical CSTR equipped with a magnetic stirrer ( $d = 25.4$  mm,  $V = 20$  mL,  $d_{\text{stirrer}} = 18$  mm, 600 rpm) and the initiator flow containing *tert*-butyl hydroperoxide (ProMinent gamma/4, stroke volume 0.03 mL/stroke, dosing flow 0.01 g/s) was added 55 mm upstream and centered to the reactor inlet via a capillary nozzle (inner diameter 1 mm) (Fig. 1c).

All chemicals were used without further purifying. Vinyl acetate, vinyl neodecanoate and Mowiol 4-88 (molecular weight ~ 31 kDa, Degree of hydrolysis 88%) were purchased in technical grade from Wacker Chemie AG, Burghausen. Ascorbic acid and ammonium iron(III) sulphate dodecahydrate were purchased in analysis grade from Sigma Aldrich. *tert*-butyl hydroperoxide was purchased as an aqueous solution ( $c = 70\%$ (w/w)) from Sigma Aldrich.

For the monomer feed a vinyl acetate-vinyl neodecanoate (Veova10®) comonomer stock system was used for emulsion polymerisation, with 0 – 20 wt% Veova10® based on total monomer content. The comonomer system is very advantageous for the investigation of fouling, as the addition of vinyl

neodecanoate increases the hydrophobicity and lowers the glass transition temperature of the polymer, which favours film formation. Polymerisation were carried out with a monomer content of 23.8 wt%. Polyvinyl alcohol was used as an emulsifier in different weight proportions (5 – 15 wt% based on monomer). The initiation was carried out by a redox initiator system consisting of *tert*-butyl hydroperoxide, ascorbic acid and ammonium iron(III) sulphate dodecahydrate in a molar ratio of 1:1:0.03. The initiator weight proportions were varied between 0.1 – 2 wt% based on monomer. As a reaction time 120 min was chosen and fouling masses after this time compared. An overview of the used recipes is given in Table 1.

The influencing variables investigated were the reactor inlet temperature (5 °C–50 °C), the initiator content (0.1 wt%–2 wt% based on monomer), the emulsifier content (5 wt%–15 wt% based on monomer), and the monomer composition given as mole fraction of vinyl acetate  $x_{\text{Vac}}$  (0.8–1.0). The total monomer content was kept constant at 23.8 wt% within the scope of this work to obtain a valid model for a substance system that delivers reproducible results in the set-up used. The total monomer content was kept lower than in typical industrial processes as fouling would be much more occurring with 50 wt% total monomer content and influencing effects can't be observed that good. So, a similar recipe with lower total monomer content was used for investigation in lab scale. For typical industrial

**Table 1** Overview of used mass flows for recipes

Dosing flow	Chemicals	Content [g/s]
continuous phase [0.15 g/s]	Water	0.144 – 0.148
	Mowiol 4-88	$1.78 \cdot 10^{-3}$ – $5.36 \cdot 10^{-3}$
	Ascorbic acid	$3.56 \cdot 10^{-5}$ – $7.12 \cdot 10^{-4}$
	ammonium iron(III) sulphate	$1.07 \cdot 10^{-6}$ – $2.14 \cdot 10^{-5}$
Monomer [0.05 g/s]	Vinyl acetate	0.04 – 0.05
	Vinyl neodecanoate	0.00 – 0.01
Water soluble Initiator [0.01 g/s]	water	$9.24 \cdot 10^{-3}$ – $9.96 \cdot 10^{-3}$
	<i>tert</i> -butyl hydroperoxide	$3.78 \cdot 10^{-5}$ – $7.56 \cdot 10^{-4}$

applications with recipes with 50 wt% or more total monomer content similar trends can be expected but in the used lab scale plant changing monomer proportions would either massively influence the conversion of the reaction or require more profound changes to the reactor. A detailed overview of the conducted experiments is given in the supplementary information. The fouling in the reactor is growing on every surface in the reactor in similar amounts. So quantification is based on differential weighting of the static mixers as they are containing more than 95% of the inner reactor surfaces and effects of the reactor walls could be neglected. All fouling masses are given as fouling masses referenced to the weight of the static mixers in the reactor where the fouling mainly occurs ( $\text{mg}_{\text{fouling}}/\text{g}_{\text{mixer}}$ ).

Conversions  $X(t)$  were calculated as the weight ratio between formed polymer  $w_p$  and total initial monomer content  $w_M$  (Eq. 1). The polymer content was measured by microwave gravimetry of the product dispersions.

$$X(t) = \frac{w_p(t)}{w_M(t=0)} \quad (1)$$

## Results

Fouling causes conversion changes in continuous polymerisations because of the changed mean residence time by loss of reactor volume. Therefore, with respect to experiments of fouling kinetics an optimal measurement point is to determine. For experiments with dynamic fouling, it is necessary to determine the point in time, when quasi stationarity of conversion is reached while fouling has not significantly reduced the reactor volume. For that purpose, the time-resolved conversion described as the proportion of formed polymer versus total monomer consumption of several reactions was observed (Fig. 2) in order to obtain the best point for in deep analytics.

Figure 2 shows that the increase in conversion is finished after two to three mean hydrodynamic residence times for the reactions. After four to five mean hydrodynamic residence times for some recipes the conversion starts decreasing because of losses of reactor volume caused by significant fouling phenomena. Concluding, the preferred spot for a comparable conversion analysis is at three mean residence times after reaction start. This is in good accordance with common literature, which summarizes that in a plug flow reactor a stationarity could be reached after three to ten residence times [38]. In this case no stationarity is reached because of the intense fouling. For further investigation this work is using the conversion after three residence times as a characteristic reaction conversion.

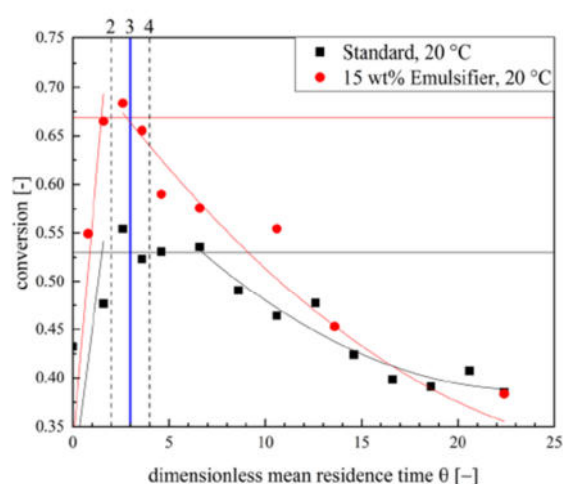


**Fig. 2** Time-dependent changes in conversion during the reaction caused by initiation and fouling processes. Shown are the standard recipe at 20 °C and a high fouling recipe for comparing the time range where no conversion decrease caused by fouling is observable

The experiments showed significant influences on the fouling mass for the reaction temperature (Fig. 3a), the initiator content (Fig. 3b), emulsifier content (Fig. 3c) and the monomer composition (Fig. 3d). Each data point in Fig. 3 indicates one experiment, so more data points represent replications on same conditions. The relationships between the influencing factors are complex and the strength of the influences, apparent from the change in the fouling masses, varies significantly between the parameters (Fig. 3). The influences of the parameters on the conversion are plotted, as the conversion in a tubular reactor is directly proportional to the reaction rate. Following the effects on reaction fouling can be compared to the effects on reaction rate (Fig. 3).

Temperature, initiator content and emulsifier content do not exert an independent influence on fouling mass, but rather influence the reaction conversion and determine by that the fouling mass. Fouling mass and conversion have similar time slopes. (Fig. 3a-c). Concluding this finding, fouling can be reduced by lower temperatures or less initiator but this decreases the reaction rate and conversion of the polymerisation so less product is formed. This demonstrates that it is possible to investigate the influences on fouling but regarding this parameters there is no possibility to obtain a industrially applicable recipe that avoids fouling.

An increased temperature and an increase in the initiator quantity accelerate the chemical reactions. The dependency of the conversion by emulsifier content is expected. Initiation takes place in the aqueous phase and the oligo-radicals subsequently migrate into micelles or precipitate and are terminated. Consequently, an increased emulsifier content leads to a higher number of latex particles and

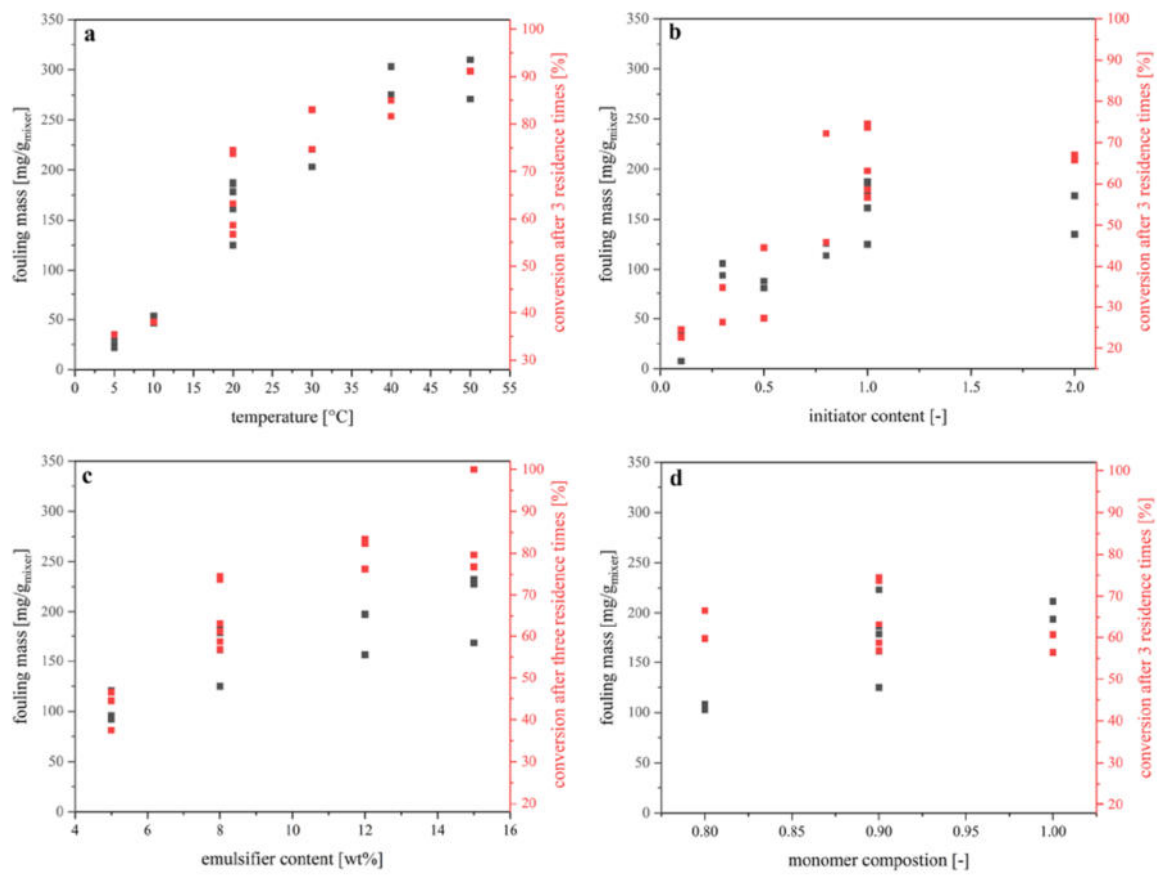


**Fig. 3** Dependency of process conditions and formulation parameters on fouling mass and conversion after three mean residence times. **a** temperature, **b** initiator, **c** emulsifier and **d** comonomer ratio

thus to a higher yield of growing chains [39]. This causes a smaller mean particle size. (Fig. 4). Particle numbers are calculated from the particle volume for spherical particles and the total volume of the monomer fraction.

The experimentally determined mean particle sizes (Fig. 4) are decreasing with increasing emulsifier content and the resulting particle number is increasing according to literature. An acceleration of the reaction is observed.

Following the above discussion, the conversion term and the monomer composition must be considered for fouling calculations. Since the conversion is not significantly correlated with the monomer composition ( $R^2=0.05$  for linear correlation) the conversion  $X$  and the monomer composition, as a mole fraction of vinyl acetate  $x_{VAc}$ , are independent of each other with regard to their influence on the formation of fouling  $m_{fouling}$  (Eq. 2).

$$m_{fouling}(X, x_{VAc}) = f(\text{conversion}) + f(\text{monomer composition}) \quad (2)$$

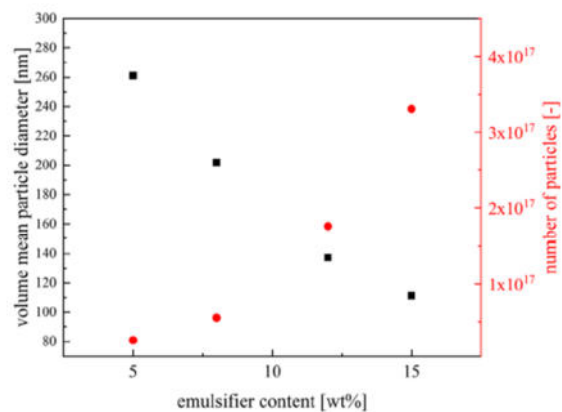


**Fig. 4** Volume mean particle diameters and the calculated number of particles against the emulsifier content

The form and factors of these terms were obtained from 56 independent experiments (Fig. 3). For the determination of the conversion term, the fouling masses (after 120 min  $m_{\text{fouling},t=120\text{min}}$ ) of the conversion-dependent process parameters are plotted against the conversion  $X$  of the reactions. The term was determined by linear fitting (Fig. 5).

In regard that only factors that influence the conversion of the reaction are changed, the fouling mass can be predicted as a function of the planned stationary conversion. Since the conversion depends on several factors the conversion term in Eq. (3) must be refined with respect to the individual conversion influences. For this purpose, the changes in the reaction conversion were determined in dependence of temperature, initiator content and emulsifier content. In order to size the influencing factors, the difference in conversion for the investigated recipe range was formed and the factors were ranked accordingly. The temperature had the strongest influence with a difference of 58% change in conversion, while emulsifier and initiator content had differences of approx. 40% change in conversion. Since the temperature has the strongest influence on the conversion, the temperature influence was determined first (Fig. 6) and the other parameters were then inserted as correction terms.

$$m_{\text{fouling},t=120\text{min}}(X_{t=3\bar{\tau}}) = 326(\pm 32.3) \frac{\text{mg}}{\text{g}}(X_{t=3\bar{\tau}}) - 29.6(\pm 20.6) \frac{\text{mg}}{\text{g}} \quad (3)$$

The temperature conversion term where best described by an Arrhenius-type exponential function (Eq. 4) which relates to the Arrhenius-theory [40] that the reaction rate can be described by an exponential function. If temperature  $T$  is the only change between the experiments is that the conversion  $X(T)$ , which results from the reaction rate

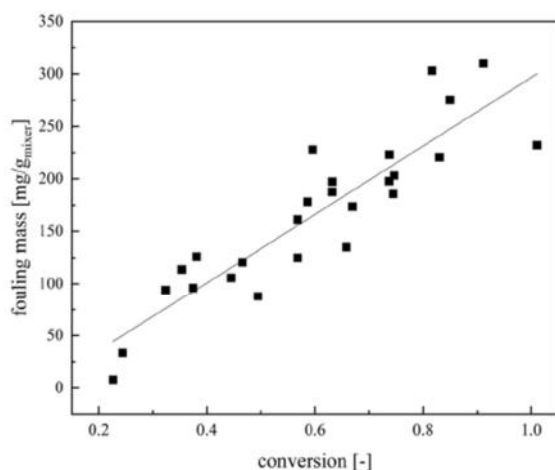


Fig. 5 Fouling mass independence of the conversion with a linear fit ( $R^2=0.898$ )

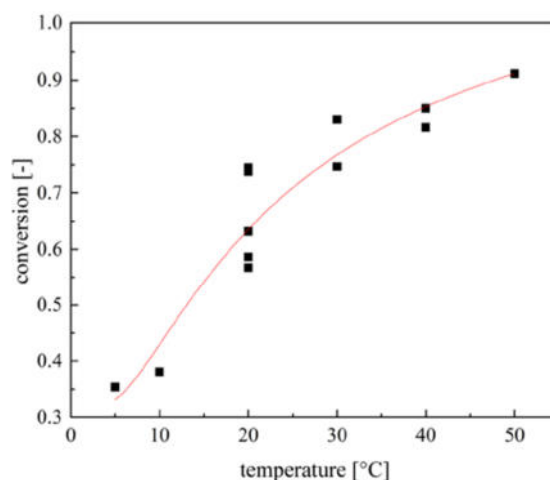


Fig. 6 Plotting conversion after 3 residence times against temperature to determine the temperature conversion term for the prediction model

could be described temperature-dependently by an Arrhenius-type function.

$$X(T)_{t=3\bar{\tau}} = A \cdot e^{-\frac{E_A}{RT}} + B$$

$$X(T)_{t=3\bar{\tau}} = 0.902(\pm 0.118) \cdot e^{-\frac{173.64+49.2K}{8.31407-273.15K}} + 0.318(\pm 0.073) \quad (4)$$

For the next step, the influence of the amount of emulsifier on the reaction conversion was plotted and then integrated into the conversion term. Regarding to Koltzenburg et al. [39] or Elias [41] the reaction rate of an emulsion polymerisation depends on the number of latices per volume [L], the monomer concentration [M], the mean number of radicals per micelle ( $\bar{n}$ ), the rate coefficient ( $k_p$ ) and the Avogadro number ( $N_A$ ) (Eq. 5).

$$-\frac{d[M]}{dt} = \bar{n} \cdot k_p \cdot [M] \cdot \frac{[L]}{N_A} \quad (5)$$

Moreover Friis and Nyhagen [42] reported an experimental correlation between the rate of polymerisation and the emulsifier content  $w_E$  to the power of 0.12 for emulsion polymerisation of vinyl acetate. This finding agrees very well with the conversion dependency in this research. Due to that the description of the conversion a function, based on this equation was chosen (Eq. 6), which considers the experimental data in literature (Fig. 7) [42].

The correlation (Eq. 6) was obtained from the experimental data.

$$X(w_E)_{t=3\bar{\tau}} = A \cdot (w_E + B)^{0.12} + C$$

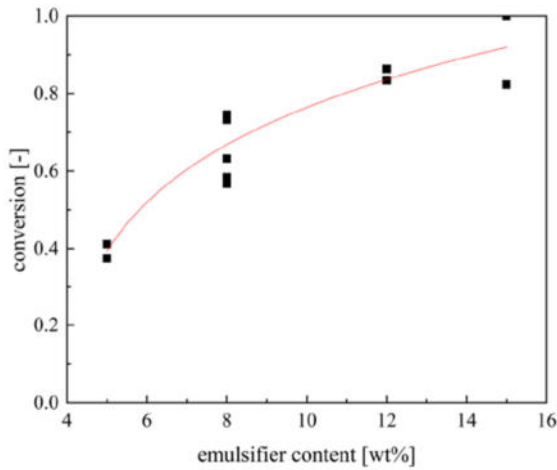


Fig. 7 Plotting conversion after 3 residence times against emulsifier content to determine the emulsifier conversion term for the prediction model

$$X(w_E)_{t=3\bar{\tau}} = 1.71(\pm 0.34) \cdot \left(\frac{w_E}{1wt\%} - 3.73(\pm 0.69)\right)^{0.12} - 1.37(\pm 0.45) \tag{6}$$

The initiator content was identified as a factor influencing the fouling mass. While the reaction rate is influenced by the initiator content, the initiator determines the conversion. Experimental investigations of the emulsion polymerisation of vinyl acetate by Friis and Nyhagen [42], Chang et al. [43] and Dunn and Taylor [44] are reporting correlations to the power of 0.5 to 0.6 for the reaction rate dependency of the initiator content. Besides the reaction rate the initiator content influences the ionic strength of the aqueous phase as the concentration of ions  $c_{ion}$  is increased so there might be effects that a higher ionic strength causes more fouling. This effect can't be denied but the concentration of ionic species in the aqueous phase is only changed by the ammonium iron(III) sulphate the change in ionic concentration is below 0.201 mmol/L (Eq. 7) and should be neglectable.

$$c_{ion} = \sum \frac{w_i}{M_i}$$

$$\Delta c_{ion} = \frac{w_{(NH_4)Fe(SO_4)_2,max} - w_{(NH_4)Fe(SO_4)_2,min}}{M_{(NH_4)Fe(SO_4)_2}}$$

$$= \frac{(0.102 - 0.005)g/L}{482.2g/mol} = 0.201 \text{ mmol/L} \tag{7}$$

The initiator content was plotted against the reaction conversion to determine the correlation (Fig. 8).

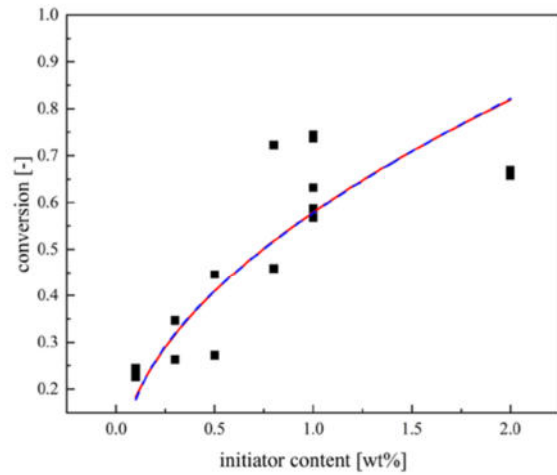


Fig. 8 Conversion after 3 residence times against initial initiator content to determine the initiator conversion term for the predictive model. Fits are showing a square root correlation (red) and a correlation to the power of 0.56 reported by Friis

Figure 8 shows a square root function correlation (Eq. 8) and a correlation to the power of 0.56 for the initiator dependence, which are both agreeing well with the kinetics of free radical polymerisation and the experimental investigations [42–44]. For this model the square root function was chosen [39].

$$X(w_I)_{t=3\bar{\tau}} = \sqrt{\frac{0.335w_I}{1wt\%}} \tag{8}$$

Temperature, initiator content, emulsifier content and the monomer ratio describe the fouling well when only one factor at time is changed. In order to improve the prediction flexibility, the influencing factors have to be combined in on prediction equation. Since the largest influencing factor was the temperature term, it was used at a starting point. The influences of the initiator and emulsifier content were included as correction terms. The reaction parameters  $T = 20 \text{ }^\circ\text{C}$ ,  $w_I = 1 \text{ wt\%}$ ,  $w_E = 8 \text{ wt\%}$  were used as fundamental recipe and as for the emulsifier and initiator content the relative change in conversion to this standard point was introduced in the complete conversion term (Eq. 9).

$$X(T, w_I, w_E)_{t=3\bar{\tau}} = X(T) \cdot \frac{X_{is}(w_I)}{X_{ref}(w_{I,ref}=1wt\%)} \cdot \frac{X_{ie}(w_E)}{X_{ref}(w_{E,ref}=8wt\%)} \tag{9}$$

After combining Eqs. (5), (6) and (7) with Eq. (8) the following equation is obtained (Eq. 10).

$$X(T, w_I, w_E)_{t=3\bar{\tau}} = \left(0.902 \cdot e^{-\frac{173.6}{8.3147T}} + 0.318\right) \cdot \sqrt{\frac{0.335w_I}{1wt\%}}$$

$$\left( \frac{\sqrt{0.335w_I}}{\sqrt{0.335w_{I,ref=1wt\%}}} \right) \cdot \left( \frac{1.71 \cdot (w_E - 3.73)^{0.12} - 1.37}{1.71 \cdot (w_{E,ref=8wt\%} - 3.73)^{0.12} - 1.37} \right) \quad (10)$$

By inserting the constants and summing up the coefficients, the following Eq. (11) is obtained.

$$X(T, w_I, w_E)_{t=37} = \left( 0.902 \cdot e^{-\frac{173.6}{8.314T}} + 0.318 \right) \cdot \left( \sqrt{w_I} \right) \cdot \left( \frac{1.71 \cdot (w_E - 3.73)^{0.12} - 1.37}{0.665} \right) \quad (11)$$

With Eq. (11) the conversion of the whole reaction could be estimated and the conversion-related fouling masses  $m_{\text{fouling}}$  could be described by combining with Eqs. (2) and (12).

$$m_{\text{fouling},t=120\text{min}}(T, w_I, w_E) = 326 \frac{\text{mg}}{\text{g}} \cdot \left( 0.902 \cdot e^{-\frac{173.6}{8.314T}} + 0.318 \right) \cdot \left( \sqrt{w_I} \right) \cdot \left( \frac{1.71 \cdot (w_E - 3.73)^{0.12} - 1.37}{0.665} \right) - 29.6 \frac{\text{mg}}{\text{g}} \quad (12)$$

Starting with Eq. (12) the coefficients were adjusted by a multivariate approach fitting all bold parameters of Eq. (12) in one step. The multivariate fitting approach agrees well to the previous described model based on single-factor evaluations as the multivariate equation shows (Eq. 13).

$$m_{\text{fouling},t=120\text{min}}(T, w_I, w_E) = 326 \frac{\text{mg}}{\text{g}} \cdot \left( 0.902 \cdot e^{-\frac{173.6}{8.314T}} + 0.841 \right) \cdot \left( \sqrt{w_I} \right) \cdot \left( \frac{1.70 \cdot (w_E - (-0.102))^{0.12} - 1.73}{0.665} \right) - 29.6 \frac{\text{mg}}{\text{g}} \quad (13)$$

Regarding to Eq. (13) the multivariate fitting approach and the single-factor evaluation model agree well so both equations could be used for the description. For the following calculations the multivariate adjusted equation was used.

In addition, the influence of the comonomer composition  $x_{\text{VAc}}$  on the fouling mass must be addressed. With increasing proportion of vinyl acetate in the polymer the fouling mass increases and can be described by a linear fit (Fig. 9) Eq. (14).

$$m_{\text{fouling},t=120\text{min}}(x_{\text{VAc}}) = 486.35 \frac{\text{mg}}{\text{g}} x_{\text{VAc}} - 271.425 \frac{\text{mg}}{\text{g}} \quad (14)$$

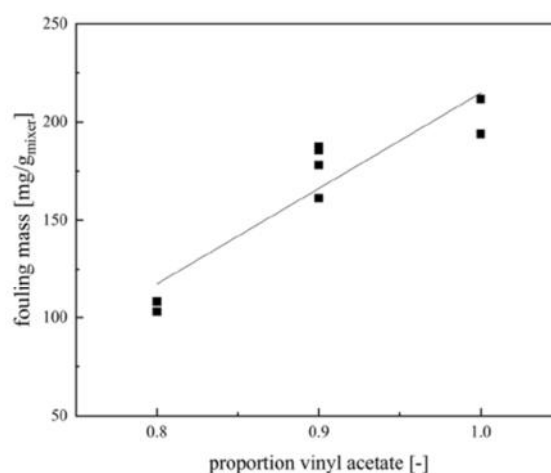


Fig. 9 Plotting of the fouling mass at  $t=120$  min against the proportion of vinyl acetate to determine the monomer composition term for the prediction model

In order to improve Eq. (2) the conversion term and the monomer composition term must be combined. For that reason, the comonomer term was transformed as a change from the standard formulation with  $x_{\text{VAc}}=0.9$  (Eq. 15) to describe the additional fouling expectations due to the changed comonomer ratio.

$$\Delta m_{\text{fouling}}(x_{\text{VAc}}) = 486.35 \frac{\text{mg}}{\text{g}} x_{\text{VAc}} - 437.625 \frac{\text{mg}}{\text{g}} \quad (15)$$

Consequently, Eq. (16) results for the entire substance system after combining all terms.

$$m_{\text{fouling},t=120\text{min}}(X_{t=37}, x_{\text{VAc}}) = \left( 326 \frac{\text{mg}}{\text{g}} (X_{t=37}) - 29.6 \frac{\text{mg}}{\text{g}} \right) + \left( 486.35 \frac{\text{mg}}{\text{g}} x_{\text{VAc}} - 437.625 \frac{\text{mg}}{\text{g}} \right) \quad (16)$$

If the explicit expression for conversion is introduced into Eq. (14) the target-independent model equation (Eq. 17) is obtained.

$$m_{\text{fouling},t=120\text{min}}(T, w_I, w_E, x_{\text{VAc}}) = 326 \frac{\text{mg}}{\text{g}} \cdot \left( 0.902 \cdot e^{-\frac{173.6}{8.314T}} + 0.841 \right) \cdot \left( \sqrt{w_I} \right) \cdot \left( \frac{1.70 \cdot (w_E + 0.102)^{0.12} - 1.73}{0.665} \right) - 29.6 \frac{\text{mg}}{\text{g}} + 486.4 \frac{\text{mg}}{\text{g}} x_{\text{VAc}} - 467.2 \frac{\text{mg}}{\text{g}} \quad (17)$$

The accuracy of the fouling prediction was determined from the scatter of the replication tests. For this purpose,

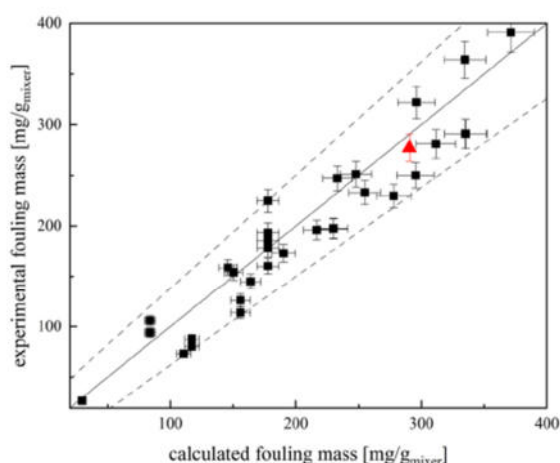


**Fig. 10** Experimentally measured fouling masses at  $t=120$  min against the model-based calculated fouling masses to validate the model. The y-error bars describe the measurement errors during the experiment, while the x-error bars indicate the intrinsic uncertainty range of the model. The solid line indicates the expected value, the dashed lines the uncertainty range of 12% given by deviation of reproduction experiments. As an example, for the red point the calculation of fouling masses is given in the supplementary information

seven tests were carried out under conditions that were as identical as possible and the results were compared. From these replications, the statistical component of the fouling can be estimated, as fouling processes always have a statistical range of variation. This results in an average scatter of the results of 12%, and therefore the prediction of the model also contains an uncertainty of 12%.

### Comparison of calculated fouling masses with experimental data

In order to validate the model, fouling masses were determined by calculation using the model equation and then compared with experimental measured data (Fig. 10).

The model predicts the fouling masses well within the uncertainties of 12% derived from the standard deviation of reproduction experiments. The calculated values and experimental fouling masses agree as well with the model. Moreover, the conversion calculated via the conversion term was compared with the measured conversion. (Fig. 11).

The description of the conversion by means of the model term corresponds approximately well with an uncertainty of  $\pm 12\%$  derived from the standard deviation of reproduction experiments based on the conversion value in the model.

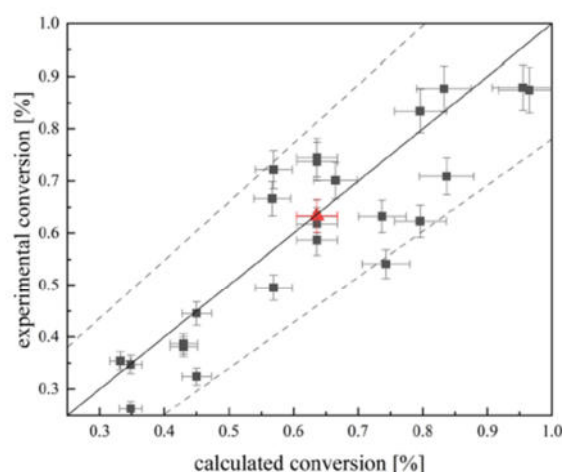


**Fig. 11** Experimentally measured conversions at  $t=120$  min against the model-based calculated conversions for specified process parameter set to validate the model. The y-error bars describe the measurement errors during the conversion determination, while the x-error bars indicate the intrinsic uncertainty range of the conversion term. As an example, the calculation of conversion for the red data point is given in the supplementary information

### Summary

A strategy for fouling quantification during continuous emulsion copolymerisation of vinyl acetate was established. For this strategy it is in the first step necessary to evaluate the influences of process and formulation parameters on the formation of deposits. Conversion and monomer composition were found to be relevant influencing factors. The conversion is mainly influenced by reaction temperature as well as initiator and emulsifier content. In the second step an experiment-based model was developed with which the expected fouling mass for emulsion polymerisations with similar recipes could be predicted in dependency of the influencing process and formulation parameters. Each influencing factor is described by a single term while process and formulation parameters which influence the same factor are connected via correction terms. For the investigated system the model can predict fouling masses with an accuracy of 12%. The presented strategy for developing a fouling prediction model could be used for different recipes as well so that a model can be obtained within short time.

**Supplementary Information** The online version contains supplementary material available at <https://doi.org/10.1007/s10965-023-03588-8>.

**Author contribution** All authors conceived the experiments, Sören Rust performed the experiments and analysed the data. The first draft of the manuscript was written by Sören Rust and all authors commented on previous versions of the manuscript. All authors read and approved the final manuscript.



**Funding** Open Access funding enabled and organized by Projekt DEAL. The work has been funded by the German Federal Ministry for Economic Affairs and Climate Action as part of the ENPRO Initiative (KoPPonA 2.0, FKZ: 03EN2004M).

**Data availability** All raw data for the modelling process are uploaded in an word document in the Attachment area and can be published in the supplementary information as well. For further data requests the authors will be available.

## Declarations

**Conflict of interest** The authors declare that they have no conflicts of interest for the submitted work.

**Open Access** This article is licensed under a Creative Commons Attribution 4.0 International License, which permits use, sharing, adaptation, distribution and reproduction in any medium or format, as long as you give appropriate credit to the original author(s) and the source, provide a link to the Creative Commons licence, and indicate if changes were made. The images or other third party material in this article are included in the article's Creative Commons licence, unless indicated otherwise in a credit line to the material. If material is not included in the article's Creative Commons licence and your intended use is not permitted by statutory regulation or exceeds the permitted use, you will need to obtain permission directly from the copyright holder. To view a copy of this licence, visit <http://creativecommons.org/licenses/by/4.0/>.

## References

- Lynch J, Sutoris HF, Zubiller J, Aumüller A (1998) Verfahren Zur Polymerisation Vinylischer Monomere. DE 196(48):811A1
- Apecetche MA, Xinlai B, Cann KJ (1996) Process for reducing polymer build-up in recycle lines and heat exchangers during polymerizations employing butadiene, isoprene, and/or styrene. US 005733988A
- Arhancet G (1998) Compositions and methods for inhibiting fouling of vinyl monomers. WO 98/47593 29
- Reid DK (1992) Antioxidant compositions and methods using p-phenylenediamine compounds and organic acid compounds. US 005128022A
- Weber M, Lattner J, McCullough L, Dickey R, Brown S, Loezos P (2010) Olefin oligomerization reaction processes exhibiting reduced fouling. WO 2010/110801 A1
- Hocking P, Sibtain F, Cheluguet E (2012) Reducing fouling in heat exchangers. CA 2797489 A1
- Tong DY (2015) Reducing polymer fouling and agglomeration in acrylate/methacrylate processes. US 2016/0102189 A1
- Cohen L (1979) Polymerization reactors coated with polymer-inhibitor complexes. US4256864
- Weimer DR, Freshour K (1979) Prevention of PVC polymer buildup in polymerization reactors using oxalyl bis(benzylidenehydrazide) and alumina. US 4145496
- Wempe L, Bauman BD (1983) Method for reducing wall fouling in vinyl chloride polymerization. US 4420591
- Cohen L (1987) Polymerization reactor coatings and use thereof. US 4696983
- Fitzwater SJ, McFadden DM (2001) Continuous process for preparing polymers. EP 1(136):505 A1
- McFadden DM, Wu RS-H (2000) The reduction of polymer fouling on reactor surfaces in a continuous process for preparing polymers. EP 1(024):149A2
- Lowell JS, Hendrickson GG, Price RJ (2018) Elimination of polymer fouling in fluidized bed gas-phase fines recovery reactors. US 2018/0105613 A1
- Lowell JS, Dooley KA, Li R, Aruho DK (2022) Systems and methods for mitigating polymer fouling. WO 2022/173784 A1
- McDonald M, Lawrence D, Williams D (1993) Polymerization reactor. WO 93/03075
- Carvalho ACSM, Chicoma DL, Sayer C, Giudici R (2010) Development of a continuous emulsion copolymerization process in a tubular reactor. Ind Eng Chem Res 49(21):10262–10273. <https://doi.org/10.1021/ie100422v>
- Kelland MA (2020) Additives for Kinetic Hydrate Inhibitor Formulations to Avoid Polymer Fouling at High Injection Temperatures: Part 1. A Review of Possible Methods. Energy Fuels 34(3):2643–2653. <https://doi.org/10.1021/acs.energyfuels.9b04040>
- Dorton MR, Gardner Sr GL (2003) Process for cleaning polymeric fouling from equipment. US 20030073595A1
- Haruyama H (2017) Solution conveying and cooling device. EP 3:203–177A1
- Saikhwan P, Chew JYM, Paterson WR, Wilson DI (2007) Swelling and Its Suppression in the Cleaning of Polymer Fouling Layers. Ind Eng Chem Res 46(14):4846–4855. <https://doi.org/10.1021/ie0615943>
- AlShehri A, Cunningham V, Amer A, Xu W, Melibari F (2021) Heat exchanger fouling determination using thermography combined with machine learning methods. WO 2021/026462 A1
- Schork FJ, Lu Fujun F (2009) Relative Rates of Branching in Emulsion and Miniemulsion Polymerization. Macromol React Eng 3(9):539–542. <https://doi.org/10.1002/mren.200900036>
- Schork FJ (2021) Monomer Transport in Emulsion Polymerization II: Copolymerization. Macromol React Eng 15(6):10–13. <https://doi.org/10.1002/mren.202100022>
- Schork FJ (2022) Monomer Transport in Emulsion Polymerization III Terpolymerization and Starved-Feed Polymerization. Macromol React Eng 16(4):2–5. <https://doi.org/10.1002/mren.202200010>
- Schork FJ (2020) Heinz Gerrens Revisited: A New Look at the Impact of Reactor Type on Polymer Chain Morphology. Macromol React Eng 14(3):1–10. <https://doi.org/10.1002/mren.201900055>
- Schork FJ (2021) Monomer Concentration in Polymer Particles in Emulsion Polymerization. Macromol React Eng 15(3):1–2. <https://doi.org/10.1002/mren.202100003>
- Krishnan S, Klein A, El-aasser MS, Sudol ED (2004) Effects of Agitation on Oxygen Inhibition, Particle Nucleation, Reaction Rates, and Molecular Weights in Emulsion Polymerization of n-Butyl Methacrylate. Ind Eng Chem Res 43:6331–6342. <https://doi.org/10.1021/ie049796r>
- Deglmann P, Hellmund M, Hungenberg KD, Nieken U, Schwede C, Zander C (2019) Side Reactions in Aqueous Phase Polymerization of N-Vinyl-Pyrrolidone as Possible Source for Fouling. Macromol React Eng 13(5):1–13. <https://doi.org/10.1002/mren.201900021>
- Neßlinger V, Welzel S, Rieker F, Meinderink D, Nieken U, Grundmeier G (2022) Thin Organic-Inorganic Anti-Fouling Hybrid-Films for Microreactor Components. Macromol React Eng 2200043:1–16. <https://doi.org/10.1002/mren.202200043>
- Ekowati Y, Msuya M, Salinas Rodriguez SG, Veenendaal G, Schippers JC, Kennedy MD (2014) Synthetic Organic Polymer Fouling Inmunicipalwastewater Reuse Reverse Osmosis. J Water Reuse Desalin 4(3):125–136. <https://doi.org/10.2166/wrd.2014.046>
- Hohlen A, Augustin W, Scholl S (2020) Quantification of Polymer Fouling on Heat Transfer Surfaces During Synthesis.

- Macromol React Eng 14(1). <https://doi.org/10.1002/mren.201900035>.
33. Hohlen A, Augustin W, Scholl S (2020) Investigation of Polymer Depositions During the Synthesis in a Heat Exchanger. *Chem-Ing-Tech* 92(5):629–634. <https://doi.org/10.1002/cite.201900130>
  34. Gottschalk N, Kuschnerow JC, Föste H, Augustin W, Scholl S (2015) Experimental Investigation on Fouling of a Polymer Dispersion on Modified Surfaces. *Chem-Ing-Tech* 87(5):600–608. <https://doi.org/10.1002/cite.201400126>
  35. Böttcher A, Petri J, Langhoff A, Scholl S, Augustin W, Hohlen A, Johannsmann D (2022) Fouling Pathways in Emulsion Polymerization Differentiated with a Quartz Crystal Microbalance (QCM) Integrated into the Reactor Wall. *Macromol React Eng* 16(2):1–8. <https://doi.org/10.1002/mren.202100045>
  36. Madani M (2017) Belagsbildung in Chemischen Reaktoren Unter Berücksichtigung von Oberflächenaspekten
  37. Bernstein C (2017) Methoden Zur Untersuchung Der Belagsbildung in Chemischen Reaktoren (Dissertation)
  38. Hertwig K, Martens L (2010) 6 Strömungstechnisch Ideale Reaktoren Für Homogene Reaktionen. In *Chemische Verfahrenstechnik*. 79–183. <https://doi.org/10.1524/9783486598698.79>.
  39. Klotzenburg S, Maskos M, Nuyen O (2014) *Polymere*; Springer Spektrum
  40. Arrhenius S (1887) Über Die Reaktionsgeschwindigkeit Bei Der Inversion von Rohrzucker Durch Säuren. *Z für Phys Chem* 4U(1):226–248
  41. Elias H-G (2002) Technische Synthesen. In *Makromoleküle Set*; John Wiley & Sons, Ltd. pp. 82–142. <https://doi.org/10.1002/9783527626557.ch4b>.
  42. Friis N, Nyhagen L (1973) A Kinetic Study of the Emulsion Polymerization of Vinyl Acetate. *J Appl Polym Sci* 17(8):2311–2327. <https://doi.org/10.1002/app.1973.070170802>
  43. Chang KHS, Litt MH, Nomura M (1981) The Reinvestigation of Vinyl Acetate Emulsion Polymerization (I) -The Rate of Polymerization. *Appl Sci Publ Ltd I*:89–136. [https://doi.org/10.1007/978-94-009-8114-0\\_6](https://doi.org/10.1007/978-94-009-8114-0_6).
  44. Dunn AS, Taylor PA (1965) The Polymerization of Vinyl Acetate in Aqueous Solution Initiated by Potassium Persulphate at 60 °C. *Die Makromol Chemie* 83(1):207–219

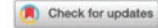
**Publisher's Note** Springer Nature remains neutral with regard to jurisdictional claims in published maps and institutional affiliations.

### 5.3 Ultrasonic and conversion-based inline fouling measurements for continuous emulsion copolymerisation of vinyl acetate

Sören Rust, Marco Osenberg, Thomas Musch, Werner Pauer

#### **Synopsis**

Inline analytics for relevant process parameters are advantageous for continuously operated processes as they reduce the time for detecting deviations in process or product properties. No time-consuming offline analysis of taken samples is needed and changes are detected immediately as they occur. Fouling is one of the important process parameters as it influences process safety and product properties at once. There are different possibilities of detecting fouling during reaction but only few are established. In this work two more sensor concepts are presented, and their suitability and limitations are discussed. Firstly, a detection based on the conversion is discussed as conversion is often monitored for process control and no further equipment is needed. Due to fouling the reaction volume is decreasing and thus the conversion of the reaction should decrease as well. A requirement for this method is that the residence time in the reactor and the reaction time are similar so that a decreased residence time caused by fouling leads to a decreased conversion. This is mostly given as reactors are optimised for the reaction and higher residence times than necessary decrease efficiency of the process. This method is suitable for detecting strong fouling, but initial deposit formation cannot be detected as the decrease in volume is not strong enough in the beginning. The other method presented is an ultrasonic-based technology which uses the difference in sound velocity between fouling and dispersion. The changes in average sound velocity (ASV) can be detected in a measurement cell so fouling layers can be detected. This method is more sensitive and can be installed scale-independent as inline or atline measurement in a bypass. Both methods agree well with gravimetric reference within a deviation below 10 %. Two suitable sensor concepts were presented and their feasibility was shown.<sup>[84,85]</sup>



OPEN

# Ultrasonic and conversion-based inline fouling measurements for continuous emulsion copolymerisation of vinyl acetate in a tubular reactor

Sören Rust<sup>1</sup>, Marco Osenberg<sup>2</sup>, Thomas Musch<sup>2</sup> & Werner Pauer<sup>1✉</sup>

One of the serious challenges for the implementation of continuous emulsion polymerisation is their significant fouling. The elucidation of time-dependent fouling processes and the development of inline analysis methods for fouling mass quantification are crucial to making progress in this area. Inline-sensor concepts based on ultrasonic measurements as well as residence time and conversion analysis were investigated regarding their suitability for the detection of time-dependent fouling formation and compared with gravimetric results in order to validate their precision. Both a set-up using a turnover analysis for determination of losses in reaction volume by fouling and an ultrasound-based measurement system detecting deposit-caused changes by evaluating the average sound velocity could be used as suitable sensor concepts. The accuracies of both sensors are below 10% deviation to fouling references.

**Keywords** Emulsion polymerization, Continuous emulsion polymerisation, Tubular reactor, Vinyl acetate, Fouling, Inline measurements

Fouling is a major challenge for various chemical processes on industrial scale. As cleaning of large-scale plants is time and cost intensive, it is advantageous to gain knowledge about possible occurring fouling during the reaction and how to avoid it to obtain an efficient process. The full understanding of fouling mechanisms is challenging and needs a lot of further research. Some empirical fouling prevention strategies were established and patented. Additives are used to reduce or avoid fouling<sup>1–7</sup>. For example polyoxyalkenes could be used for fouling reduction in solution polymerisation of ethylene co- and homopolymers<sup>6</sup> or alkyl and aryl phthalates prevent fouling for the polymerisation of acrylates, methacrylate or acrylic acid<sup>7</sup>. In different applications coatings of the equipment were described as solution for fouling reduction<sup>8–11</sup>. Monolayer coatings with polyvinyl alcohol and the disodium salt of bisphenol A are advantageous for the polymerisation of vinyl halides or vinylidene monomers<sup>8</sup> or water dispersion coatings of alumina oxalyl bis(benzylidene)hydrazide<sup>9</sup> respectively aqueous selenous acid<sup>10</sup> can be used for vinyl chloride polymerisation. Besides chemical concepts for fouling reduction there are mechanical concepts as well which are using special reactor concepts<sup>12–17</sup>. McFadden et al.<sup>13</sup> reduced fouling during continuous polymerization by highly precise control of monomer streams and process parameters. Lowell et al.<sup>14</sup> optimized the geometry of the reactor to reduce fouling for gas phase polymerisation. Carvalho et al.<sup>17</sup> reported that an oscillatory flow reactor causes a fouling free continuous emulsion polymerization at lab scale. Moreover, for some specialized applications the addition of comonomers to the recipe is described like for Kinetic Hydrate Inhibitor Formulations<sup>18</sup>. Another approach instead of preventing fouling is the optimization of cleaning concepts, so the efficiency could be increased by efficient cleaning. Olefinic polymer deposits for example can be efficiently cleaned by circulating high boiling aromatic hydrocarbon solvents in the reactor and afterwards recovering them by flash separation<sup>19</sup>. Haruyama<sup>20</sup> developed a mechanical cleaning strategy of polymeric fouling by polymerizing in the gap between two tempered tubes built into each other, which can be tempered independently of each other for cleaning, so that the reaction gap is closed by material expansion or contraction and removes polymer residues<sup>20</sup>.

<sup>1</sup>Institute for Technical and Macromolecular Chemistry, University of Hamburg, Bundesstraße 45, 20146 Hamburg, Germany. <sup>2</sup>Chair of Electronic Circuits, Ruhr-University Bochum, Universitätsstraße 150, 44801 Bochum, Germany. ✉email: werner.pauer@chemie.uni-hamburg.de

Saikhwan et al.<sup>21</sup> reported temperature and pH conditions where cleaning of non-cross-linked acrylate-styrene copolymers is easily done by taking advantage of the swelling behavior.

Regarding fouling kinetics or mechanisms there are less publications. For wastewater treatment there are precise mechanistic studies by Ekowati et al.<sup>22</sup> who reported that cationic polymers cause fouling on reverse osmosis membranes. It was possible to predict the time dependent fouling masses and distinguish between reversible fouling that could be removed by chemical cleaning and irreversible fouling that influenced the efficiency of the membranes permanently.<sup>22</sup> Regarding homogeneous polymerisation reactions Deglmann et al.<sup>23</sup> reported the fouling processes in the free radical polymerisation of N-vinyl pyrrolidone are caused by radical transfer reactions leading to terminal double bonds which are crosslinked afterwards. This crosslinking increases the molecular weight significantly and leads to deposit formation.<sup>23</sup> Neßlinger et al.<sup>24</sup> performed solvent polymerisation of N-vinyl pyrrolidone and evaluated the fouling masses. They investigated the influences of coated reactor surfaces on fouling masses and their suitability for fouling prevention.<sup>24</sup>

The kinetics of emulsion polymerization are described in multiple publications by different research groups, for example Smith and Ewart<sup>25</sup>, Chern<sup>26</sup>, Gilbert<sup>27</sup>, Schork and many others<sup>27–35</sup>. The state of the art regarding modelling development of particle size distributions in emulsion polymerisation and discussing coagulation is well described by Vale et al.<sup>36</sup>. Especially continuous emulsion polymerisation in tubular reactors and approaches for modelling them are discussed here<sup>36</sup>. The fouling behaviour during emulsion polymerisation of vinyl acetate is described in literature as well. Different publications are discussing some parts of this topic<sup>37–39</sup>. Carvalho et al.<sup>17</sup> performed continuous emulsion copolymerisation of vinyl acetate and *n*-butyl acrylate in a tubular reactor and found that fouling caused problems which could be solved by oscillating pulsed flow control and internal sieve plates in the reactor. The oscillating flow results in short periods of turbulent flow control and prevents fouling by high shear rates while the internal sieve plates improve radial mixing and reduce side reactions<sup>17</sup>. Emulsion copolymerisation of vinyl acetate and vinyl esters were investigated regarding to their fouling on heated or cooled surfaces and compared with commercial polyvinyl acetate dispersions. The influences of temperature and surface modifications on fouling masses show that higher temperatures lead to higher fouling masses. For surface modifications no general trend could be observed as it is highly dependent on the other process parameters<sup>37–39</sup>. Hohlen et al.<sup>38</sup> compared fouling of reactive emulsion polymerisation systems with fouling of non-reactive polymer dispersions. Reactive polymerisation systems cause much higher fouling masses than non-reactive so polymerisation fouling is the major part. Moreover, the morphology of the fouling is given by the pathway of formation so the dominant fouling process can be concluded optically from the fouling morphology<sup>38</sup>.

On the field of fouling quantification technologies there are different approaches described<sup>40–44</sup>. For example Böttcher et al.<sup>40</sup> reported an inline measurement technique for monitoring fouling masses during emulsion copolymerisation of *n*-butyl acrylate and methyl methacrylate using a quartz crystal microbalance with dissipation monitoring. They reported two different pathways for heat-transfer fouling, the first one leading to thin fouling films with no further growth after formation and the other resulting in continuously growing thick fouling<sup>40</sup>. In fouling intense polymerisation processes it is commonly practiced to detect the changes in the reactor weight<sup>41,42</sup>. At low fouling masses this method is not as precise as a quartz crystal microbalance but for stronger fouling a quartz crystal microbalance does not work robust enough so the weighting of the whole reactor or parts of them is more suitable. Osenberg et al.<sup>43,44</sup> proved in previous work the general suitability of ultrasonic fouling detection for polymerisation processes as the solvent polymerisation of polyurethanes<sup>43,44</sup>.

Concluding these publications there is much published work about fouling reduction or prevention but less literature which addresses scientific approaches to fouling processes. Most of the scientific publications are focussed on mechanistic influences or temperature effects so there are no publications addressing time-resolved fouling behaviour for the continuous emulsion polymerisation process of vinyl acetate copolymers. This work investigates the fouling behaviour of continuous emulsion polymerisations of vinyl acetate vinyl ester copolymers and develops and ultrasonic measurement approach as well as and conversion based method for inline fouling quantification.

## Exp. section

The experiments were carried out in a tubular lab reactor set-up of the type Fluitec ContiPlant LAB' with CSE-X static mixing elements (Fig. 1a). The half-shell reactor has a channel diameter of  $d = 12$  mm and filled with CSE-X static mixing elements a resulting volume of  $V = 45.5$  mL. Temperature control of reactor and ultrasonic measurement cell was achieved by a cryostat of the type Julabo FP50 tempering the double jacket to a constant inlet temperature, closed loop temperature controlled at the jacket inlet (Fig. 1b).

The experimental procedure and recipe were chosen similar as in previous work and are described detailed here for better understanding with the included differences for this task<sup>45</sup>. The dosing was achieved by three solenoid-driven diaphragm metering pumps ProMinent' Gamma. The monomers, vinyl acetate and vinyl neodecanoate (VeoVa10'), (ProMinent gamma/4-1, stroke volume 0.13 mL/stroke, dosing flow 0.05 g/s) and the emulsifier solution containing poly(vinyl alcohol), Ascorbic acid and ammonium iron(III)sulphate (ProMinent gamma/5, stroke volume 0.16 mL/stroke, dosing flow 0.15 g/s) were pre-emulsified in a cylindrical CSTR equipped with a magnetic stirrer ( $d = 25.4$  mm,  $V = 20$  mL,  $d_{\text{stirrer}} = 18$  mm, 600 rpm) and the initiator flow containing *tert*-butyl hydroperoxide (ProMinent gamma/4, stroke volume 0.03 mL/stroke, dosing flow 0.01 g/s) was added 55 mm upstream and centered to the reactor inlet via a capillary nozzle (inner diameter 1 mm) (Fig. 1c)<sup>45</sup>.

All chemicals were used without further purifying. Vinyl acetate, vinyl neodecanoate and Mowiol 4–88 (molecular weight ~ 31 kDa, Degree of hydrolysis 88%) were purchased in technical grade from Wacker Chemie AG, Burghausen. Ascorbic acid and ammonium iron(III) sulphate dodecahydrate were purchased in analysis grade from Sigma Aldrich. *tert*-Butyl hydroperoxide was purchased as an aqueous solution ( $c = 70\%$ (w/w)) from Sigma Aldrich<sup>45</sup>.

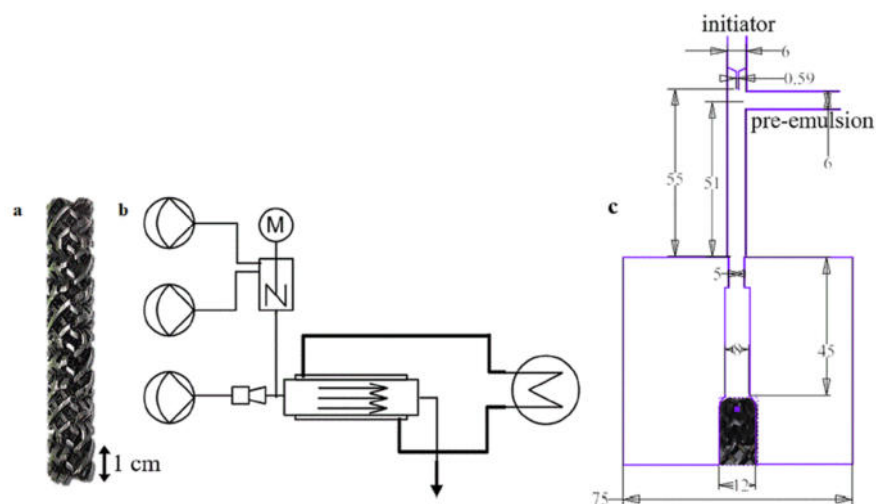


**Figure 1.** (a) Picture of the static mixers type CSE-X, (b) schematic structure of the reactor plant, (c) detailed plan of the initiator nozzle.

For the monomer feed a vinyl acetate-vinyl neodecanoate (VeoVa10<sup>®</sup>) comonomer stock system was used for emulsion polymerisation, with 10 wt% VeoVa10<sup>®</sup> based on total monomer content. Polymerisation were carried out with a monomer content of 23.8 wt%. Polyvinyl alcohol was used as an emulsifier in weight proportions of 8 wt% based on monomer. The initiation was carried out by a redox initiator system consisting of *tert*-butyl hydroperoxide, ascorbic acid and ammonium iron(III) sulphate dodecahydrate in a molar ratio of 1:1:0.03. The initiator was used in weight proportions of 1 wt% based on monomer<sup>45</sup>. The mean hydrodynamic residence time of the reactor is approximately four minutes which is comparable to the time for reaching full conversion. The runtime of the experiments was varied between 20 and 180 min.

Two ultrasonic measuring cells were developed by the chair of electronic circuits at the Ruhr-University Bochum. To favor fouling to settle in the measuring cell, the flow profile was designed in a way that allows for regions with small flow velocities, since previous work has shown that higher flow velocities reduce fouling<sup>44</sup>. The measurement cells were made of 1.4404 stainless steel. To couple the ultrasonic signals into the emulsion phase, a coupling path (Fig. 2, yellow part) made of polyetheretherketone (PEEK) is used, since the acoustic impedance (AI) of PEEK better matched with the AI of the emulsion than the AI of stainless steel. Thus, more energy can be coupled into the sensing element, resulting in a higher dynamic range. The measurement cells are cylindrical in shape, with different dimensions leading to different dwell times and dead volumes. The first measurement cell (Fig. 2a) has a height of  $h_c = 10$  mm and a radius of  $r_c = 15$  mm concluding to a cell volume

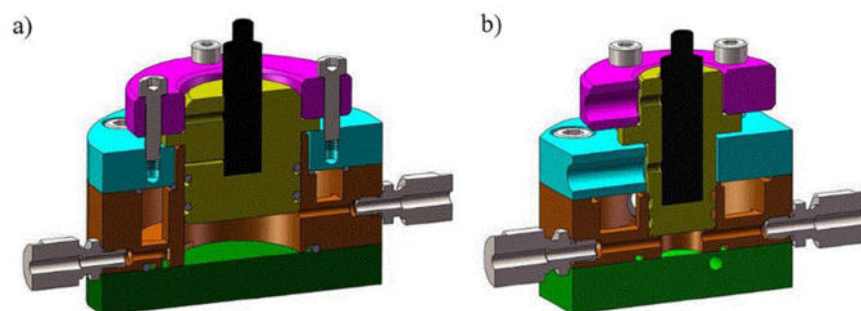


**Figure 2.** CAD models of the ultrasonic measurement cells, the coupling path (yellow) is made of PEEK, all other parts are made of stainless steel 1.4404, (a) measurement cell with large volume, (b) optimized measurement cell with smaller volume.

of  $V_c = 7.0$  mL with large, fouling intense dead zones. The second measurement cell (Fig. 2b) has an optimised geometry with less dead zones. The dimensions are a height of  $h_c = 7.5$  mm and a radius of  $r_c = 8$  mm concluding to a cell volume of  $V_c = 1.5$  mL. A cell with higher volume would be more sensitive to early stages of the deposit formation because of the low flow velocities but will not represent the situation in the reactor well. Concluding the second measurement cell with smaller volume was considered and detailed investigated. A sectional view of the computer aided design (CAD) models is shown in Fig. 2.

An ultrasonic transducer with a center frequency of  $f_{ct} = 4.8$  MHz (6 mm aperture diameter, 4.02 MHz bandwidth, Olympus Corp., USA, model V310-SM) was used for measurement because the emulsion causes high signal attenuation at higher frequencies. At the selected center frequency, still a best spatial resolution is ensured with sufficient signal-to-noise ratio. The ultrasonic transducer is excited with an experimental MOSFET output stage, this generates a pulse with a pulse length of  $t_{PA} = 100$  ns and a voltage of  $U_{PA} = 50$  V. To decouple the reflection signals from the excitation a passive decoupling is used. For protection of the amplifiers and analog filters, an analog voltage limiter is applied to limit the received signals to  $U_{Lim} = 0.7$  V, ensuring that the receiving circuitry is not damaged. The signals are filtered with a 6th order bandpass filter with a lower cutoff frequency of  $f_{cl} = 0.5$  MHz and an upper cutoff frequency of  $f_{cu} = 20$  MHz. To digitize the signals, an oscilloscope (Rohde & Schwarz GmbH, Germany, model RTO 1004) with a sampling frequency of  $f_{sp} = 500$  MSps is used. The measurement set-up is shown graphically as a block diagram (Fig. 3).

To enhance the signal to noise ratio, the mean value is formed from 25 individual measurements and a digital band pass filter is used to suppress any interference that is outside the useful frequency range. To determine reflection times and signal powers, the envelope of the time signal is evaluated. For this purpose, a Gaussian fit is performed with the Curve Fitting Toolbox of Matlab™ in the calculated in-coupling and out-coupling reflection time sections. The Gaussian fit provides a good representation of times and signal powers, since many measurement points are incorporated for the fit. From these data, the average sound velocity (ASV) of the phases in the measurement cell can now be evaluated over the coupling time  $t_1$  and the back-wall reflection time  $t_2$  (Eq. 1).

$$c_{ASV} = \frac{h_c}{t_1 - t_2} \quad (1)$$

All fouling masses are given as fouling masses referenced to the weight of the static mixers in the reactor where the fouling mainly occurs ( $\text{mg}_{\text{fouling}}/\text{g}_{\text{reactor}}$ ). Conversions  $X(t)$  were calculated as the weight ratio between formed polymer  $w_p$  and total initial monomer content  $w_M$  (Eq. 2). The polymer content was measured by microwave gravimetry of the product dispersions.

$$X(t) = \frac{w_p(t)}{w_M(t=0)} \quad (2)$$

For gel permeation chromatography (GPC) a set-up using tetrahydrofuran as eluent with a flow rate of 1 mL/min was used. The set-up contained in order of use a Knauer K-4002 2-channel Degasser, a FLOM Intelligent Pump AI-12-13 and a Knauer Smartline 3800 Autosampler with 20  $\mu\text{L}$  sample loop. As columns one PLgel 10  $\mu\text{m}$  Guard followed by two PLgel 10  $\mu\text{m}$  MIXED-B columns by Agilent Technologies were used. The detection was performed by a Schambeck SFD GmbH RI 2000 detector measuring refractive index. All measurements were calibrated with linear polystyrene standards of different molecular weights, so the obtained molecular weights are qualitative and not quantitative.

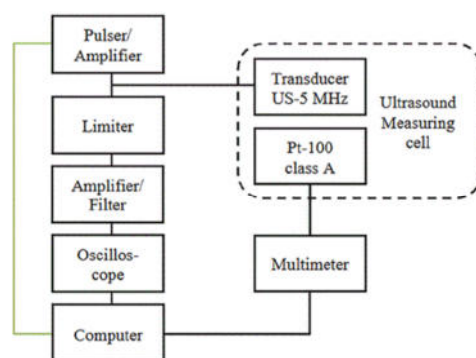


Figure 3. Block diagram of the ultrasonic measurement set-up.

## Results

For the development of inline-sensor concepts to monitor time-dependent fouling formation it is in the first step necessary to establish a robust and reproducible polymerisation which results in reproducible fouling masses. In the second step the time and space resolved fouling deposition can be quantified. In further experiments these data will be used to evaluate possible sensor concepts regarding their suitability and precision.

### Investigation of a suitable polymerisation

An emulsion copolymerisation of vinyl acetate and vinyl neodecanoate was chosen as test system for the fouling detection. The polymer properties of the products from reproduction experiments were investigated to validate the reproducibility of the reaction. For this purpose, the molecular weights of the emulsion polymers and the deposit of three different reactions under same conditions were determined by qualitative GPC and compared (Fig. 4). Moreover, the molecular weights of the emulsion polymers of two additional reactions from sensor testing were included.

Very similar molecular weights for all emulsion polymers as well as all deposits were obtained, with the molecular weight of the emulsion polymers always being lower than that in the fouling, so the polymerisation process is reproducible and the polymeric products are comparable.

The molecular weight of the emulsion polymer, the deposit and the deposit in the first part of the reactor were compared as well. The deposit in the first part of the reactor was investigated as the conversion there is lower and a broader molecular weight distribution is expected, if the deposits are caused by polymerisation fouling (Fig. 5).

The molecular weights of the emulsion polymers are significantly lower than those of the deposits (Fig. 5), indicating that the polymeric properties of the two phases do not match. In particular, the molecular weight distribution of the fouling at the reactor inlet is of interest, as it is much broader than the others. It ranges from very low molecular weights to the high molecular weights of the deposits. This indicates that polymerisation fouling is the dominant process, since at the reactor inlet at low radical concentrations significant monomers as well as oligomers remain in the deposit, i.e., polymerisation takes place in a film on the reactor wall and no sedimented particles are responsible for the fouling. The increased molecular weights in the deposits are presumably since the initiation takes place in the aqueous phase and therefore, due to the lower surface-to-volume ratio, fewer radicals enter the film on the reactor wall than the micelles, so that termination occurs later there.

The statistical deviation of fouling deposition was determined by replication tests. For this purpose, seven tests were carried out under conditions that were as identical as possible and the deviation was calculated. The statistical component results in an average deviation of 12% which indicates the range of scattering including measurement errors.

### Time and space resolved fouling deposition

First, the average fouling masses of the entire reactor were determined gravimetrically and their development over time was investigated. Since it is known that the temperature also exerts an influence on the fouling<sup>45</sup>, the influences of the temperature are investigated as well (Fig. 6). This data could be used later for calibrating the sensors.

The overall fouling in the reactor is linear, i.e. the formation of initial fouling neither inhibits the fouling as would be expected from a reduction in the surface energy, nor does the deposit formation increase due to the more uneven surface. The linear correlations of the time-dependent fouling exist for all investigated temperatures (Fig. 6). Only the slope of the linear function is different due to the changed temperature and describes the temperature dependence of the fouling. This indicates that nothing changes mechanically in the selected

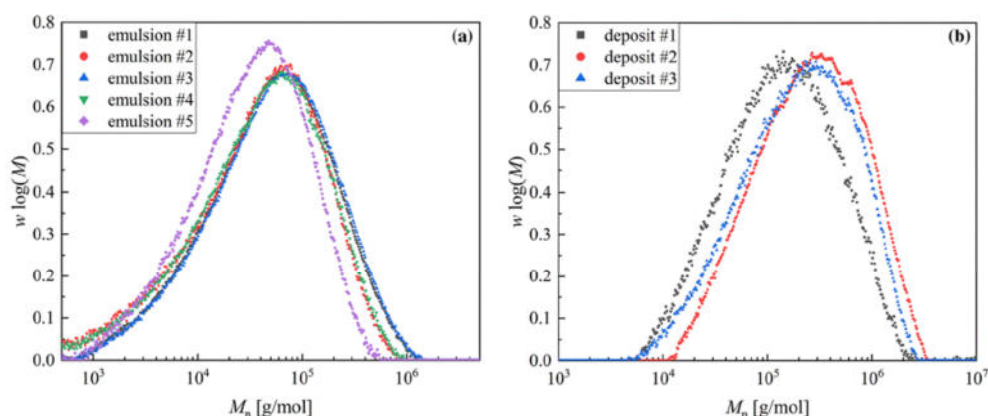


**Figure 4.** Plot of the qualitative molecular weight distribution of emulsion polymers from five different reproduction experiments (a) and deposits from three of this reproduction reactions (b) at same conditions at 20 °C to confirm reproducibility.



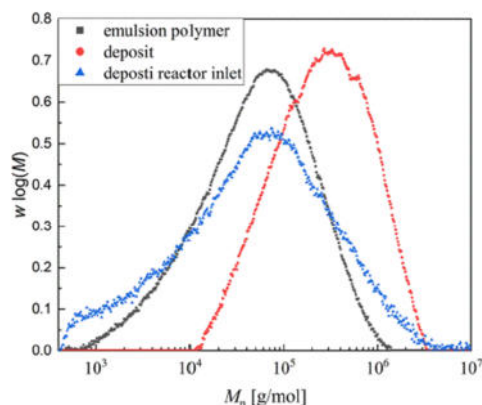


Figure 5. Plot of the molecular weight distribution of emulsion polymer, deposit and deposit at the reactor inlet for comparison of the polymeric properties for an experiment at 20 °C.

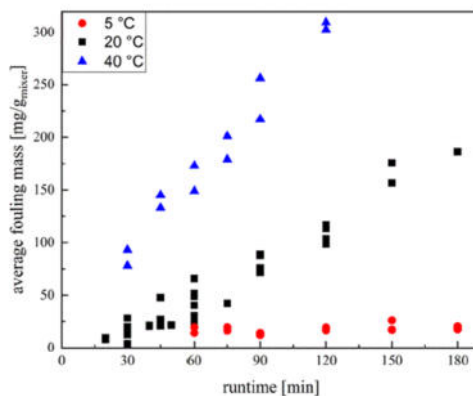


Figure 6. Plot of the mean fouling masses of the total reactor over the runtime of the experiment at different temperatures.

temperature range, since a mechanistic change would usually be accompanied by a different time-related behaviour. For the fouling masses at 5 °C the slope of linear correlation is close to zero and in the shown time-interval the offset in fouling caused by dead zones in the reactor dominates the time-dependent fouling trend.

The reaction progresses along the reactor and the fouling is depending on the conversion<sup>45</sup>. It is to be expected that higher fouling masses occur at the reactor outlet than at the inlet, since higher conversions are achieved there. For this purpose, the fouling masses of the individual static mixers were compared with the mean values of the overall reactor (Fig. 7).

The fouling largely reflects the expected conversion process in the reactor (Fig. 7). This agrees well with the literature<sup>45</sup>, which predicts a strong conversion dependence of the fouling. An exception to this is the first static mixer, in which the deposit formation is significantly increased. This is probably due to increased dead zones at the reactor inlet and deficits in the initial mixing<sup>46</sup>. Both favour an increased fouling, since the conversions are increased locally and the shear rates are also reduced by dead zones, so that sedimentation is favoured. After a minimum of fouling in static mixers two and three, the deposit formation then increases along the reactor and reaches its maximum near the reactor outlet. For technical implementation, the most fouling-intensive point is usually the most important, as this is most likely to lead to critical situations. Therefore, the time-dependent fouling of the last static mixer was compared with the average fouling mass for the whole reactor (Fig. 8).

The fouling formation at the reactor outlet is initially above the reactor mean. With increasing runtime, the deposit formation at the reactor outlet reaches a plateau and hardly increases any further. This course is attributed to that with increasing fouling, the flow velocity in the remaining channel volume is increased, so that further

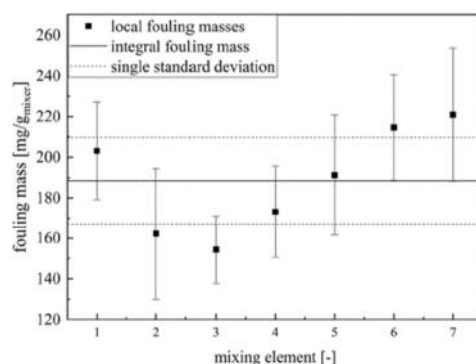


**Figure 7.** Plot of the mean fouling masses of the entire reactor and the fouling masses of the individual static mixers at a runtime of 120 min and a temperature of 20 °C.

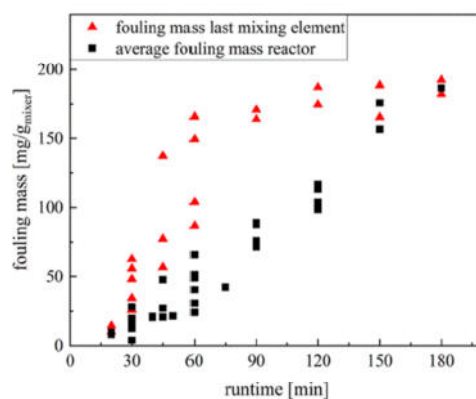


**Figure 8.** Plot of the mean fouling masses of the total reactor and the fouling masses of the last mixing element (ME7) over the runtime of the test at 20 °C.

fouling is reduced due to the shear rates. Thus, a saturation is reached after which the fouling increase slightly. This saturation is reached at different times due to the different rates of fouling along the reactor, so that the mean value increases linearly for a long time, while saturation is already reached close to the reactor outlet.

#### Conversion based online fouling sensing

The observation of the volume loss due to the fouling is a possible measurement method for fouling quantification. Here the volume loss was determined by conversion observation. Prerequisite for this is that the hydrodynamic residence time of the process corresponds approximately to the reaction time, so that a volume loss during the reaction directly influences the conversion. If the residence time is significantly higher than the reaction time, declines in conversion by reduced reaction volume will be detectable only at late fouling stages. Complete conversions would still be achieved even if the volume was reduced by significant fouling masses. In the set-up investigated here, the hydrodynamic residence time in the reactor was about 4 min, while the reaction time until complete thermal conversion of the investigated substance system in the batch reactor at 20 °C was about 3.5 min. In the batch process an increase in reactor temperature of about 20 °C was observed. In the continuous tubular reactor with improved cooling capacity compared to the batch reactor, the reaction time would therefore be somewhat longer and thus above the hydrodynamic residence time, so that the method is suitable here.

For this purpose, the reaction conversion at the reactor outlet was measured at regular intervals and the percentage conversion decrease over the runtime was determined. The conversion is directly proportional to the reaction volume at constant temperature and dosing currents, the decrease in conversion can be used to conclude the degree of filling in the reactor (Fig. 9).

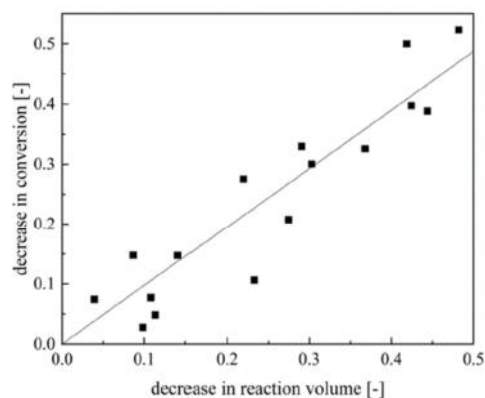


**Figure 9.** Plot of the decrease in conversion against the decrease in reaction volume for the experiments at 20 °C. The decrease in conversion is compared with the calculated decrease in reaction volume by gravimetrically determined reactor filling from the fouling masses in the reactor.

The indirect determination of fouling masses by the decrease in conversion is in good agreement ( $R^2 = 0.96$ ) with the direct, gravimetric determination. To confirm that the regression requirements were met, the normal distribution of the residuals was analysed using Shapiro–Wilk. The test showed a significant normal distribution ( $p > 0.05$ ). The determination of fouling masses by conversion analysis results in similar reactor fillings, the deviation of which lies within the measurement errors of the methods caused by conversion analytics or statistical deviations in fouling processes. Despite all possible deviations, the coverage of both methods is within 5%, so that the statistical deviation in the investigated fouling processes with 12% is significantly higher than the measurement errors. This method can be inline, online or atline depending on the method for determining the conversion. In this case, a real-time microwave gravimetric determination of conversions was used, so the method is between online and atline. The conversion could be easily accessed inline by calibrated RAMAN-spectroscopy as previously published<sup>47</sup>. Concluding, the real-time conversion analysis is a good strategy to quantify the amount of fouling fast. Although the conversion-based determination of the fouling masses is well practicable as a laboratory method, it is unsuitable for larger plants or routine operation due to the high effort involved.

#### Inline fouling sensing using ultrasonic techniques

The ultrasonic measuring technique can determine material characteristics which will be discussed as opportunity for fouling measurement. Since the reactor outlet was identified in the above considerations as the most fouling-intensive and therefore most critical point, the measuring cell was placed directly behind the reactor outlet. The fouling behaviour of the measuring cell was compared with the average fouling in the reactor (Fig. 10a) as well as the fouling at the reactor outlet (Fig. 10b) to validate that the measuring cell is representative of the fouling situation inside the reactor.

The average fouling masses of the reactor is not linear correlated with the fouling masses in the measurement cell. The measurement cell is especially in the beginning more sensitive to fouling deposition than the average reactor (Fig. 10a). In comparison the fouling at the last static mixer in the reactor agrees well with the gravimetrically determined fouling masses in the measuring cell (Fig. 10b). It is noticeable that for the whole runtime investigated up to 120 min there is a linear correlation between both fouling masses ( $R^2 = 0.77$ , Shapiro–Wilk  $p > 0.05$ ). It was chosen a regression of the type  $y = ax + b$  as there is a constant offset in fouling mass in the measurement cell caused by small dead zones, which is described by parameter  $b$ . With the measuring cell, the course of the reactor end can be mapped well, so that it is suitable for describing the fouling behaviour.

Since the section with the most fouling is usually the most interesting, this method can represent this well. Further, it is still crucial to consider the directly accessible measurement variables of the ultrasonic measurement technology in which this trend can be depicted to obtain a useable technology. The average sound velocity (ASV) in the measuring cell is media dependent, so it is a promising approach for detecting fouling (Fig. 11).

During the first 15 min of the experiment, the reaction has not reached stationarity so the average sound velocity is fluctuating (Fig. 11). These fluctuations of the ASV at the beginning of the measurement are caused by the low homogeneity of the pre-emulsion containing monomer droplets, micelles and water. About 7 min after starting the experiment first reaction can be detected in the measurement cell. This is expected as the hydrodynamic mean residence time for the reactor, connecting tubes and measurement cell is between 5 and 6 min. It can be recognized by the temperature increase due to the exothermic reaction but also visually by the resulting product. The curve of the average sound velocity clearly indicates the start of the reaction by the strong reduction of the average sound velocity, reaching a constant level with reaching the stationarity of the process after 15 min. In the following the fouling starts and the ASV is increasing as the solid fouling has a higher sound

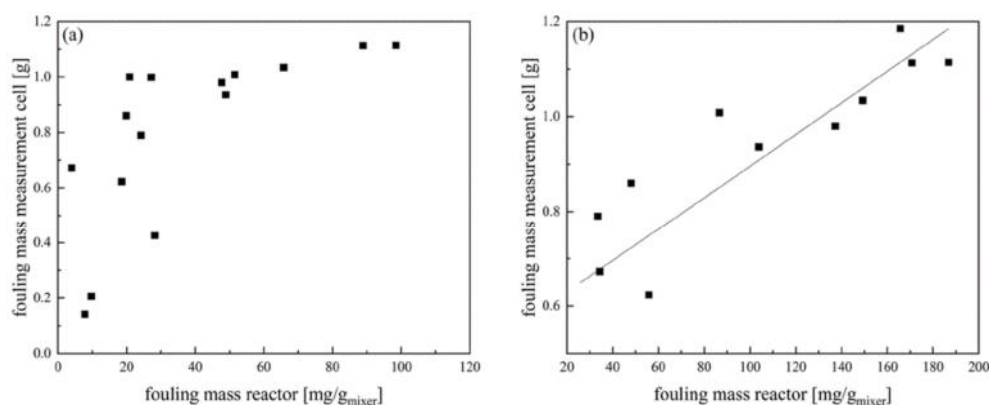


**Figure 10.** Plot of the fouling masses in the measurement cell against the average fouling masses of the reactor (a) and the fouling masses of the last static mixer (ME7) (b) for experiments at 20 °C.

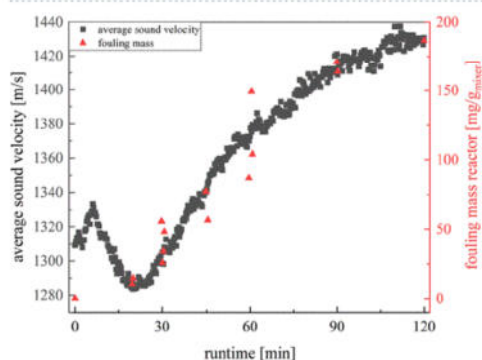


**Figure 11.** Plot of the fouling masses of the measuring cell and the average sound velocity against the runtime for one experiment at 20 °C.

velocity than the emulsion. Time-resolved gravimetrically determined fouling masses correlate well with the change in average sound velocity indicating that the sound velocity is representing deposit formation. For validation the fouling mass in the measurement cell for 16 experiments are plotted against the difference in average sound velocity (Fig. 12).

The fouling mass and the average sound velocity correlates with  $R^2 = 0.98$  (Shapiro–Wilk  $p > 0.05$ ). Concluding, the average sound velocity is suitable for inline monitoring of the fouling masses in the reactor.

As proof of the conceptual suitability of the measurement technique, a complete deposit formation cleaning cycle was followed using ultrasonic measurement technology. First, the fouling in the measuring cell and reactor was observed and then the cleaning of the reactor was followed using acetone (Fig. 13). Both the fouling mass before cleaning and the cleaning result were confirmed gravimetrically and optically.

The average sound velocity of acetone was measured as reference for cleaning. After that, the reaction was started and after 12 min the stationarity was reached and fouling growth can be observed. The runtime was set to 30 min and after that the experiment was ended and the measurement cell was rinsed with compressed air. In the next step acetone was used for cleaning and the decrease of the fouling layer can be observed starting 37 min after initiation. After 15 min of cleaning the average sound velocity reaches the level of pure acetone, so there should be no more fouling in the measurement cell which is confirmed visually. Only in the corners of the measuring cell outside the measuring path could small amounts of deposits still be detected optically, but these could not be measured because the measuring path was completely free of fouling. Further optimisation of the measuring cell is necessary here so that there are no undetectable zones, and the behaviour of the reactor can be described even more precisely.

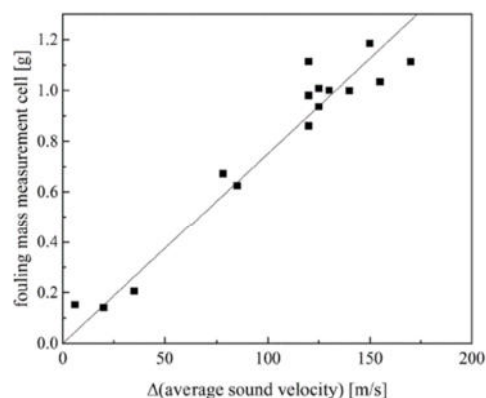


**Figure 12.** Plot of the fouling masses of the measuring cell against the change in mean sound velocity for experiments at 20 °C.

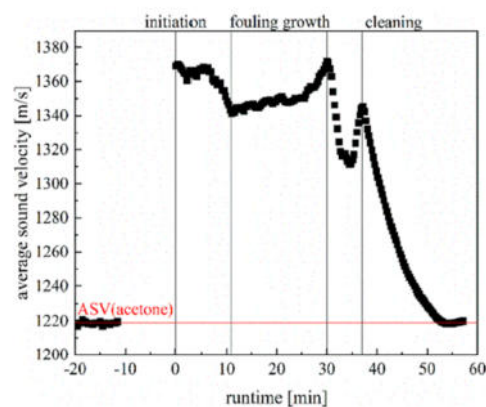


**Figure 13.** Plot of a complete deposit formation-cleaning cycle as proof of the conceptual suitability of the measurement technique at 20 °C.

### Summary

Two suitable sensor concepts were established, one monitoring fouling processes via conversion analysis and one using ultrasonic measurement techniques or fouling quantification. In the first case the loss in reaction volume caused by fouling was measured by the decrease in conversion during the reaction. In the second case the deposit formation was monitored by tracking the changes in average sound velocity in the measurement cell, which are substance-dependent and therefore caused by the formation of deposits. Both methods agree well with gravimetric references and reach deviations below 10%. Deposit formation is mainly caused by polymerisation fouling and for the average reactor value a linear fouling trend can be observed. This is caused by local differences in fouling behaviour as the conversion influences the fouling speed. The most intense fouling occurs at the reactor end causing a higher slope in fouling growth but reaching a saturation after 60 min as increased flow velocities reduce further fouling. Thus, the time-dependent fouling processes during continuous emulsion copolymerisation of vinyl acetate could be determined.

### Data availability

All data generated or analysed during this study are included in this published article and its Supplementary Information files.

Received: 30 October 2023; Accepted: 11 February 2024  
 Published online: 19 February 2024

## References

- Lynch, J., Sutoris, H. F., Zubiller, J., & Aumüller, A. Verfahren zur polymerisation vinyllischer monomere. DE 196 48 811 A 1 (1998).
- Apecetche, M. A., Xinlai, B., & Cann, K. J. Process for reducing polymer build-up in recycle lines and heat exchangers during polymerizations employing butadiene, isoprene, and/or styrene. US005733988A (1996).
- Arhancet, G. compositions and methods for inhibiting fouling of vinyl monomers. WO 98/47593 29 (1998).
- Reid, D. K. Antioxidant compositions and methods using p-phenylenediamine compounds and organic AOD compounds. US005128022A (1992).
- Weber, M., Lattner, J., McCullough, L., Dickey, R., Brown, S., & Loezos, P. Olefin oligomerization reaction processes exhibiting reduced fouling. WO 2010/110801 A1 (2010).
- Hocking, P., Sibtain, F., & Cheluget, E. Reducing fouling in heat exchangers. CA 2797 489, A1 (2012).
- Tong, D. Y. Reducing polymer fouling and agglomeration in acrylate/methacrylate processes. US 2016/0102189 A1 (2015).
- Cohen, L. Polymerization reactors coated with polymer-inhibitor complexes. US4256864 (1979).
- Weimer, D. R., & Freshour, K. Prevention of pvc polymer buildup in polymerization reactors using oxalyl bis(benzylidenehydrazide) and alumina. US4145496 (1979).
- Wempe, L., & Bauman, B. D. Method for reducing wall fouling in vinyl chloride polymerization. US4420591 (1983).
- Cohen, L. Polymerization reactor coatings and use thereof. US4696983 (1987).
- Fitzwater, S. J., & McFadden, D. M. Continuous process for preparing polymers. EP 1 136 505 A1 (2001).
- McFadden, D. M., & Wu, R. S.-H. The reduction of polymer fouling on reactor surfaces in a continuous process for preparing polymers. EP 1 024 149 A2 (2000).
- Lowell, J. S., Hendrickson, G. G., & Price, R. J. Elimination of polymer fouling in fluidized bed gas-phase fines recovery reactors. US 2018/0105613 A1 (2018).
- Lowell, J. S., Dooley, K. A., Li, R., & Aruho, D. K. Systems and methods for mitigating polymer fouling. WO 2022/173784 A1 (2022).
- McDonald, M., & Lawrence, D., & Williams, D. Polymerization reactor. WO 93/03075 (1993).
- Carvalho, A. C. S. M., Chicoma, D. L., Sayer, C., & Giudici, R. Development of a continuous emulsion copolymerization process in a tubular reactor. *Ind. Eng. Chem. Res.* 49(21), 10262–10273. <https://doi.org/10.1021/ie100422v> (2010).
- Kelland, M. A. Additives for kinetic hydrate inhibitor formulations to avoid polymer fouling at high injection temperatures Part 1. A review of possible methods. *Energy Fuels* 34(3), 2643–2653. <https://doi.org/10.1021/acs.energyfuels.9b04040> (2020).
- Dorton, M., & Gardner Sr., G. Process for cleaning polymeric fouling from equipment. US 20030073595A1 (2003).
- Hanyama, H. Solution conveying and cooling device. EP 3 203 177 A1 (2017).
- Saikhwan, P., Chew, J. Y. M., Paterson, W. R., & Wilson, D. I. Swelling and its suppression in the cleaning of polymer fouling layers. *Ind. Eng. Chem. Res.* 46(14), 4846–4855. <https://doi.org/10.1021/ie0615943> (2007).
- Ekowati, Y. et al. Synthetic organic polymer fouling in municipal wastewater reuse reverse osmosis. *J. Water Reuse Desal.* 4(3), 125–136. <https://doi.org/10.2166/wrd.2014.046> (2014).
- Deglmann, P. et al. Side reactions in aqueous phase polymerization of N-vinyl-pyrrolidone as possible source for fouling. *Macromol. React. Eng.* 13(5), 1–13. <https://doi.org/10.1002/mren.201900021> (2019).
- Neßlinger, V. et al. Thin organic-inorganic anti-fouling hybrid-films for microreactor components. *Macromol. React. Eng.* 2200043, 1–16. <https://doi.org/10.1002/mren.202200043> (2022).
- Smith, W. V. & Ewart, R. H. Kinetics of emulsion polymerization. *J. Chem. Phys.* 16, 592–599. <https://doi.org/10.1002/app.1965.070090410> (1948).
- Chern, C. S. Emulsion polymerization mechanisms and kinetics. *Prog. Polym. Sci.* 31(5), 443–486. <https://doi.org/10.1016/j.progpolymsci.2006.02.001> (2006).
- Thickett, S. C. & Gilbert, R. G. No title. *Polymer (Guildf)*. 48, 6965–6991. <https://doi.org/10.1016/j.polymer.2007.09.031> (2007).
- Schorck, F. J. & Lu Fujun, F. Relative rates of branching in emulsion and miniemulsion polymerization. *Macromol. React. Eng.* 3(9), 539–542. <https://doi.org/10.1002/mren.200900036> (2009).
- Schorck, F. J. Monomer transport in emulsion polymerization II: Copolymerization. *Macromol. React. Eng.* 15(6), 10–13. <https://doi.org/10.1002/mren.202100022> (2021).
- Schorck, F. J. Monomer transport in emulsion polymerization III terpolymerization and starved-feed polymerization. *Macromol. React. Eng.* 16(4), 2–5. <https://doi.org/10.1002/mren.202200010> (2022).
- Schorck, F. J. Heinz Gerrens revisited: A new look at the impact of reactor type on polymer chain morphology. *Macromol. React. Eng.* 14(3), 1–10. <https://doi.org/10.1002/mren.201900055> (2020).
- Schorck, F. J. Monomer concentration in polymer particles in emulsion polymerization. *Macromol. React. Eng.* 15(3), 1–2. <https://doi.org/10.1002/mren.202100003> (2021).
- van der Hoff, B. M. E. Kinetics of emulsion polymerization. *Adv. Chem.* 9, 6–31. <https://doi.org/10.1002/app.1965.070090410> (1962).
- Elizalde, O., Aramendia, E., Ilundain, P. & Tauer, K. *Aqueous Polymer Dispersions* (Springer, 2004).
- van Herk, A. M. *Chemistry and Technology of Emulsion Polymerisation, 2nd edition* (Wiley, 2013).
- Vale, H. M. & McKenna, T. F. Modeling particle size distribution in emulsion polymerization reactors. *Prog. Polym. Sci.* 30(10), 1019–1048. <https://doi.org/10.1016/j.progpolymsci.2005.06.006> (2005).
- Hohlen, A., Augustin, W. & Scholl, S. Quantification of polymer fouling on heat transfer surfaces during synthesis. *Macromol. React. Eng.* 14, 1. <https://doi.org/10.1002/mren.201900035> (2020).
- Hohlen, A., Augustin, W. & Scholl, S. Investigation of polymer depositions during the synthesis in a heat exchanger. *Chem. Ingenieur Technik* 92(5), 629–634. <https://doi.org/10.1002/cite.201900130> (2020).
- Gottschalk, N., Kuschnerow, J. C., Föste, H., Augustin, W. & Scholl, S. Experimental investigation on fouling of a polymer dispersion on modified surfaces. *Chem. Ingenieur Technik* 87(5), 600–608. <https://doi.org/10.1002/cite.201400126> (2015).
- Böttcher, A. et al. Fouling pathways in emulsion polymerization differentiated with a quartz crystal microbalance (QCM) integrated into the reactor wall. *Macromol. React. Eng.* 16(2), 1–8. <https://doi.org/10.1002/mren.202100045> (2022).
- Madani, M. Belagsbildung in Chemischen Reaktoren Unter Berücksichtigung von Oberflächenaspekten (2017).
- Bernstein, C. Methoden Zur Untersuchung Der Belagsbildung in Chemischen Reaktoren (Dissertation) (2017).
- Förster, J., Tebrügge, J., Osenberg, M., Westerdick, S., von Grothuss, E., Behrendt, F., & Vogt, M. A9.2 Fouling detection in polymerization processes by ultrasound echo measurements. In *SMSI 2021—Sensors and Instrumentation*; AMA Service GmbH, Von-Münchhausen-Str. 49, 31515 Wunstorf, Germany, 2021; Vol. 48, 99–100. <https://doi.org/10.5162/SMSI2021/A9.2>.
- Osenberg, M. et al. Ultrasound based fouling detection in polymerization processes polymerization process. *Sens. Messtechnik* 303, 272–274 (2022).
- Rust, S. & Pauer, W. Formulation and process determined fouling prediction for the continuous emulsion co polymerization of vinyl acetate. *J. Polym. Res.* 30(6), 1–11. <https://doi.org/10.1007/s10965-023-03588-8> (2023).
- Förster, J., Fritsch, T., Tebrügge, J., Musch, T., Osenberg, M., Haspel, D., Pauer, W., Rust, S., Klinkert, A., Augustin, W., Scholl, S., Melchin, T., & Eckl, B. *Schlussbericht Zum Verbundprojekt: „KoPPonA 2.0“—Kontinuierliche Polymerisation in Modularen*,

- Intelligenten, Gegen Belagbildung Resistenten Reaktoren—Teilvor-Haben: Verfahrensentwicklung Und Betriebliche Umsetzung Für Die Emulsionspolymerisation* (2023).
47. Jacob, L. I. & Pauer, W. Scale-up of emulsion polymerisation up to 100 L and with a polymer content of up to 67 Wt%, monitored by photon density wave spectroscopy. *Polymers (Basel)* **14**, 8. <https://doi.org/10.3390/polym14081574> (2022).

#### Author contributions

All authors conceived the experiments, S.R. and M.O. performed the experiments and analysed the data. The first draft of the manuscript was written by S.R. and M.O., T.M. and W.P. commented on previous versions of the manuscript. All authors read and approved the final manuscript.

#### Funding

Open Access funding enabled and organized by Projekt DEAL. The work has been funded by the German Federal Ministry for Economic Affairs and Climate Action as part of the ENPRO Initiative (KoPPonA 2.0, FKZ: 03EN2004E,I,M). We acknowledge financial support from the Open Access Publication Fund of Universität Hamburg.

#### Competing interests

The authors declare no competing interests.

#### Additional information

**Supplementary Information** The online version contains supplementary material available at <https://doi.org/10.1038/s41598-024-54321-4>.

Correspondence and requests for materials should be addressed to W.P.

Reprints and permissions information is available at [www.nature.com/reprints](http://www.nature.com/reprints).

**Publisher's note** Springer Nature remains neutral with regard to jurisdictional claims in published maps and institutional affiliations.



**Open Access** This article is licensed under a Creative Commons Attribution 4.0 International License, which permits use, sharing, adaptation, distribution and reproduction in any medium or format, as long as you give appropriate credit to the original author(s) and the source, provide a link to the Creative Commons licence, and indicate if changes were made. The images or other third party material in this article are included in the article's Creative Commons licence, unless indicated otherwise in a credit line to the material. If material is not included in the article's Creative Commons licence and your intended use is not permitted by statutory regulation or exceeds the permitted use, you will need to obtain permission directly from the copyright holder. To view a copy of this licence, visit <http://creativecommons.org/licenses/by/4.0/>.

© The Author(s) 2024

## 5.4 KoPPonA 2.0 – Continuous polymerisation in modular, intelligent, fouling resistant reactors – Subproject: Process development and implementation for emulsion polymerisation.

In this chapter the sections of the project report discussing the results at the University of Hamburg are shown. These are the pages 56 – 74. The full report can be requested at the Technische Informationsbibliothek (TIB), Hannover.<sup>[86]</sup>

Jan Förster, Thomas Fritsch, Jan Tebrügge, Thomas Musch, Marco Osenberg, Dominik Haspel, Werner Pauer, **Sören Rust**, Annika Klinkert, Wolfgang Augustin, Stephan Scholl, Timo Melchin, Bernhard Eckl

### **Synopsis**

Fouling is highly challenging for industrial processes. The knowledge about fouling processes and methods to measure fouling are widely unknown. Especially polymerisation processes tend to high fouling masses. Following this a research project was founded to investigate the fouling behaviour during different polymerisation processes with industrial relevance. One of the chosen polymerisations was the emulsion polymerisation of vinyl acetate copolymers. The approach of this research project was different to the publications stated before, as here lots of topics were investigated superficially and some were discussed deeper. This causes a wide range of topics addressed in the report. Some of them have been published in scientific papers with more research, and others have been investigated more detailed but are so far unpublished work. These are discussed more detailed in chapter 6.

Fouling behaviour on different scales was analysed and compared. This enables the transfer of gained knowledge to different scales and validation if fouling is scale-dependent or not. Moreover, chemical fouling characterisation as well as characterisation of the dispersions obtained were research goals of the project as the product properties are important for comparing the results from different partners. Another part was the development of different sensors for inline fouling detection in the tubular reactor which were carried out in cooperation with engineering partners. The sensors were developed, optimised, and validated for the different polymerisations. Moreover, the reactor used in the project was a newly developed PFR which was characterised regarding mixing and residence time behaviour to analyse effects of the reactor on the polymerisation.



### 3.2 Wissenschaftlich-technisches Ergebnis

Die ITMC-UH ist mit fünf Schwerpunktthemen

- Bestimmung der Mikrovermischung von Fluiden in kontinuierlichen Reaktoren mit statischen Mischelementen
- Entwicklung eines geeigneten Referenzsystems für die Belagscharakterisierung
- Entwicklung eines orts aufgelösten, faseroptischen Temperatursensors zur Belagsdetektion
- Chemische Untersuchung der Belagsbildungsprozesse
- Entwicklung von Belagsvermeidungsstrategien und Belagsvorhersagemodellen.

im KoPPonA-Projekt vertreten, in denen wissenschaftlich-technische Ergebnisse erzielt wurden. Zudem hat die ITMC-UH zusammen mit weiteren Projektpartnern Ergebnisse auf dem Feld der Sensorapplikation in das vorliegende Emulsionsstoffsystem erzielt. Im Folgenden sind die wissenschaftlich-technischen Ergebnisse der ITMC-UH nach Arbeitspaketen geordnet kurz dargestellt.

#### 3.2.1 AP 1 Entwicklung und Evaluation von Sensor- und Messtechniken zur Belagserkennung und -quantifizierung

##### AP 1.2 Entwicklung und Bau einer Teststrecke sowie Implementierung von Sensormesstechnik zur Belagsdetektion in den Versuchsanlagen

###### Wesentliche wissenschaftlich-technische Ergebnisse:

- Aufbau der Versuchsanlage zur Belagsdetektion
- Geeignete Reinigungsrezeptur für die Belagsentfernung liegt vor
- Belagsbildung wurde in Umpumpversuchen quantifiziert
- Belagsquantifizierung kann mit guter Übereinstimmung chemisch sowie gravimetrisch erfolgen
- Die Auswahl einer passenden Messtechnik ist abgeschlossen
- Die faseroptische Temperaturmessung wurde im Modellaufbau erprobt
- Der Einbau und die Erprobung von Glasfasern in einem 3D-gedruckten Rohrreaktor wurde erfolgreich abgeschlossen
- Die online Temperaturmessung bei Emulsionspolymerisation in 3D-gedrucktem Rohrreaktor mittels FOS wurde durchgeführt

Im Fluitec-Halbschalenreaktor wurde im Laborversuchstand (Abbildung 3.1) eine ausreagierte Polymeremulsion bei 80 °C im Kreis gefördert und die Belagsmenge in Abhängigkeit der Zeit ermittelt.

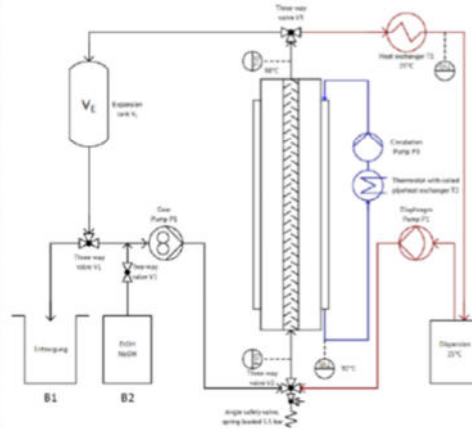


Abbildung 3.1: Versuchsstand mit zugehörigem R&I-Schema.

Hierfür wurde eine Dispersion aus VAc/Versa10 verwendet, welche in Zeiträumen von 1 bis 40 Stunden im Kreis gefördert wurde. Die Belagsmenge wurde chemisch und gravimetrisch untersucht und verglichen. Die gravimetrische Quantifizierung erfolgte durch Differenzwägen des getrockneten Reaktors vor und nach dem Versuch. Die chemische Belagsquantifizierung erfolgte über eine Reinigung des Reaktors mit einer 8 molaren NaOH-Lösung und Ethanol im Massenverhältnis von 1:1. Diese wurde bei 80 °C für drei Stunden im Kreis gefördert und anschließend über den Feststoffgehalt der Reinigungslösung sowie das verwendete Volumen die Belagsmenge ermittelt. Die Belagsmengen stimmen mit mittleren Abweichungen unter 10 % überein (Abbildung 2)

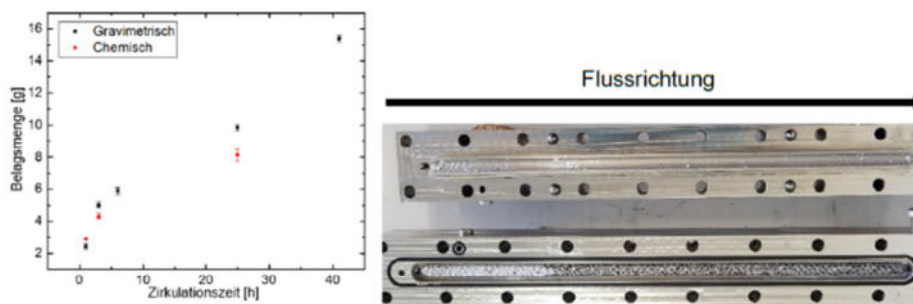


Abbildung 3.2: Auftragung der Belagsmengen gegen die Umpumpzeit sowie Blick in den Halbschalenreaktor nach Durchführung des Versuches.

Durch Öffnen des Reaktors nach Versuchsdurchführung wurde die Verteilung des Belages im Reaktor bestimmt. Es ist deutlich zu erkennen, dass der Belag hauptsächlich an den statischen Mischelementen in der Nähe des Reaktoreinganges ausgebildet wird (Abbildung 3.2). Nach

dem ersten Drittel des Reaktors sind nur noch geringe Belagsanhaftungen erkennbar, welche mit zunehmender Entfernung zum Eingang weiter abnehmen. Es wird vermutet, dass dies auf die Temperaturunterschiede zwischen auf 80 °C temperiertem Reaktor und nicht temperierter Dispersion bei 20 °C, die am Reaktoreingang am größten sind zurückzuführen ist.

Als Methode zur *inline*-Belagsdetektion sind Gasfasern als faseroptische Sensoren etabliert worden. Nachdem die Erprobung im Testkörper mit Wasser erfolgreich war und die Software zur Auslesung mehrerer Fasern parallel fertiggestellt wurde, wurde eine erste Belagsbildung durch Einführen von Papierschichten zwischen Testkörper und Temperiermedium simuliert (Abbildung 3.3).

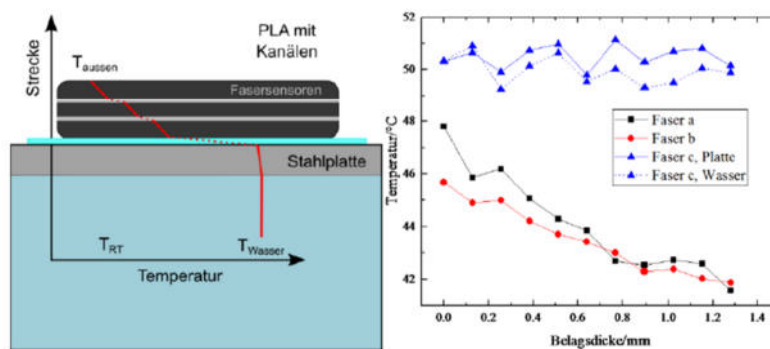


Abbildung 3.3: Skizze des Versuchsaufbaus zur Belagssimulation sowie Auftragung der Temperaturverläufe in Abhängigkeit der Anzahl an Papierschichten.

Aus der Veränderung der Temperatur bei unterschiedlichen Anzahlen an Papierschichten konnte gezeigt werden, dass die faseroptischen Sensoren zur Belagsdetektion geeignet sind. Anschließend wurden zwei Faserkanäle in die Wand eines 3D-gedruckten Rohrreaktors eingedrückt und mit Fasern versehen (Abbildung 3.4). Es konnte gezeigt werden, dass die Temperaturen an den Fasern den Temperaturverlauf der Polymerisation widerspiegelt und auch zeitliche Veränderungen zu erkennen sind, die mit der zunehmenden Belagsbildung korrelieren.

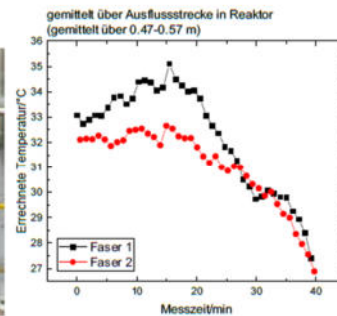
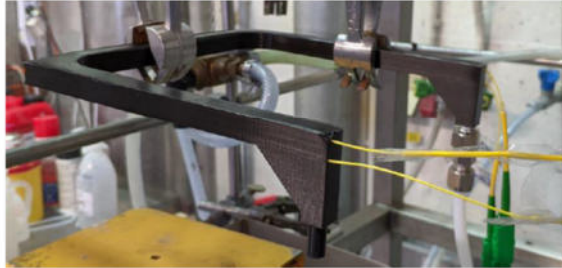


Abbildung 3.4: Aufbau des 3D-gedruckten Reaktors mit implementierten Glasfasern und Auftragung der zeitlichen Temperaturentwicklung im besonders belagsträchtigen Endsegment des Reaktors.

Zusammenfassend wurde das Arbeitspaket termingerecht abgeschlossen und die Arbeit an den darauf aufbauenden Arbeitspaketen aufgenommen.

### AP 1.3 Einsatz und Bewertung unterschiedlicher Mess- und Sensortechniken in den Versuchsanlagen

#### Wesentliche wissenschaftlich-technische Ergebnisse:

- Chemische Belagscharakterisierung erfolgt
- Faseroptische Sensoren in Halbschalenreaktor implementiert
- Auslesung der Temperaturen möglich
- Kalorimetrische Messungen durch externe Kalibrierung in Planung
- Charakterisierung der Mischgüte im Halbschalenreaktor

Die während der Polymerisationen erhaltenen Beläge wurde chemisch mittels unterschiedlicher analytischer Methoden

- Gelpermeationschromatographie
- Löslichkeitsversuche
- Quellversuche
- Gelgehaltsbestimmung

charakterisiert. Zunächst wurden Restfeuchte sowie lösliche Bestandteile untersucht. Dazu wurden frische Reaktionsbeläge bis zur Massekonstanz getrocknet und der Gewichtsverlust gravimetrisch ermittelt. Bei den untersuchten Belägen wurden Restfeuchten zwischen 30 % und 40 % gemessen. Die Gelgehaltsbestimmung erlaubte Rückschlüsse auf die Vernetzung der Beläge. Bei einer Soxhlet-Extraktion der Beläge wurden Gelgehalte von ca. 45-55 % gemessen, während die korrespondierende Emulsion bei gleicher Behandlung Gelgehalte von unter 10 % aufwies. Da eine Soxhlet-Extraktion teilweise bei Verschlaufungen der Polymere zu falschen

Ergebnissen führt, wurde der Gelgehalt ebenfalls durch mehrstündiges Kochen unter Reflux in THF und anschließende Filtration bestimmt, wobei für die Emulsion Gelgehalte von unter 2 % und für die Beläge Gelgehalte von unter 5 % erhalten wurden, sodass davon ausgegangen werden kann, dass auch die Beläge weitgehend unvernetzt sind, jedoch stärker verschlufft sind, als die Emulsion. Dies deckt sich mit der Untersuchung der Molekulargewichte mittels GPC, bei welcher die Beläge mit ca. 400 000 – 500 000 g/mol nur ein doppelt so hohes mittleres Molekulargewicht wie die Emulsion aufwiesen. Abschließend wurde die Quellbarkeit der Beläge untersucht, hierbei wurden Quellgehalte von ca. 400 % - 500 % ermittelt, wobei kalt lösliche Bestandteile der Beläge nicht berücksichtigt wurden.

Ein faseroptischer Sensor wurden in die Bohrungen des Halbschalenreaktors eingebracht. Hierzu wurden alle Bohrungen im selben Abstand zur Reaktormitte durch dieselbe Glasfaser ausgelesen, sodass das Temperaturprofil längs des Reaktors durch einen faseroptischen Sensor dargestellt werden kann, während die Wärmeleitung zwischen Reaktor und Temperiermedium durch den faseroptischen Sensor gemessen werden kann (Abbildung 3.5).



Abbildung 3.5: Ansicht des Reaktoraufbaus mit eingebautem faseroptischem Sensor zur ortsaufgelösten Temperaturmessung längs und quer zum Reaktor.

Da die Reaktionen von verschiedenen Personen durchgeführt werden sollen, wurde zuerst mit BasicScan eine Software geschrieben, welche einfach zu bedienen ist. Sie ermöglicht nach kurzer Einweisung das Datenerfassen mit den faseroptischen Sensoren. Des Weiteren wurden mehrere Thermoelemente in eine Bohrung eingebaut, die den gleichen Abstand zum Temperiermedium und zum Reaktorinneren besitzt wie die Fasern. Mithilfe dieser herkömmlichen Temperaturmessung ist ein direkter Vergleichswert zu den Fasermessungen gegeben. Die Rohdaten, die aus der Fasermessung erhalten werden, sind Dämpfungsinformationen. Diese erfordern eine Kalibrierung, um sie in absolute Temperaturwerte umrechnen zu können. Zuerst wurde dies aber übergangen und die Auswertung auf relative Temperaturänderungen begrenzt, da zunächst

untersucht werden soll, ob die Fasern in dieser Weise zur Temperaturmessung eingesetzt werden können, oder ob zu starke Spannungen auftreten, welche die Messergebnisse der Fasern verzerren.

In Abbildung 3.6 ist eine beispielhafte Messung einer belagsbildenden Reaktion gezeigt. Die Dämpfung skaliert antiproportional zu einer Temperaturerhöhung, weswegen die Ausschläge über die vier Messstrecken trotz Temperatursenkung in den positiven Bereich gehen. Diese Messung wurde bei einer eingestellten Temperatur von 20 °C durchgeführt. Die vier Messstrecken sind deutlich durch Temperaturabweichungen zu der Umgebung zu sehen.

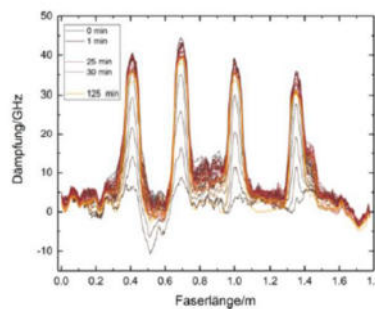


Abbildung 3.6: Faseroptische Verfolgung einer belagsbildenden Reaktion mit einer Faser, die viermal durch den Halbschalenreaktor gewunden wurde.

Abbildung 3.7 zeigt die zeitliche Signaländerung einer der Messstrecken durch den Reaktor bei derselben Reaktion.

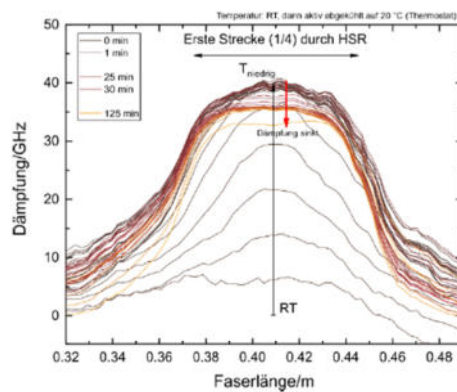


Abbildung 3.7: Erste Faserstrecke aus Abbildung 7.

Wie in Abbildung 3.7 zu erkennen ist, kann die ca. 8 cm lange Querstrecke durch den Halbschalenreaktor erkannt werden. Außerdem ist zu erkennen, wie die Temperaturänderung zu Beginn der Messung eine Spitze ausbildet, was geschieht, weil das Temperiermedium durch einen

zentralen Kanal gepumpt wird. Die Wärmeleitung im Stahl führt dann dazu, dass sich das erwartete Plateau an der Stelle der Querbohrung ausbildet. Nach einiger Zeit kommt es trotz konstanter Temperatur im Reaktor zu einem vermeintlichen Temperaturanstieg, wie durch die sinkende Dämpfung erkennbar ist. Dies war zuerst vermutlich darauf zurückzuführen, dass die Fasern durch ihre Verlegung und ihre Plastikschuttschicht unter mechanischer Spannung stehen, die sich mit der Zeit verändern. Das Problem der Spannungen im System ist im Moment das größte Hindernis betreffend einer reproduzierbaren und genauen Temperaturmessung mit den Glasfasern. Dies ist allerdings bereits in Bearbeitung. In der Vergangenheit konnte gezeigt werden, dass nackte Glasfasern nicht nur schneller auf Temperaturänderung reagieren, sondern auch weniger zu Verzerrung neigen.

Durch mehrere Messungen dieser Art konnte ein Temperaturprofil entlang des Halbschalenreaktors gemessen werden. Wie auch in Abbildung 3.8 zu erkennen, ist die größte Temperaturänderung bei der zweiten Querbohrung zu erkennen. Die Messstrecken waren vom Eingangsende des Halbschalenreaktor dabei jeweils 56 mm, 153 mm, 295 mm, 332 mm und 433 mm entfernt.

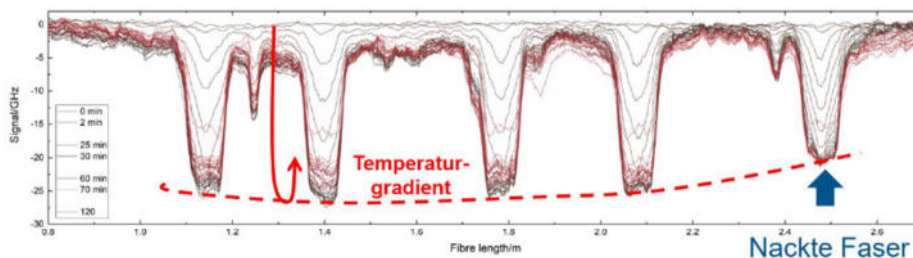


Abbildung 3.8: Temperaturgradient entlang des Halbschalenreaktors, illustriert mithilfe der Fasersensoren.

Diese Funde wurden mithilfe von Thermoelementen überprüft. Wenn die sich über die Reaktionszeit ändernde Dämpfung des Signals durch eine mit Thermoelementen messbare Temperaturänderung zurückführen ließe, wären die Fasersensoren weniger durch mechanische Spannungen beeinflusst als gedacht.

In Abbildung 3.9 sind die Temperaturverläufe von Thermoelementen gezeigt, die in ähnliche Positionen wie die Glasfasern zuvor eingeführt wurden. Die Positionen waren vom Eingangsende des Halbschalenreaktor dabei jeweils 56 mm, 120 mm, 332 mm und 433 mm entfernt.

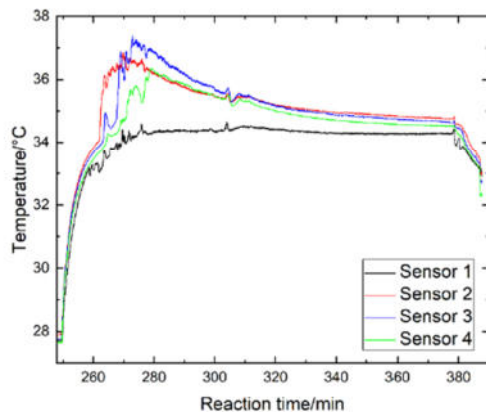


Abbildung 3.9: Thermoelementmessungen analog zu den Messungen mit den Fasersensoren.

Es kann in der Tat gesehen werden, dass es ein Temperaturmaximum im Reaktorverlauf gibt. Des Weiteren kann erkannt werden, dass der Temperatureauschlag sich durch den Reaktor propagiert und die Sensoren daher zeitlich versetzt auf die exotherme Reaktion reagieren. Anschließend fallen die Temperaturen wieder ab, was durch Belagsbildung erklärt werden könnte. Der sich bildende Belag sollte dazu führen, dass der effektive Durchmesser des Reaktors kleiner wird und dadurch die zeitabhängige Initiierung der exothermen Reaktion weiter hinten im Reaktor stattfindet. Des Weiteren sollte die Temperatur abnehmen, da die Belagsschicht thermisch isoliert.

Außerhalb des Halbschalenreaktors konnte dasselbe Verhalten bestätigt werden.

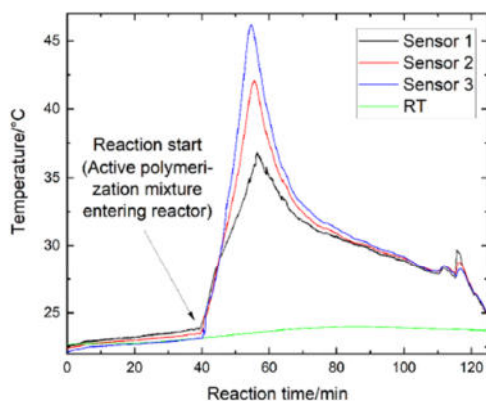


Abbildung 3.10: Thermoelementmessungen in einem 50 cm langen 3D gedruckten Reaktor ohne äußere Temperierung.



Der Reaktor hat einen Innendurchmesser von 12 mm und ist die in Abbildung 3.11 gezeigt geformt. Der abgebildete Abschnitt ist 16 cm lang und es können mehrere Abschnitte aneinandergereiht werden. Für die hier gezeigten Messungen wurden jeweils drei dieser Abschnitte kombiniert um einen ca. 50 cm langen Reaktor zu kreieren. Der Reaktor besitzt ein Loch in das ein Thermoelement in den Reaktionsstrom eingeführt werden kann.



Abbildung 3.11: Geometrie des 3D gedruckten PLA Reaktors.

Der Reaktor passt fest in ein Modul, in das bis zu drei faseroptische Sensoren integriert werden können. In der Rundung wurde Thermopaste verstrichen, sodass es keine Luftlücke entsteht und die Temperaturmessung beeinflusst.



Abbildung 3.12: Modul für den Reaktor aus Abbildung 3.11 für faseroptische Temperaturmessungen.

Die Belagsdetektion die in den vorgehenden Thermoelementmessungen gezeigt wurde, konnte mithilfe der faseroptischen Messungen bestätigt werden. Der erwartete Temperaturverlauf einer exothermen Reaktion in einem nicht temperierten Rohrreaktor enthält ein Temperaturmaximum, welches ohne Belagsbildung während der gesamten Reaktionszeit stationär stabil sein müsste. Das Maximum liegt in dem verwendeten Aufbau hinter dem Reaktorausgang, aber trotzdem können Beobachtungen gemacht werden.

In der folgenden Heatmap ist zu sehen, dass das Temperaturmaximum der Reaktion hinter dem Reaktorausgang liegt. Diese Messung entspricht der Thermoelementmessungen in Abbildung 3.10.

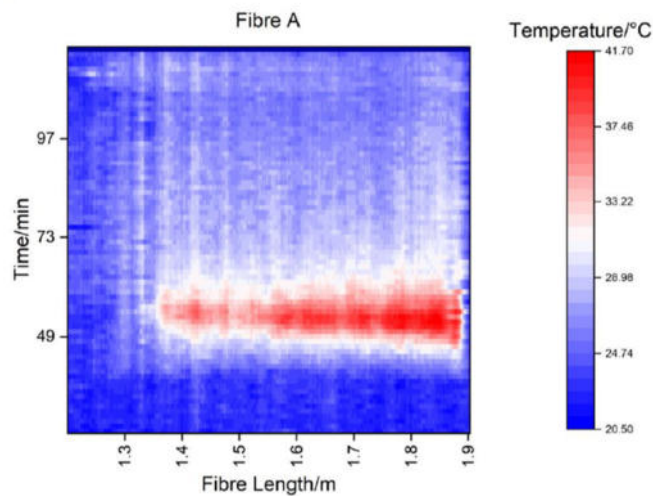


Abbildung 3.13: Heatmap der faseroptischen Messung im 3D gedruckten PLA Reaktor während einer Belagsträchtigen Reaktion.

Es kann zusammenfassend festgestellt werden, dass Belag im Halbschalenreaktor, sowie in einem 3D gedruckten PLA Reaktor detektiert werden konnte. Der Belag führt dazu, dass das gemessene Temperaturprofil entlang der Rohrreaktoren weiter nach hinten verschoben wird, und zu abnehmender Temperatur im Reaktormantel. Dies bestätigt die ursprünglichen Annahmen. Eine Belagsquantifizierung durch Temperaturmessung konnte noch nicht durchgeführt werden.

#### AP 1.4 Übertragung erfolgreicher Messmethoden auf die anderen Stoffsysteme

##### Wesentliche wissenschaftlich-technische Ergebnisse:

- Test der Ultraschallmesstechnik zusammen mit RUB-EST im Wacker-Stoffsystem
- Bisherige Ergebnisse sehen vielversprechend aus, benötigen jedoch noch weitere Messungen zur Validierung der Aussagen
- Anpassung der Geometrie der Ultraschallmesszelle zur Optimierung der Strömungsverhältnisse durchgeführt, Verbesserung der Ergebnisse erzielt
- Stabsonde (CEMOS) ist beständig gegenüber dem verwendeten Stoffsystem, nicht aber gegenüber der Reinigungslösung, daher Ausbau vor Reinigung nötig
- Erprobung der Stabsonde zusammen mit CEMOS durchgeführt
- Es wird vermutet, dass die Stabsonde als Belagsdetektor nicht geeignet ist, da die Sensitivität gegenüber dem Feststoffgehalt höher ist als gegenüber einer Belagsbildung

Zusammen mit der RUB-EST wurde die Ultraschallmesszelle am Hamburger Laborversuchsstand im Wackerstoffsystem erprobt. Dazu wurden sowohl Saat-Emulsionspolymerisationen als auch ab initio Emulsionspolymerisationen durchgeführt, bei welchen die Messzelle vor den Reaktor geschaltet war. Eine neue Messzellegeometrie mit vergrößerten Zu- und Abläufen

wurde entwickelt, welche auch vom Strömungsbild optimiert wurde. Mithilfe der Messzelle konnte bestätigt werden, dass eine Zunahme der Dämpfung während der Reaktion zu beobachten ist, die auf Belagsbildung zurückzuführen ist. Nach weiteren Optimierungen der Messzelle und Messmethode ist es möglich, mit der Belagsbildung in der Messzelle die Belagsbildung im letzten Reaktordrittel nahezu zu simulieren und somit die zeitliche Belagsbildung im Reaktor abzubilden. Zudem ist es ebenfalls möglich, durch die Messtechnik auch eine Reinigung des Reaktors zu überwachen und somit analytikbasiert einen sicheren closed-loop-Betrieb zu ermöglichen. Weitere Details zu diesen Ergebnissen sind im Bericht der RUB-EST dargestellt.

Die Erprobung der Stabsonde im Hamburger Labor Versuchs wurde gemeinsam mit CEMOS durchgeführt. Vorversuche zur Beständigkeit zeigen, dass die Sonde gegenüber der Reaktionsdispersion beständig ist, die Reinigung erfolgt mechanisch, da die Sonde nicht dauerhaft gegenüber der Reinigungslösung ist. Erste Messungen im Versuchsstand zeigten zunächst einen erfolgsversprechenden Verlauf des Messsignals, da dieses während der Reaktion signifikant anstieg und nach einiger Zeit eine Sättigung erreichte. Weitergehende Untersuchungen legen jedoch die Vermutung nahe, dass der Anstieg des Messsignals auf eine Zunahme des Festkörpergehalts der Dispersion zurückzuführen ist und nicht wie zunächst angenommen auf eine Belagsbildung. Dabei besteht die Möglichkeit, dass durch den Festkörpergehalt der Dispersion die Sättigung des Detektors bereits erreicht wird und weitere Veränderungen durch Beläge somit nicht mehr detektierbar sind. Auch eine Validierung der Ergebnisse zeigt, dass die Störeinflüsse im System aufgrund von Veränderungen im Festkörpergehalt sowie statistischen Einflüssen größer sind als die zu erwartenden Belagssignale, sodass eine erfolgreiche Belagsdetektion mit diesem Stabsonden-Aufbau im Emulsions-Stoffsystem nicht realisierbar erscheint.

### 3.2.2 AP 2 Quantitatives Monitoring von Belagsbildungsvorgängen in spez. Zellen und Reaktoren der Firmenbeispiele

#### AP 2.2 Belagsbildungsversuche mit integrierter Messtechnik im Laborreaktor

##### Wesentliche wissenschaftlich-technische Ergebnisse:

- Modellierung der Wärmeübergänge des Halbschalenreaktors
- Ermittlung geeigneter Positionen zur Implementierung der faseroptischen Sensoren
- Charakterisierung der Mischgüte im Halbschalenreaktor
- Charakterisierung der Vermischung, insbesondere der Initialvermischung, im Polymerisationsaufbau
- Durchführung von Versuchen zu unterschiedlichen Prozessbedingungen

Der Halbschalenreaktor wurde hinsichtlich seiner Wärmedurchgänge im zu untersuchenden Betriebsbereich simuliert. Anhand der Simulationen wurden gemeinsam mit Fluitec für die Messaufgabe geeignete Positionen zur Implementierung der Glasfasern in den Reaktor identifiziert und von Fluitec ein entsprechender Reaktor gefertigt. (Abbildung 3.14).

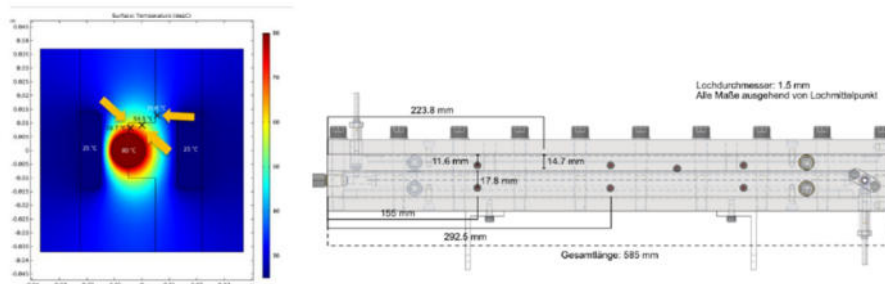


Abbildung 3.14: Simulation der Wärmedurchgänge des Halbschalenreaktors samt zunächst ausgewählter Längsbohrungen sowie Skizze samt nun geplanter Tangentialbohrungen.

Nach Lieferung des Halbschalenreaktors wurde dieser in den Versuchsstand integriert und Emulsionspolymerisationen durchgeführt. Es wurde deutlich, dass der Hauptteil des Belags sich an den statischen Mischelementen bildet, sodass die gravimetrische Belagsquantifizierung ausschließlich auf die Mischelemente bezogen wurde. Dadurch ist eine Ortsauflösung der Belagsbildung im Reaktorverlauf möglich, da jedes Segment einzeln betrachtet werden kann. Bei den ab initio Emulsionspolymerisationen variiert der Belagsschwerpunkt je nach Reaktionsbedingungen. Oft befindet er sich im letzten Reaktordrittel, da die Belagsneigung mit zunehmendem Umsatz der Polymerisation steigt. Lediglich bei Reaktionsbedingungen, die sehr frühzeitig hohe Umsätze erzielen, ist der Belagsschwerpunkt in die erste Reaktorhälfte verschoben.

Der Halbschalenreaktor mit Vormischer wurde auf seiner Mikromischgüte mittels der Villermaux-Dushman Reaktion charakterisiert. Aufgrund der Reproduktionstoxizität von Borsäure wurden Experimente durchgeführt, um einen guten Ersatz hierfür zu finden. Hierbei wurden TRIS [tris(hydroxymethyl)aminomethan und Phosphorsäure untersucht. Das Puffersystem auf Basis von TRIS wurde mit Perchlor- und Schwefelsäure getestet. Aufgrund von diesen Experimenten und Untersuchungen des Verhältnisses von  $\text{HPO}_4^{2-}$  und  $\text{H}_2\text{PO}_4^-$  konnte festgestellt werden, dass die Ionenstärke die Kinetik der Villermaux-Dushman Reaktion beeinflusst und in Berechnungen einfließen muss. Die Reaktionsordnung der Villermaux-Dushman Reaktion mit Phosphatpuffer wurde untersucht. Sie beträgt in Summe 5, bestehend aus der Abhängigkeit der Säurekonzentration ( $\text{H}^+$ ) – 2, der Iodatkonzentration ( $\text{IO}_3^-$ ) – 1, und der Iodidkonzentration ( $\text{I}^-$ ) – 2. Die Reaktionsgeschwindigkeitskonstante wurde in Abhängigkeit der Ionenstärke  $\mu$  festgestellt. Die Mikromischzeiten wurden mit einem erweiterten Inkorporationsmodell berechnet.

$$k = k_0 \cdot f_{\text{Dushman}} = -1.93(\pm 0.06) \cdot \frac{\sqrt{\mu}}{1 + \sqrt{\mu}} + 0.40(\pm 0.02) \cdot \mu \quad (3.1)$$

Mithilfe von Saccharose wurden Lösungen verschiedener Viskositäten hergestellt und das Mischverhalten in Abhängigkeit der Viskosität und der Mischgeschwindigkeit in einem Bulkreaktor untersucht. Abbildung 3.15 stellt die Triiodidkonzentration (mindere Mischgüte) in Abhängigkeit der Viskosität für verschiedene Rührgeschwindigkeiten dar.

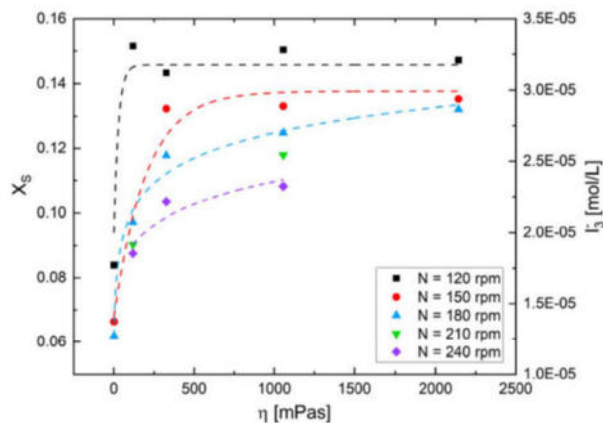


Abbildung 3.15: Ergebnisse von Villermaux-Dushman Versuchen in einem Bulkreaktor bei verschiedenen Viskositäten.

Im Halbschalenreaktor mit Vormischer und ohne Vormischer wurden Mikromischversuche im Viskositätsbereich zwischen 1–1000 mPas durchgeführt. Es wurden pulsationsarme Zahnradpumpen, Exzentrerschneckenpumpen und nicht hubsynchronisierte, pulsationsstarke Hubmembranpumpen bezüglich der Mikromischgüte miteinander verglichen. Die Mikrovermischung wurde für verschiedene Mischergeometrien, wie dem CSE-X/4 4.7 mm, CSE-XD/6 12.3 mm und dem CSE-X/8 G 12.3 mm, mit unterschiedlichen Einlaufkonfigurationen bei Volumenströme von 5–290 mL/min untersucht.

Für den Säurestrom wurde eine 1/16“ Kapillare und ein 8 mm Einlass eingesetzt. Es wurden Mikromischzeiten zwischen 0.02-1.6 s gemessen, wobei der CSE-X/4 mit Vormischer zur effektivsten Mikrovermischung führte. Die Ergebnisse sind in Abbildung 3.16 dargestellt.

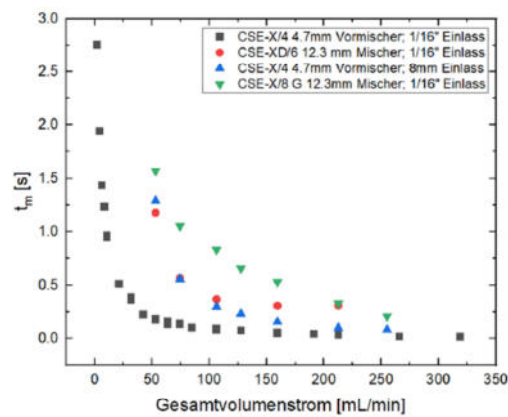


Abbildung 3.16: Mikromischzeiten für verschiedene Konfigurationen in wässriger Lösung.

Zudem wurde die Belagsbildung in Abhängigkeit der Initialvermischung im Halbschalenreaktor untersucht und dabei festgestellt, dass die Belagsbildung des ersten Mischelementes stark von der Einmischung des Initiatorstroms abhängt (Abbildung 3.17).

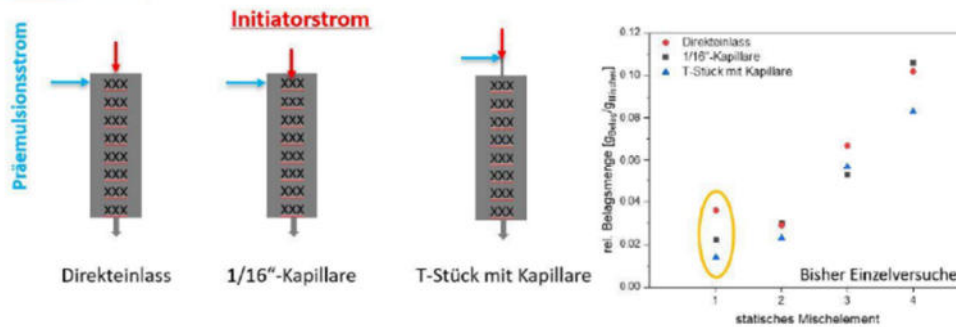


Abbildung 3.17: Darstellung der Einmischungsgeometrien sowie der Belagsmengen betrachtet auf die Mischelemente.

Aus den Versuchen geht hervor, dass die Belagsbildung der Versuche nahezu reproduzierbar verläuft, einzig die Belagsmenge im Eingangssegment weicht zwischen den Aufbauten stark voneinander ab, sodass die Vermutung naheliegt, dass die Initialvermischung einen erheblichen Einfluss auf die Belagsbildung aufweist. Ab dem zweiten Mischelement ist die Einmischung durch die statischen Mischelemente hinreichend gut, sodass Initialeffekte ausgeglichen werden und die Belagsbildung sich angleicht.

Zudem wurde die Abhängigkeit der Belagsbildung von der Monomerzusammensetzung, der Reaktionstemperatur, sowie Rezepturparametern, wie Initiator- und Emulgatoranteil untersucht. Die Auswertung der Versuche legt nahe, dass es signifikante Einflüsse der gewählten Parameter auf die Belagsbildung gibt (Abbildung 3.18).

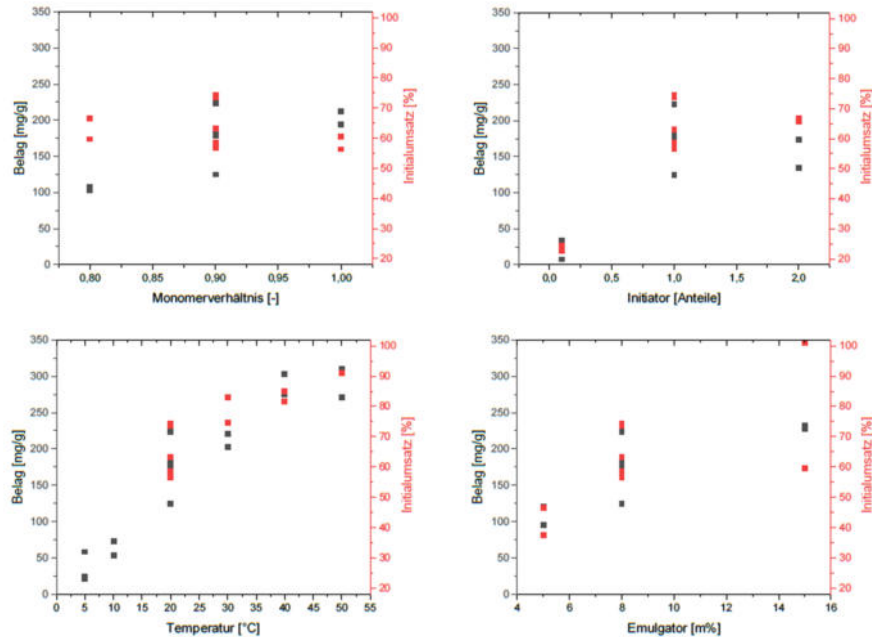


Abbildung 3.18: Auswertungsgrafiken der Versuche zur Untersuchung der Rezeptur- und Prozesseinflüsse auf die Belagsbildung, oben links Zusammenhang zwischen Comonomer-Zusammensetzung und Belagsmasse, oben rechts Auftragung des Einflusses der Initiatormenge auf die Belagsmasse, unten links Einfluss der Reaktionstemperatur auf die Belagsmasse und unten rechts Einfluss der Emulgatormenge auf die Belagsmasse.

Aus Abbildung 3.18 geht hervor, dass alle untersuchten Parameter einen direkten oder indirekten Einfluss auf die Belagsmasse aufweisen. Um direkte von indirekten Einflüssen zu unterscheiden, wurde der Initialumsatz der Reaktion in Abb. 6 ebenfalls mit aufgetragen, um zu differenzieren, welche der Einflussgrößen umsatzbedingt in Erscheinung treten und welche einen darüberhinausgehenden Einfluss haben. So wurde festgestellt, dass Initiator- und Emulgatorgehalt sowie Temperatur lediglich einen Einfluss auf den Reaktionsumsatz und dadurch mittelbar auch auf die Belagsmasse ausüben. Dabei ist der Einfluss des Umsatzes der Größte auf die Gesamtbelagsmenge. Zudem weist Monomerzusammensetzung einen Einfluss auf die Belagsbildung auf, welcher in der erhöhten Klebrigkeit der Polymere mit steigendem Vinylacetat-Anteil zu begründen ist und unabhängig von Umsatz oder Polymeranteil ist. Diese Untersuchungen stellen ein spannendes wissenschaftlich-technisches Ergebnis dar, welches aber die



wirtschaftliche Nutzung fraglich erscheinen lässt, da alle Belagsvermeidungsstrategien die hieraus hervorgehen die Effizienz des Prozesses herabsetzen würden und somit an Wirtschaftlichkeit einbüßen.

### 3.2.3 AP 3 Modellhafte Beschreibung von Belagsbildungsvorgängen

#### Wesentliche wissenschaftlich-technische Ergebnisse:

- Versuchsplan zur Belagsvorhersage durchgeführt
- Aus Versuchsplan wurden Temperatur, Emulgator- und Initiatorkonzentration sowie Comonomer-Verhältnis als relevante Größen ermittelt
- Direkte Einflüsse auf die Belagsbildung haben der Umsatz und die Monomierzusammensetzung
- Umsatz wird beeinflusst durch Temperatur, Emulgator- und Initiatorkonzentration
- Aus Experimenten wurden Modellterme für alle Einflussgrößen entwickelt und zu einer Modellgleichung kombiniert
- Belagsvorhersage für vergleichbare Rezepturen mit Abweichungen unter 15 % möglich

Aus den Einflussfaktoren aus Abbildung 3.18 geht hervor, dass alle Faktoren einen Einfluss auf die Belagsbildung ausüben. Aus den experimentellen Daten konnte darüber hinaus ein mathematisches Modell zur Belagsvorhersage entwickelt werden, welches es ermöglicht, die Belagsmasse anhand der gewählten Werte für die Parameter mit einer Genauigkeit von 15 % abzuschätzen. Dabei wurde als Gesamtgleichung für das Modell Gleichung 3.2 erhalten. Die detaillierte Herleitung der Gleichung ist aktuell zur Publikation eingereicht.

$$\begin{aligned}
 m_{\text{fouling}}(T, [I], [E], x_{VAc}) = & \\
 3.26 \cdot \left( 90.24 \cdot e^{-\frac{173.6}{8.314T}} + 31.75 \right) \cdot (\sqrt{[I]}) & \\
 \cdot \left( \frac{(-0.612 \cdot [E] + 22.5) \cdot \frac{(1.24 \cdot 10^{25} [E])}{N_L}}{65.016} \right) & \quad (3.2) \\
 + 486.4 x_{VAc} - 467.2 &
 \end{aligned}$$

Um das Modell zu Validierung wurden mit dem Modell Belagsmassen für bestimmte Versuchsbedingungen berechnet und mit experimentell gemessenen Belagsmassen verglichen (Abb. 3.19).

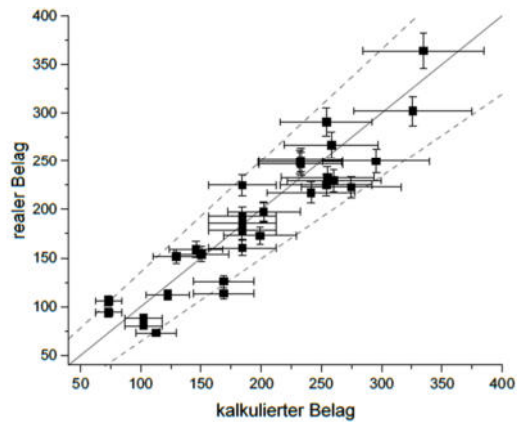


Abbildung 3.19: Darstellung der experimentell gemessenen Belagsmassen gegenüber den modellbasiert berechneten Belagsmassen zur Validierung des Modells. Die y-Fehlerbalken beschreiben die Messfehler während des Experiments, während die x-Fehlerbalken den intrinsischen Unsicherheitsbereich des Modells angeben. Die durchgezogene Linie gibt den erwarteten Wert an, die gestrichelten Linien den Unsicherheitsbereich.

Aus Abbildung 3.19 ist zu erkennen, dass das Modell zur Vorhersage der Belagsmassen im betrachteten Rezepturfenster gut geeignet ist und meist im angegebenen Unsicherheitsbereich liegt.

### 3.3 Fortschreibung des Verwertungsplans

Seitens der ITMC-UH als akademischem Partner waren als Verwertung Publikationen sowie die Präsentation auf wissenschaftlichen Tagungen geplant. Die wissenschaftlichen Ergebnisse wurden bereits in peer reviewed Publikationen zu Mikrovermischung und *inline*-Analytik für Emulsionspolymerisationen veröffentlicht. Weitere 3 drei Publikationen zu Einflüssen auf die Belagsbildung im untersuchten Stoffsystem sowie Sensorkonzepten in konkreter Planung und werden in den nächsten Monaten umgesetzt. Auch langfristig nach Projektende stehen die Erkenntnisse aus dem Projekt damit der zur Verfügung und auch an der ITMC-UH werden an das Projekt vertiefende Arbeiten einzelner Aspekte angeschlossen, um weiteren wissenschaftlich-technischen Nutzen zu erzielen. Insbesondere auf dem Feld der faseroptischen Temperaturmessung sind noch weitreichende Arbeiten in Planung. Zudem ist ein weiteres Projekt zur Untersuchung von hydrophilen Beschichtungen bei der kontinuierlichen Emulsionspolymerisation in Zusammenarbeit mit der Universität Paderborn sowie der Wacker Chemie in Planung. Folglich werden auch nach Projektende die wissenschaftlichen Erkenntnisse genutzt und an einer Fortführung der Projektziele gearbeitet.

### 3.4 Arbeiten, die zu keiner Lösung führten

Im Rahmen des Projektes konnten nicht alle Ideen erfolgreich umgesetzt werden. Das Hauptziel einen kontinuierlichen Betrieb der gewählten Polymerisation im Technikumsmaßstab umzusetzen wurde nicht erreicht, da eine hinreichende Belagsvermeidung im Stoffsystem nicht gelang. So konnten zwar zahlreiche Erkenntnisse zur Belagsbildung gewonnen werden, diese führten allerdings nicht zur Findung eines Betriebszustandes, der bei sinnvollen Prozessbedingungen Reaktionszeiten von mehr als 5 Stunden zuließ. Somit war eine Realisierung im Technikumsmaßstab nicht möglich. Zudem wurden im Rahmen des Projektes keine Lösungen für die Implementierung mancher Sensorkonzepte erzielt. So konnte die Stabsonde, deren theoretische Eignung für das Emulsions-Stoffsystem bei der TUBS gezeigt werden konnte, nicht erfolgreich in den Versuchsstand der ITMC-UH implementiert werden, da im genutzten Aufbau die Störeffekte durch veränderliche Festkörpergehalte und statistische Effekte größer waren als eine belagsinduzierte Signaländerung. Auch für die Implementierung der faseroptischen Temperaturmessung in den Halbschalenreaktor konnte im Projekt keine Lösung gefunden werden, da diese zwar eine sehr gute Eignung in Testständen zeigen, die Wärmeleitung des Edelstahl aber eine Detektion thermischer Effekte in den Bohrungen des Halbschalenreaktors sehr herausfordernd macht.

### 3.5 Präsentationsmöglichkeiten für den Nutzer

Sämtliche wesentlichen Erkenntnisse der ITMC-UH wurden detailliert dokumentiert und wurden oder werden publiziert. Somit stehen die Ergebnisse allen Interessenten in Form von Veröffentlichungen zur Verfügung und können auch präsentiert bzw. zitiert werden. Zudem wurden detaillierte Berichte verfasst, die ebenfalls mit allen Projektpartnern geteilt wurden und als Basis für mögliche Präsentationen dienen können. Dabei sind vertrauliche Abschnitte als diese gekennzeichnet, sodass Interessenkonflikte eindeutig vermieden werden. Für weitergehende Präsentationen steht die ITMC-UH möglichen Interessenten auch jederzeit zur Verfügung und unterstützt diese bei ihren Vorhaben.

## 6. Unpublished Work

This thesis approaches the topic of fouling during continuous emulsion polymerisation on different ways. Some parts of the investigated topics have been published in scientific articles, but many findings were not published so far. Some of them are here shortly presented as there are interesting results which did not lay within the scope of the published topics. Lots of this could be published with intensified research on these topics as well and the chosen publications above are just the most promising parts. Moreover, the reactor setup was characterised before the conduction of polymerisation reactions inside. Some aspects of this are presented here.

### 6.1 Residence time characterisation of the tubular reactor

The residence time distribution is one relevant characteristic of every reactor. The residence time distribution enables disclosures to dead zones and short-circuit currents in the reactor. For that purpose, the residence time distribution of the used tubular reactor was investigated and the suitability of measured residence times for fouling quantification evaluated.

The residence times were measured by adding colour-marker directly at the inlet of the tubular reactor and detecting the output signal photometrically. This signal was compared with the calculated mean hydrodynamic residence time. If short-circuit currents exist, colour-marker can be detected before reaching the hydrodynamic residence time. Dead zones would also cause a tailing of the colour-marker because the marker remains in the dead zones and is released later. The reactor volume is  $V_R = 45.5$  mL, and the total mass flow rate was set to  $\dot{m} = 12.6$  g/min. The hydrodynamic residence time  $\tau_{hyd}$  can be calculated using equation 1.<sup>[87]</sup> For the calculation of the hydrodynamic residence time, the mass flow must be converted into the volume flow using the density of the system.

$$\tau_{hyd} = \frac{V_R}{\dot{V}} = \frac{V_R}{\frac{\dot{m}}{\rho_{mean}}} = \frac{V_R}{\frac{\dot{m}}{\sum(w_i \cdot \rho_i)}} \quad (1)$$

As simplification the density of water can be used, so that mass flow and volume flow are the same. The hydrodynamic residence time with this simplification is calculated to  $\tau_{hyd,ideal} = 3.61$  min. For a more precise approach the densities of the monomers must be considered. With the densities of vinyl acetate  $\rho_{Vac} = 0.94$  g/cm<sup>3</sup> and vinyl neodecanoate  $\rho_{VeoVa} = 0.88$  g/cm<sup>3</sup> the volume flow rate is a bit increased, and the hydrodynamic residence time decreases to  $\tau_{hyd,real} = 3.55$  min. The difference between both residence times is below the precision of the reactor set-up so that there is no need to consider the densities of the

components of the system. The hydrodynamic residence time for this tubular reactor is  $\tau_{\text{hyd}} = 3.6$  min.

The real residence times were measured using a colour-marker and water determining the coloration of samples taken at the inlet and outlet of the reactor. The recovery rate of the colour-marker was determined as 79.3 % and measured intensities were area standardised for evaluation of residence times. A gaussian approach was chosen to fit the real residence time distribution (Figure 6).

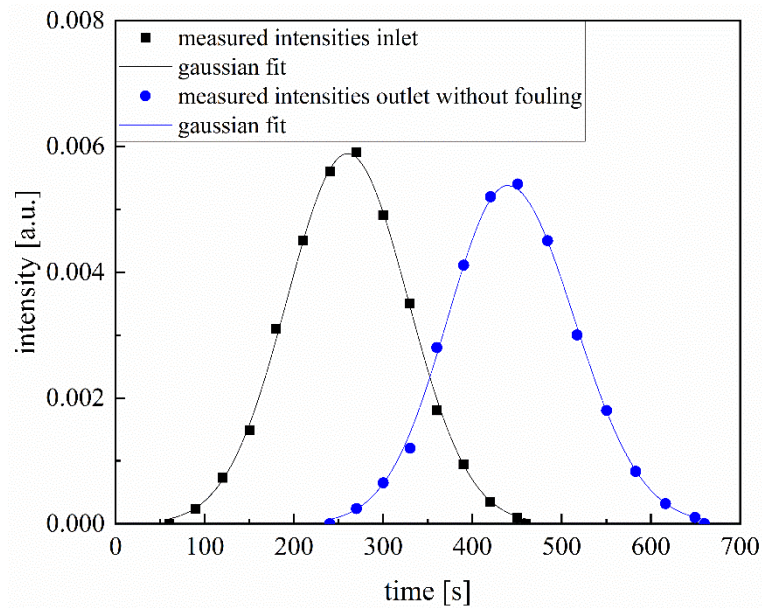


Figure 6: Residence time measurements for the tubular reactor without fouling using colour-markers in water. The intensities of colouration were measured at the inlet and outlet of the reactor photometrically and the mean residence time was determined as time between the mean inlet signal and mean outlet signal.

The real residence time distribution measured for the reactor without fouling results in a mean residence time of  $\tau_{\text{real}} = 3.1$  min which is lower than the hydrodynamic residence time with  $\tau_{\text{hyd}} = 3.6$  min. This indicates that not the whole reactor shows an even flow profile and dead zones are present. Moreover, the real residence time distribution at the outlet (420 s from first marker-signal to last marker-signal) is wider than the one of the inlet (380 s) and tailing of the signal can be observed, which indicates dead zones in the reactor. Concluding, the reactor has a non-ideal flow profile with significant dead zones that are reducing the mean residence time about 15 % compared to the hydrodynamic residence time. With the hydrodynamic residence time and variance of the residence time distribution the BODENSTEIN number can be calculated.<sup>[88]</sup> For the reactor, a BODENSTEIN number of 22.4 was obtained, which indicates a continuous flow with low back mixing.

In the next step, residence time measurements with the same procedure were carried out in a rinsed tubular reactor with intense fouling to compare the measured residence times and evaluate if fouling can be detected by this characteristic reactor parameter (Figure 7). Measurements were carried out using water and colour-marker.

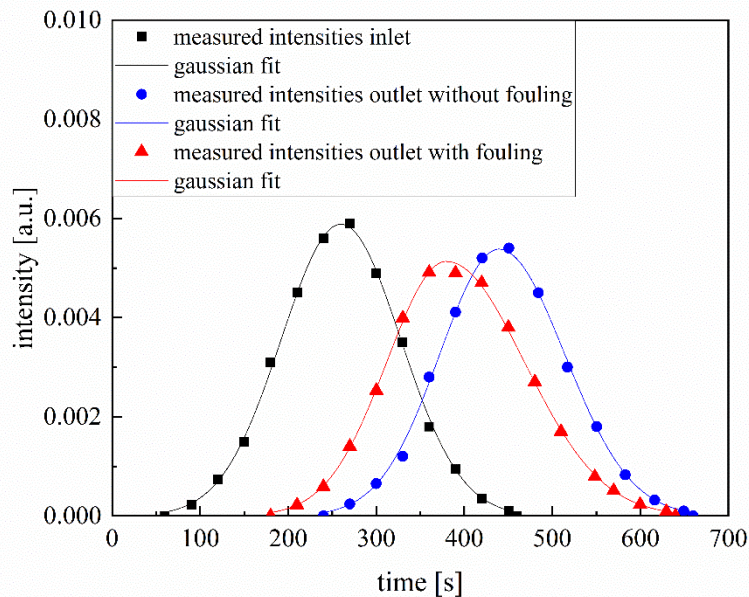


Figure 7: Residence time measurements for fouling detection in the reactor. A reactor containing fouling produced by the standard recipe was used and after rinsing with water the residence time was measured using water and colour-marker.

The residence time distribution is significantly affected by the fouling in the reactor. The mean real residence time with fouling is  $\tau_{\text{real,foul.}} = 2.2$  min which is significantly reduced to the real residence time for the empty reactor  $\tau_{\text{real}} = 3.1$  min. As reference the reactor filling with fouling was determined gravimetrically by differential weighting of the reactor before and after the reaction, resulting that 55 % of the reactor volume are filled with deposits. The decrease in residence time is 30 % and with that lower than the calculated filling of the reactor by gravimetric methods. Compared with the hydrodynamic residence time  $\tau_{\text{hyd.}} = 3.6$  min, the residence time with fouling is 40 % reduced, which is comparable to the gravimetrically reactor filling. The comparability of this is given as the formation of deposits is favoured in dead zones. The whole reactor volume has to be considered for comparing fouling and not only the even flowed parts. Moreover, the tailing of the residence time distribution is much stronger with fouling in the reactor (480 s from first marker-signal to last) as there are more complex flow profiles and colour-marker can be retained in the fouling. All in all, fouling affects the residence time distribution in two ways. Firstly, the mean residence time is reduced by fouling. For high fouling masses a reactor filling can be estimated with residence time measurement. Secondly, the residence time distribution is getting wider with more fouling occurring and tailing of the signal is more significant, so dead zones are increasing and the flow profile is less ideal.

## 6.2 Cleaning procedures for polymerisation reactors

The reactor cleaning is a crucial point in the field of fouling research as one possible strategy can be an efficient cleaning of the reactor when fouling occurs. A first cleaning strategy is described in literature<sup>[89,90]</sup> but there are further optimisations possible so cleaning of deposits was investigated here. Different approaches were examined for deposits formed by emulsion polymerisation, both chemical and mechanical cleaning was tested. As factors the remaining fouling mass, the total time from end of the reaction to start of the next reaction and the scale-up potential was evaluated. All cleaning concepts were firstly tested with the static mixers type CSE-X (see ch. 5.2, p. 42, Fig. 1a) in a batch cleaning process and the most promising of them afterwards transferred to continuous cleaning of the whole reactor.

For chemical cleaning, the reactor was washed with solvents that show a good solubility for the polymer. Solvents tested were acetone and methanol as well as mixtures containing alkaline solvents. The advantage of alkaline is that ester bonds are hydrolysed and the solubility in hydrophilic solvents is increased. For this reason, mixtures containing sodium hydroxide or potassium hydroxide in water combined with methanol or ethanol were investigated. The temperature dependency of the cleaning was examined as well.

In literature a cleaning by mixing 50 wt.% 8 mol/L aqueous sodium hydroxide and 50 wt.% ethanol was discussed. The mixture was circulated for three to six hours at 80 °C in the reactor. It was shown that the cleaning of deposits formed from circulating non-reactive polymer dispersions was successful.<sup>[86,89,90]</sup> A recovery of the cleaning solution was not discussed. Concluding, this method is both time and resource consuming and seems not efficient on industrial scale but reaches good cleaning results on lab-scale.

Alkaline cleaning as described in the publications mentioned above<sup>[89,90]</sup> causes changes in the structure of fouling but is not suitable for efficient cleaning. The white deposit is changed to a more dense, yellowish polymer but is not solved in the cleaning solution. Even 24 h of treatment with cleaning solution at 60 – 80 °C do not remove the deposits completely. This agrees with literature as polyvinyl alcohol is poorly soluble in organic solvents and even hot water.<sup>[91]</sup> Cleaning can be reached by repeated treating the static mixers in hot alkaline solution followed by boiling water to dissolve the formed polyvinyl alcohol. With this procedure most fouling can be removed and only small aggregates of fouling remain at spots which are bad accessible. Concluding the effort for cleaning the static mixers in a batch process, this approach was not transferred to continuous cleaning.

Solvent cleaning of the static mixers was performed with acetone, methanol and tetrahydrofuran as all three solvents dissolve the polymer emulsion sufficient. A disadvantage of tetrahydrofuran is that the emulsifier polyvinyl alcohol is insoluble so that even small amounts of the emulsifier cannot be removed with this solvent. The polyvinyl acetate copolymer is partially soluble in all of the solvents at 20 °C. With acetone the deposits are swelling within minutes but dissolving is a slow process which needs more than 48 h. At elevated temperatures the solubility is improved. With acetone under reflux cleaning with residues below 2 % is possible within 3 h in batch cleaning. As this was the best examined chemical approach the transfer to continuous cleaning without dismantling of the reactor was performed. One major aspect in continuous cleaning is the accessibility of fouling as its coincidences that fouling occurs primarily on dead zones. Dead zones are the most difficult to clean by rinsing the reactor as exchange is very slow there. Moreover, boiling solvents cannot be handled safely in continuous PFRs so that acetone at 20 °C and 50 °C was used for cleaning. Both can achieve reduction in fouling, especially in zones with high flow velocities but the residues after cleaning are higher as dead zones are addressed insufficient and diffusion of polymers is very slow. An increased temperature reduces the cleaning time but the effect is lower than in batch cleaning as the accessibility of dead zones remains a problem.

Besides chemical cleaning concepts it was investigated if cleaning can be more efficient with addition mechanical influences. For that purpose, the batch cleaning with acetone was compared with cleaning in acetone in an ultrasonic bath to improve diffusion and fasten dissolving of the polymer. The cleaning times for the static mixers could be reduced from several hours without ultrasonic treatment to few minutes with ultrasonic treatment. For fouling intense cleaning situations two or three repetitions of the cleaning and rinsing were necessary to remove the deposits fully. For lab-scale applications the time from end of one reaction to the start of the next reaction was between 1.5 h and 2 h, which allows efficient cleaning. Any further optimisation in cleaning time would not increase efficiency as the preparation of the next reaction needs the same amount of time and both can be done parallel. This procedure was chosen as resource-friendly and efficient cleaning concept with minimal use of solvent and time. The scale-up potential is challenging as concepts which need a deconstruction of the reactor set-up are not favourable on larger scale.

Concluding different cleaning strategies were tested and some of them are useful and efficient on lab-scale but none of them seems promising on industrial scale. So, the scale-up potential is still a challenge to solve in cleaning procedure in an industrial process.



### 6.3 Influences of reactor coating on fouling masses

Reactor coatings with various materials are described in literature to reduce fouling during polymerisation reactions.<sup>[49–52]</sup> Previous work showed that surface materials which reduce the surface energy by their low surface energies could reduce polymerisation fouling so that polymer fouling is dominant and total fouling masses are significantly decreased. Moreover, a smoothed surface would reduce polymer fouling as reported.<sup>[92]</sup> The coating of static mixers or the complete reactor would be expensive, so in a first step circular sample plates ( $d = 29\text{mm}$ ) were coated via atomic layer deposition (ALD) and the fouling behaviour on them observed. The plates with hydrophilic and hydrophobic coatings were implemented in the measurement cell for ultrasonic measurements<sup>[85]</sup> as it was easily accessible for testing and samples can be removed and analysed. The coatings tested were a hydrophilic titanium dioxide ( $\text{TiO}_2$ ) coating with a water contact angle (WCA) of  $11^\circ - 14^\circ$  and a hydrophobic polydimethylsiloxane (PDMS) coating with a water contact angle of  $150^\circ - 160^\circ$ . The coatings were compared with sample plates of the same electropolished stainless steel without coating. All experiments were performed using the standard recipe published before for comparability.<sup>[85]</sup> For all experiments a runtime of 45 min was chosen and the amount of fouling as well as the cleaning behaviour was investigated.

The stainless-steel reference plates result in fouling masses between 4.3 g and 4.9 g. The deposit was strong attached to the plates and cleaning was only with mechanical work or solvent possible. The hydrophobic PDMS coating does not result in a reproducible reduction of fouling mass but the adhesion of fouling at the coated surface was weaker and deposits can be removed by rinsing with water easily. A possible explanation for this is that the adhesion to coated surfaces is lower and therefore the fouling can be removed easier. After rinsing a thin film remains at the surface which can be removed mechanically. For hydrophilic titanium dioxide coatings, the fouling mass in the measurement cell was reduced but the variance between three experiments was large with 0.2 g to 3.0 g deposit on the sample plates. The adhesion of the deposits is again weaker than on stainless steel and deposits can be removed by rinsing with water and only a few micrometres thick film remains on the surface (Fig. 8).

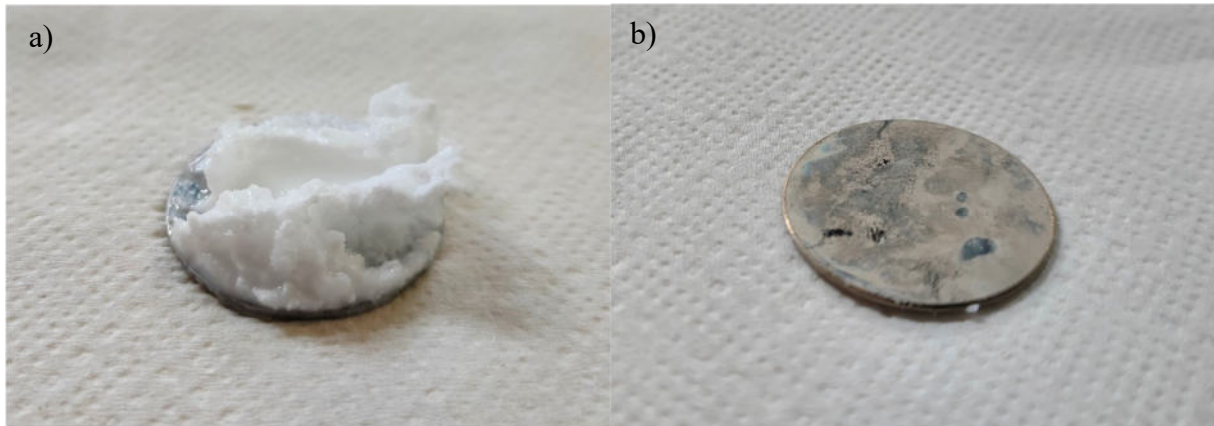


*Figure 8: sample plates hydrophilic coated with titanium dioxide a) directly after 45 min polymerisation in the measurement cell and b) after rinsing with water showing the thin, remaining fouling layer.*

There are two possible explanations for this finding. On one hand, fouling can still occur on the coated surfaces and only mechanical or chemical cleaning is improved with the coatings to increase efficiency. On the other hand, fouling grows at the uncoated sides of the measurement cell and reaches the sample plate during growth. Only the thin film is directly deposited on the plate, so this film is difficult to clean and the rest can be removed as it was never attached to the coated areas. For evaluating this it would be necessary to coat larger parts of the reactor to prevent growing of fouling from uncoated surfaces to the coated. An evaluation of the influences on fouling masses should be the next step to investigate coatings for fouling reduction or increased cleaning efficiency as results are promising so far.

## 6.4 Chemical properties of polyvinyl acetate dispersions

In emulsion polymerisation the most relevant properties are the particle size of the dispersion and the molecular weight distribution of the resulting polymer. The stability of the dispersion is important as well as instable dispersions change their properties fast after production. For many applications the reaction conversion is relevant as volatile organic compounds like monomers are not allowed in the products and removing them is mostly expensive and time consuming. All these parameters must be considered for comparing different polymer dispersions. The polymer properties of the obtained dispersions and their dependency of the production process were investigated.

The reaction conversion of the polymerisation is strongly dependent on reaction conditions. Regarding the emulsion copolymerisation of vinyl acetate conversions between 20 % and 100 % can be realised by choosing suitable formulations and process parameters. For the standard recipe<sup>[84]</sup> the initial conversion is between 65 % and 85 % and decreases with time as fouling reduces reaction volume.<sup>[85]</sup> Higher reaction conversions can be reached by increased initiator content, higher temperature, or higher residence times. For high solid content polymerisations, the reaction conversion is mostly between 40 % and 60 % and can be increased to 80 % but high conversions cause challenges in dispersion stability and flow control. If residence times were set to a point where full reaction conversion is reached, the flow velocity is so low that sedimentation and with that even more fouling occurs. Concluding, for emulsion polymerisations with monomer contents above 30 wt.% the chosen reactor design is not favourable and a second stage for post-polymerisation would improve conversion and product properties as reaction conversion and flow velocities can be adjusted. Compared with batch reactions the conversion in continuous reactors is decreased as batch reactors reach full conversion with residual monomer contents below 1 % for a wide range of formulations. For continuous operated polymerisation full conversion is more challenging as cooling capacity is higher which reduces conversion. The residence time must be adjusted for every recipe to obtain full conversion. On the other hand, reaction control is increased as cooling capacity is increased, and reaction temperature can be adjusted precise which allows more control for product properties. Concluding, the conversion is in continuous operation mostly lower than in batch polymerisation and reaching the same conversion is more effort in continuous operation. Otherwise, process control is increased, and same conversions can be reached with adjustments in residence time.

The particle sizes of the obtained dispersions were analysed by dynamic light scattering (DLS) and disk centrifuge. Both methods are widely used for particle size measurement in polymer dispersions.<sup>[93]</sup> The particle sizes of dispersions investigated in this work varied between 80 nm and 350 nm related to the used conditions. The strongest correlation is given by the emulsifier content, which determines the number of formed micelles and with that the particle size of the dispersion. Number mean particle sizes are reproducible between 180 nm and 230 nm, for deviations the emulsifier content must be changed significantly. Compared with batch polymerisation for the same recipe no change in particle sizes depending on operation mode is observed. Only if process parameters are preventing a stable process, there are different particle sizes in continuous operation. Concluding, in this case the particle size as important product property is not affected by the operation mode of the process, so for vinyl acetate copolymers a change in process can be achieved without changing product properties. This is important for polymers as they are products by process and their applications depend highly on polymeric properties.

The stability of the dispersions was investigated as well to detect if operation mode changes the properties of the dispersion. For investigation of dispersion stability two analysis were carried out. Firstly, the dispersions were evaluated optically if there is visible phase separation or sedimentation. Moreover, the mean particle size of the same dispersion samples was measured via DLS over time and the change in particle sizes was analysed for quantifying agglomeration. The most important parameter for emulsion stability is the emulsifier content as the emulsifier stabilises the latices. Emulsifier contents between 2 wt.% and 25 wt.% based on monomer content were investigated. Both, less and too much emulsifier causes a decrease in emulsion stability. For emulsions with less than 4 wt.% emulsifier content, the optical evaluation detects heavy sedimentation and phase separation within hours or days. Dispersions with an emulsifier content of 4 wt.% are stable on short terms but show slow sedimentation within weeks. Polymer dispersions with emulsifier contents of 8 wt.% to 12 wt.% are optically stable for at least 30 days at 25 °C without showing sedimentation. After 90 days at 25 °C most of the samples are still stable but some are starting to sediment. Above 16 wt.% emulsifier content the sedimentation increases slightly, and dispersion stability is reduced. This can be caused by the emulsifier polyvinyl alcohol which tends to form clusters which are less stable than dissolved molecules.<sup>[91]</sup> The particle sizes of some samples of dispersion which are optically stable were measured over time to detect changes caused by agglomeration and ripening (Figure 9).

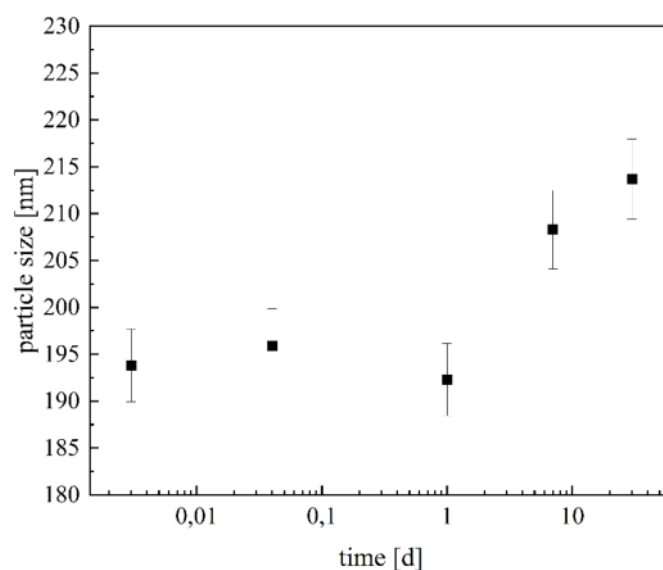


Figure 9: Development of particle sizes of polymer dispersion samples of the standard recipe with 8 wt.% emulsifier<sup>[85]</sup> over time to detect agglomeration. As the time intervals were wide, a logarithmic scale was chosen.

The mean particle size of the dispersion is stable for at least one day but is slowly increasing over weeks. This indicates that agglomeration and ripening is occurring in the polymer dispersions but it is a slow process which affects the product properties in the first weeks neglectable. After 30 days the mean particle size is 10 % increased but sedimentation is still not visible. Concluding, the particle size of the dispersion is changing with storage but most recipes are stable and sedimentation can be observed first after more than 30 days. The stability of dispersions obtained from batch polymerisation and continuous polymerisation is completely comparable and no difference given by the operation mode can be detected.

The molecular weights of the polymer dispersions were evaluated as well as it is an important product property. Number mean molecular weights between 10 kg/mol and 150 kg/mol were obtained. The most dispersion had number mean molecular weights between 25 kg/mol and 40 kg/mol. Molecular weights were influenced by process parameters as initiator concentration and monomer content as expected, because the monomer to initiator ratio is changed and termination and growth influenced. There was no significant influence of the operation mode on molecular weights of the polymer as no time or concentration limitation was given by the operation mode.

All in all, the product properties of the polymer dispersion are not dependent on the operation mode and polymers with same properties as in batch polymerisation can be obtained with continuous plug flow reactors. The most difficult parameter is the monomer conversion where adjustments in residence time are necessary to obtain comparable results, but molecular weights, particle sizes and dispersion stabilities are independent of operation. Concluding, the product properties allow a transfer to continuous polymerisation.

## 6.5 Chemical properties of polyvinyl acetate deposits

The chemical properties of the fouling material were analysed as well. While particle size and dispersion stability are important parameters for the product emulsion, for the fouling these cannot be determined. Here the important parameters are solubility and swelling behaviour in different solvents as well as the molecular weight of the polymers obtained. The molecular weights are significantly higher in deposits than in the dispersion but have already been discussed briefly in one of the publications.<sup>[85]</sup> The main point will be solubility and swelling behaviour of the polymer to determine possible branching and crosslinking which would influence the solubility. As solvents methanol, acetone and tetrahydrofuran were used. The soluble share at 20 °C and under reflux was measured and a swelling rate of the gel fraction determined. For analysing the soluble share under reflux two procedures were carried out, a Soxhlet extraction and dissolving in boiling solvent and filtration after 24 h of boiling. The results of both methods are not comparable as dissolving long-chain polymers takes time and in a Soxhlet extraction there is a time-limitation which increases gel fraction. For evaluation the fresh deposits from the tubular reactor were used. These deposits contain 30 % to 40 % of volatile compounds which were determined by differential weighting and drying the deposits at 120 °C for 24 h. This fraction is mainly water, but small amounts of remaining monomer are most likely included as well. For Soxhlet extraction the deposits were dried and a gel fraction of 45 % to 55 % of the dried mass obtained. As solvents acetone and tetrahydrofuran were used and both solvents were comparable in gel fraction content resulting. The gel fraction after boiling 24 h in the solvents and filtration afterwards is with 2 % to 5 % of the fresh deposit mass and 3 % to 8 % based on dried deposits much lower than the gel fraction determined by Soxhlet extraction (Figure 10). This indicates that the molecular weights in the deposits are entangled but no significant crosslinking is present. As the gel fraction is that small swelling tests do not appear significant.

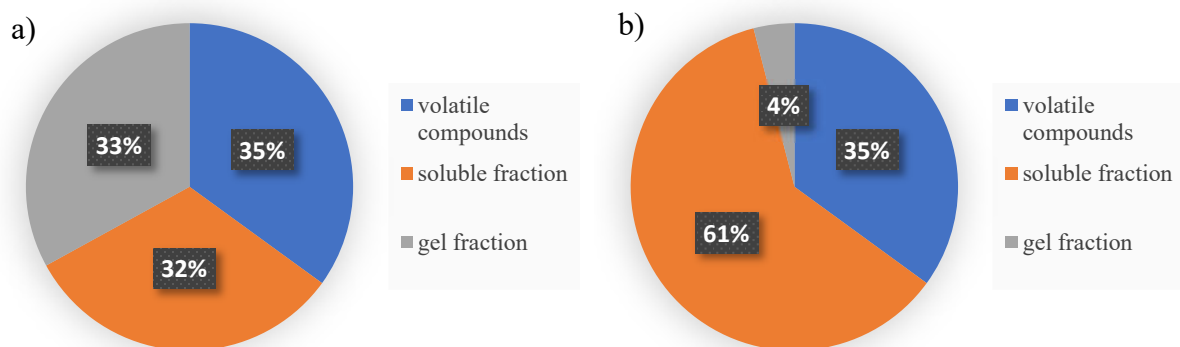


Figure 10: Visualisation of the composition of the deposits depending on the extraction method a) Soxhlet and b) boiling for 24 h.

## 6.6 Influences of comonomer composition on polymerisation and product properties

The comonomer composition is one of the parameters directly influencing the fouling mass.<sup>[84]</sup> Following it is a promising approach to change the comonomer composition for reducing fouling. The polymer properties are likely influenced by the change in comonomer composition as well, so the influences were investigated.

The comonomer composition is changed gradually between pure vinyl acetate and 50 wt.% vinyl neodecanoate and glass transition temperature and monomer conversion measured for comparison of product properties. Vinyl neodecanoate is a monomer with a larger sidechain so the free volume of the polymer should be increased and following the glass transition temperature should decrease. For conversion there may be a sterically hindrance that reduces conversion. The conversion during batch copolymerisation of vinyl acetate and vinyl neodecanoate were measured (Figure 11).

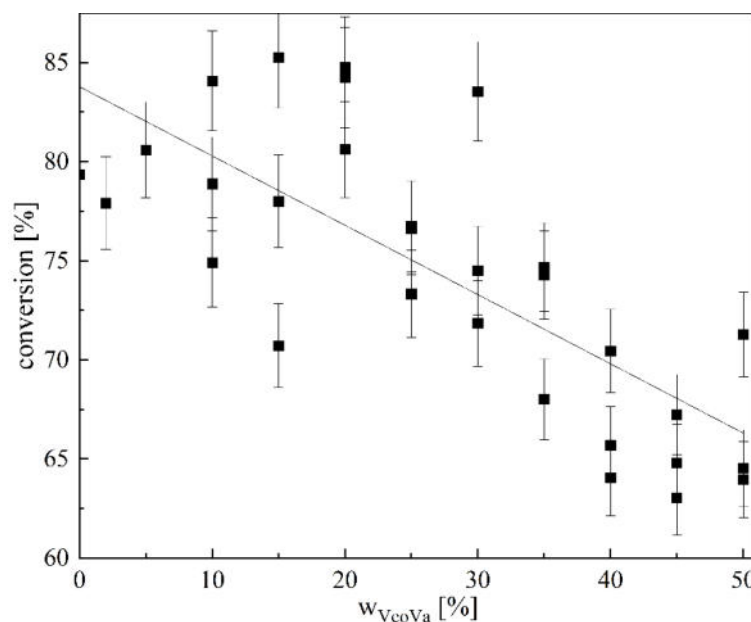


Figure 11: Monomer conversion of the polymerisation depending on the comonomer composition.

The conversion is strongly influenced by the monomer composition, for vinyl neodecanoate contents up to 20 wt.% the conversion of the polymerisation is not significantly influenced. An increased share of vinyl neodecanoate reduces the conversion significantly. This is caused by sterically hindrance of the vinyl neodecanoate. Particle sizes and molecular weights of the formed polymer are not significantly influenced by the comonomer composition. The glass transition temperature is another parameter which was investigated as it should be influenced by the monomer composition (Figure 12).

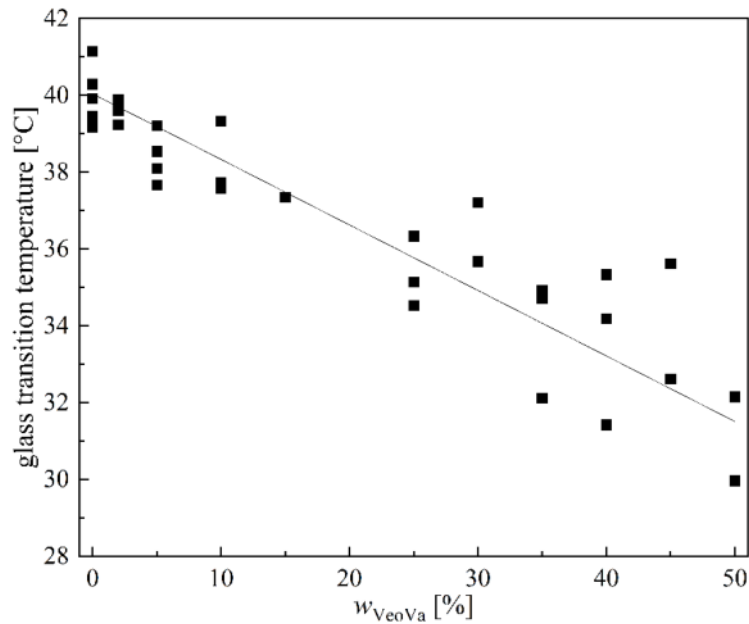


Figure 12: Correlation between glass transition temperature and comonomer composition given as weight fraction of vinyl neodecanoate.

The glass transition temperature is strongly decreased by an increased amount of vinyl neodecanoate. This is in good accordance with theory but changes the product properties of the polymer dispersion. In literature the glass transition temperature for polyvinyl acetate homopolymer is given with 28 °C.<sup>[94]</sup> For polyvinyl neodecanoate homopolymer a glass transition temperature of -3 °C<sup>[95]</sup> is published, so the glass transition temperatures of the copolymers should be between this values depending on their composition. The glass transition temperatures found in the experiments are generally higher than in literature described but the trends agree well. The comparison between batch polymerisation and continuous polymerisation shows no differences caused by operation mode. Concluding, the comonomer composition is an important parameter for adjusting the product properties but is not influenced by the operation mode of polymerisation.



## 7. Discussion

Fouling is and will always be an important topic for industrial processes, especially for polymerisation processes. An all-encompassing solution for this challenge would be a big benefit but this is nearly impossible to reach as every process and every recipe is very different and the reasons for fouling are various. For that reason, every process must be investigated detailed and improvements for that process can be found.

In this work various aspects regarding fouling during continuous emulsion polymerisation of vinyl acetate were discussed. Even for this system no global solution for fouling prevention could be obtained but lots of insights were gained and different improvements were made.

In the first part the fundamentals were set, and a robust and reproducible setup was investigated. For this reason, a recipe previously similar used for emulsion polymerisation in batch and continuous PFR was investigated and optimised for high solid, fouling intense polymerisations.<sup>[8,96]</sup> A redox-initiated polymerisation was chosen as it is similar to industrial processes and a wide temperature range is accessible. The initial conversions of the standard polymerisation were constantly between 75 % and 90 % in the used reactor and polymer conversion decreases with time caused by fouling and the resulting loss in reaction volume. With changes in the recipe the initial conversion can be reduced to 20 % – 30 % or increased to nearly full conversion. The mean particle size in batch as well as continuous operation is normally between 180 nm and 220 nm but can be adjusted by changes in the recipe from 100 nm to 300 nm to obtain stable dispersions. This particle sizes and conversions are comparable with other publications in academic research. In industrial processes the conversion must be higher so usually reaction time is increased to reach full conversion and a low concentration of volatile organic compounds (VOC). The fouling mass of this standard recipe was reproducible with an accuracy of 15 %. Fouling will never occur perfectly reproducible as lots of statistical effects affect the fouling formation so that a deviation in fouling mass will always be found and must be measured. With a deviation of 15 % in fouling masses it is possible to analyse effects on fouling formation that are stronger than this deviation. This should be possible for most effects if parameter ranges are chosen wide enough. Concluding, a standard recipe was established, and the reproducibility and robustness proven and quantified.

With the knowledge about a standard recipe and the deviations within the recipe was varied and effects on the fouling mass, conversion and molecular weight of the polymer were analysed. In the first step, the single-factor influences were investigated to determine the factors which

influence the fouling. Investigated factors were the comonomer composition, the concentration of initiator and emulsifier, and the temperature. All these factors influence the fouling mass in the reactor which is in good accordance with the theory. The difference is that some factors are directly influencing the fouling mass and others are influencing the conversion and the conversion influences the fouling mass. The conversion of reactions is more commonly investigated in kinetic studies than fouling masses. Influences of temperature and initiator concentration on conversion and reaction rate are widely described.<sup>[14,23,24]</sup> For emulsifier content and comonomer composition there are less information. In this work it was shown that emulsifier content as well influences the conversion and fouling mass only indirectly. This can be explained by the rate of termination which is related to the probability of growing chains to nucleate. The more emulsifier is available the higher is the probability that an initiated oligoradical in water phase is stabilised and can grow further in a micelle. So, the conversion is directly influenced by the emulsifier content. For the comonomer composition there is no influence on conversion discussed in literature. This agrees well with the experimental results because the fouling mass is influenced by this factor, but the conversion is kept constant. The influences of all factors were quantified, and a prediction of fouling masses was possible. Besides the single-factor evaluation there can be multi-factor effects that affect the fouling mass. For that purpose, a multivariate approach was chosen to validate the single-factor evaluation. Both approaches lead to very similar results so that both can be used but the multivariate model is always the better option as it combines everything. With this model a fouling prediction is possible for unknown recipes in this formulation field. The precision of this prediction is given by the statistical deviation of 15 % in fouling masses discussed above. Concluding, it is possible to determine the influences on fouling masses and predict fouling masses for new recipes. This model can be transferred to different formulations as well and can reduce experimental effort for fouling prediction. Unfortunately, in this polymer system the fouling is directly proportional to the conversion so, fouling reduction is coupled with conversion decrease which is not favourable.

Fouling reduction or prevention can be achieved with two pathways. Firstly, a chemical approach in changing the recipe is possible but is ruled out for this polymerisation. Secondly, an approach in reactor design can be followed. For this purpose, the optimisation of residence time distribution or reactor surfaces can be used. The residence time distribution in the used reactor was investigated and residence time measurements show a tailing of the marker signal that indicates dead zones in the reactor. Dead zones are a serious challenge for fouling prevention as low flow velocities favour sedimentation and thus fouling processes. Moreover,

the properties of polymerisation in dead zones are completely different to the desired polymerisation and molecular weights and stabilisation are different. This points out that the PFR with static mixers is not the favourable reactor for continuous emulsion polymerisation or a special design must be developed. Another possibility is the coating of the reactor surfaces which can reduce surface energy and decrease the interactions with the reactor surfaces. Hydrophilic and hydrophobic coatings were investigated on sample plates and both coating types show influences on the fouling processes. The fouling cannot be completely prevented but fouling masses can be reduced and above all the cleaning effort can be reduced significantly as the adhesion of the deposits is lower. Concluding, coatings of reactor surfaces can improve the situation especially for efficient cleaning as well as fouling reduction.

Another important part was the development of analytical methods for fouling detection and inline particle size measurement. The particle size measurement in emulsion polymerisation is mostly performed by dynamic light scattering (DLS). This method needs time and resource consuming sampling, diluting the samples, and measuring them. An inline measurement technology which is compatible with high solid contents as well as fast measurements is promising as improvement for the efficiency of the process. Moreover, for continuous processes it is possible to react fast on changed product properties and adjust the process so that the product quality is kept constant. Turbidity is one characteristic property of any dispersion which is mainly influenced by the concentration and shape of particles. Particle size is another parameter as different sized particle show different scattering behaviour. In emulsion polymerisation the number of particles is approximately constant after nucleation stage so that no changes in particle concentration are expected. Changes in turbidity can be correlated with the particle size in stable dispersions where agglomeration is not dominant. The measured turbidity values were correlated with particle sizes determined by dynamic light scattering (DLS) and disk centrifuge. Both methods result in an agreement of the values, but DLS is more precise in correlation as both are light scattering methods referring to the same mean diameter while disk centrifuge as sedimentation method refers to another mean diameter. A calibration of turbidity values and mean particle sizes was obtained and validated. The method was able to measure particle sizes between 100 nm and 250 nm for this polymerisation with a precision below 5 % deviation. An advantage is the fast and automatic processing of the data to obtain particle sizes within seconds. Disadvantageous is that this method is highly dependent on the recipe and process so for every changed process a new calibration is necessary. Moreover, precision is below the level of conventional methods like DLS but within the scope of industrial relevance. Concluding, this method is well suitable for monitoring a production process for

detecting divergences from specifications but is less suitable for academic particle size measurement in changing environments.

The detection of fouling in reactors is an important challenge as fouling is a safety risk and influences product properties. Fouling can occur in various processes and the reasons for fouling are diverse. In this case fouling during emulsion polymerisation was investigated and suitable detection methods investigated. For lab-scale the weighting of the reactor gives information about fouling masses in the reactor<sup>[73,74]</sup> but this is not applicable on industrial scale. The development of sensor concepts that are applicable scale-independent was another goal. Different measured variables were addressed and some sensors successful established. A first idea was to detect fouling by changes in residence time distribution as fouling decreases the reaction volume and with that the residence time. Colour-marker measurements were performed for residence time characterisation of the reactor, and this can be compared with measurements for the reactor with fouling, especially at fouling intense situations. The residence time is decreased for the reactor containing deposits and the tailing of the outlet signal increases as more dead zones are formed by deposits. This method is generally suitable but demands a high effort as the polymerisation must be stopped and colour-marker measurements must be performed. This decreases the efficiency of this method. Therefore, this method is not favourable for industrial purposes.

The detection of a reduced reaction volume for indicating fouling was followed further and a method based on reaction conversion was established. If the reaction time and residence time are similar, which is often given for high efficiency of the processes, a decrease in reaction volume will cause a decreased conversion as residence time is shorter. Moreover, the conversion of reactions is often followed for monitoring the process and so this can be used for indirect fouling measurement as well. Fouling masses calculated by decrease in conversion and gravimetrically references agree well so this method is suitable for detecting and quantifying fouling inline. Advantageous is that this method is efficient as it does not require additional equipment if conversion is already detected. A challenge can be the detection limit for fouling as conversion is only significantly influenced if the reaction volume is significantly reduced and small amounts of fouling cannot be detected with this method.

Different other approaches which were based on optical and scattering technologies were promising first but did not reach the reproducibility and robustness needed as the detection area was too small and the situation in the reactor was not pictured reliable. Electrochemical impedance spectroscopy for fouling detection was tested as well and is promising for small

amounts of fouling with very low detection limits but the upper detection limit is reached soon and fouling intense processes can only be monitored for minutes until saturation is reached.<sup>[79]</sup> A promising approach is the ultrasonic measurement technology. A measurement cell is attached inline, or atline for larger scales, and the average sound velocity (ASV) is monitored. The ASV is media-dependent so fouling will cause a change in ASV. Fouling masses in the measurement cell were determined gravimetrically and correlated with the change in ASV measured. The results are in good accordance with the fouling masses of the reactor end which is plausible as the measurement cell is placed at the outlet of the reactor. The same fouling trends are detected, and the most fouling intense point is monitored. Moreover, the fouling growth and cleaning of the measurement cell can be monitored so besides fouling growth the cleaning can be supervised as well. This is an advantage for process efficiency as cleaning can be optimised and automated. A challenge here are dead zones as cleaning of these needs more time and cannot be detected. Concluding, for an optimised reactor with less dead zones this technology would be able to guarantee precise cleaning as well as fouling measurement but for the real reactor small amounts of fouling remained in the dead zones.

All in all, various aspects of fouling during continuous emulsion polymerisation of vinyl acetate were investigated and progress in different fields achieved. The knowledge about fouling processes and fouling pathways was improved and prediction models for fouling generated. The inline analytics for emulsion polymerisation improved both for particle size measurement and fouling detection. Different approaches were investigated and successfully their suitability and limitations shown.

## 8. References

- [1] *Plastics – the Facts 2022*; 2022.
- [2] *Emulsion Polymers Market By Product (Vinyl Acetate Polymers, Styrene-Butadiene Latex, Acrylics, and Others), By Application (Adhesives, Paper & Paperboard Coatings, Paints & Coatings, and Others), and By Region-Global and Regional Industry Trends, Competi*; 2022.
- [3] Research and Markets. *Global Vinyl Acetate Market Report 2013-2018 & 2023*; 2019.
- [4] Wacker Chemie <https://www.wacker.com/cms/de-de/home/home.html>.
- [5] Lovell, P. A.; El-Asser, M. A. *Emulsion Polymerization and Emulsion Polymers*, 1st editio.; JOHN WILEY & Sons Ltd.: Chichester, West Sussex, 1997.
- [6] van Herk, A. M. *Chemistry and Technology of Emulsion Polymerisation*, 2nd editio.; John Wiley & Sons Inc: New York, 2013.
- [7] Hernandez, H.; Tauer, K. *Heterophase Polymerization: Basic Concepts and Principles*; Jenny Stanford Publishing Pte. Ltd., 2021.
- [8] Schroeter, B. L. *Kinetik von Redoxinitiatoren Für Die Emulsionspolymerisation*, University of Hamburg, Hamburg, 2018.
- [9] Zhang, S.; Zhang, Q.; Shang, J.; Mao, Z. sha; Yang, C. Measurement Methods of Particle Size Distribution in Emulsion Polymerization. *Chinese J. Chem. Eng.* **2021**, *39*, 1–15. <https://doi.org/10.1016/j.cjche.2021.03.007>.
- [10] Priest, W. J. Particle Growth in the Aqueous Polymerization of Vinyl Acetate. *J. Phys. Chem.* **1952**, *56*, 1077–1082.
- [11] Cal, C. De; Leiza, R.; Asua, M.; Butte, A.; Storti, G.; Morbidelli, M. Emulsion Polymerization. In *Handbook of Polymer Reaction Engineering*.; Meyer, T., Keurentjes, J., Eds.; WILEY-VCH Verlag GmbH & Co. KGaA: Weinheim, 2005; p 249ff.
- [12] Chern, C. Principles and Applications of Emulsion Polymerization. *Prog. in. Polym. Sci.* **2006**, *31*, 443–486.
- [13] Chern, C. *Principles and Applications of Emulsion Polymerization*, 1st editio.; JOHN WILEY & Sons Ltd.: New Jersey, 2008.
- [14] Chern, C. S. Emulsion Polymerization Mechanisms and Kinetics. *Prog. Polym. Sci.* **2006**, *31* (5), 443–486. <https://doi.org/10.1016/j.progpolymsci.2006.02.001>.
- [15] Chern, C. S.; Chen, Y. C. Stability of the Polymerizable Surfactant Stabilized Latex Particles during Semibatch Emulsion Polymerization. *Colloid Polym. Sci.* **1997**, *275*, 124.
- [16] Schork, F. J. Monomer Transport in Emulsion Polymerization II: Copolymerization. *Macromol. React. Eng.* **2021**, *15* (6), 10–13. <https://doi.org/10.1002/mren.202100022>.
- [17] Schork, F. J.; Lu Fujun, F. Relative Rates of Branching in Emulsion and Miniemulsion Polymerization. *Macromol. React. Eng.* **2009**, *3* (9), 539–542. <https://doi.org/10.1002/mren.200900036>.

- [18] Schork, F. J. Heinz Gerrens Revisited: A New Look at the Impact of Reactor Type on Polymer Chain Morphology. *Macromol. React. Eng.* **2020**, *14* (3), 1–10. <https://doi.org/10.1002/mren.201900055>.
- [19] Schork, F. J. Monomer Concentration in Polymer Particles in Emulsion Polymerization. *Macromol. React. Eng.* **2021**, *15* (3), 1–2. <https://doi.org/10.1002/mren.202100003>.
- [20] Schork, F. J. Monomer Transport in Emulsion Polymerization III Terpolymerization and Starved-Feed Polymerization. *Macromol. React. Eng.* **2022**, *16* (4), 2–5. <https://doi.org/10.1002/mren.202200010>.
- [21] Thickett, S. C.; Gilbert, R. G. Emulsion Polymerization: State of the Art in Kinetics and Mechanisms. *Polymer (Guildf)*. **2007**, *48*, 6965–6991. <https://doi.org/https://doi.org/10.1016/j.polymer.2007.09.031>.
- [22] Smith, W. V.; Ewart, R. H. Kinetics of Emulsion Polymerization. *J. Chem. Phys.* **1948**, *16*, 592–599. <https://doi.org/10.1002/app.1965.070090410>.
- [23] van der Hoff, B. M. E. Kinetics of Emulsion Polymerization. *Adv. Chem.* **1962**, *9*, 6–31. <https://doi.org/10.1002/app.1965.070090410>.
- [24] Friis, N.; Nyhagen, L. A Kinetic Study of the Emulsion Polymerization of Vinyl Acetate. *J. Appl. Polym. Sci.* **1973**, *17* (8), 2311–2327. <https://doi.org/10.1002/app.1973.070170802>.
- [25] Brunier, B. Modeling of Pickering Emulsion Polymerization, Université Claude Bernard, Lyon, 2017.
- [26] Nomura, M.; Harada, M.; Nakagawara, K.; Eguchi, W.; Nagata, S. The Role of Polymer Particles in the Emulsion Polymerisation of Vinyl Acetate. *J. Chem. Eng. Jpn.* **1971**, *4*, 160ff.
- [27] Asua, J. M.; Sudol, E. D.; El-Aasser, M. S. Radical Desorption in Emulsion Polymerization. *J. Polym. Sci. Part A Polym. Chem.* **1989**, *27* (12), 3903–3913. <https://doi.org/10.1002/pola.1989.080271203>.
- [28] Babar, M. Continuous Emulsion Copolymerisation of Vinyl Acetate and VeoVa 10 Using Taylor Reactor, Wissenschaft & Technik Verlag, Hamburg, 2012.
- [29] Hayashi, S.; Hojo, N. No Title. *Makromol. Chem.* **1976**, *177*, 1215–1219.
- [30] Allen, K. C.; Baines, S. J.; Dorian, P. Durch Ein Phosphattensid Stabilisierte Emulsionen Eines Vinylacetat/Ethylen-Polymeren. DE 000060218951 T2, 2002.
- [31] Martin, P. S.; Smith, O. W.; Bassett, D. R. Proceedings of the Waterborne. *High-Solids, Powder Coatings Symp.* **1991**, *18*, 279–308.
- [32] Smith, O. W.; Collins, M. J.; Martin, P. S.; Bassett, D. R. New Vinyl Ester Monomers for Emulsion Polymers. *Prog. Org. Coatings* **1993**, *22*, 19–25.
- [33] Erbil, H. Y. *Vinyl Acetate Emulsion Polymerization and Copolymerization with Acrylic Monomers*; CRC Press LLC: Florida, 2000.
- [34] Rätzsch, M.; Schneider, W.; Musche, D. Reactivity of Ethylene in the Radically Initiated Copolymerization of Ethylene with Vinylacetate. *J. Polym. Sci. Part A-1 Polym. Chem.* **1971**, *9*, 785–790.

- [35] Bartl, H. Kontinuierliches Verfahren Zur Herstellung von Copolymerisat-Dispersionen. DE 000002309368 C3, 1973.
- [36] Poljansek, I.; Fabjan, E.; Burja, K.; Kukanja, D. No Title. *Prog. Org. Coatings* **2013**, *76*, 1798–1804.
- [37] Watkinson, P.; Wilson, D. I. Chemical Reaction Fouling: A Review. *Can J. Chem. Eng.* **1997**, *14*, 361.
- [38] Hohlen, A.; Augustin, W.; Scholl, S. Quantification of Polymer Fouling on Heat Transfer Surfaces During Synthesis. *Macromol. React. Eng.* **2019**, *1900035*.
- [39] Ekowati, Y.; Msuya, M.; Salinas Rodriguez, S. G.; Veenendaal, G.; Schippers, J. C.; Kennedy, M. D. Synthetic Organic Polymer Fouling Inmunicipalwastewater Reuse Reverse Osmosis. *J. Water Reuse Desalin.* **2014**, *4* (3), 125–136. <https://doi.org/10.2166/wrd.2014.046>.
- [40] AlShehri, A.; Cunningham, V.; Amer, A.; Xu, W.; Melibari, F. Heat Exchanger Fouling Determination Using Thermography Combined with Machine Learning Methods. WO 2021/026462 A1, 2021.
- [41] Lynch, J.; Sutoris, H. F.; Zubiller, J.; Aumüller, A. Verfahren Zur Polymerisation Vinylischer Monomerer. DE 196 48 811 A I, 1998.
- [42] Apecetche, M. A.; Xinlai, B.; Cann, K. J. Process for Reducing Polymer Build-Up in Recycle Lines and Heat Exchangers during Polymerization Employing Butadien, Isoprene, and/or Styrene. US005733988A, 1996.
- [43] Arhancet, G. Compositions and Methods for Inhibiting Fouling of Vinyl Monomers. Wo 98/47593 29, 1998.
- [44] Reid, D. K. Antioxidant Compositions and Methods Using P-Phenylendiamine Compounds and Organic AOD Compounds. US005128022A, 1992.
- [45] Weber, M.; Lattner, J.; McCullough, L.; Dickey, R.; Brown, S.; Loezos, P. Olefin Oligomerization Reaction Processes Exhibiting Reduced Fouling. WO 2010/110801 A1, 2010.
- [46] Hocking, P.; Sibtain, F.; Cheluget, E. Reducing Fouling in Heat Exchangers. CA 2797489 A1, 2012.
- [47] Tong, D. Y. Reducing Polymer Fouling and Agglomeration in Acrylate/Methacrylate Processes. US 2016/0102189 A1, 2015.
- [48] Kelland, M. A. Additives for Kinetic Hydrate Inhibitor Formulations to Avoid Polymer Fouling at High Injection Temperatures: Part 1. A Review of Possible Methods. *Energy and Fuels* **2020**, *34* (3), 2643–2653. <https://doi.org/10.1021/acs.energyfuels.9b04040>.
- [49] Cohen, L. Polymerization Reactors Coated With Polymer-Inhibitor Complexes. US4256864, 1979.
- [50] Weimer, D. R.; Freshour, K. Prevention of PVC Polymer Built-up in Polymerization Reactors Using Oxalyl Bis(Benzylidenhydrazine) and Alumina. US4145496, 1979.
- [51] Wempe, L.; Bauman, B. D. Method for Reducing Wall Fouling in Vinyl Chloride Polymerization. US4420591, 1983.



- [52] Cohen, L. Polymerization Reactor Coatings and Use Thereof. US4696983, 1987.
- [53] Fitzwater, S. J.; McFadden, D. M. Continuous Process for Preparing Polymers. EP 1 136 505 A1, 2001.
- [54] McFadden, D. M.; Wu, R. S.-H. The Reduction of Polymer Fouling on Reactor Surfaces in a Continuous Process for Preparing Polymers. EP 1 024 149 A2, 2000.
- [55] Lowell, J. S.; Hendrickson, G. G.; Price, R. J. Elimination of Polymer Fouling in Fluidized Bed Gas-Phase Fines Recovery Eductors. US 2018/0105613 A1, 2018.
- [56] Lowell, J. S.; Dooley, K. A.; Li, R.; Aruho, D. K. Systems and Methods for Mitigating Polymer Fouling. WO 2022/173784 A1, 2022.
- [57] McDonald, M.; Lawrence, D.; Williams, D. Polymerization Reactor. WO 93/03075, 1993.
- [58] Carvalho, A. C. S. M.; Chicoma, D. L.; Sayer, C.; Giudici, R. Development of a Continuous Emulsion Copolymerization Process in a Tubular Reactor. *Ind. Eng. Chem. Res.* **2010**, *49* (21), 10262–10273. <https://doi.org/10.1021/ie100422v>.
- [59] Dorton, M.; Gardner Sr., G. Process for Cleaning Polymeric Fouling from Equipment. US 20030073595A1, 2003.
- [60] Haruyama, H. Solution Conveying and Cooling Device. EP 3 203 177 A1, 2017.
- [61] Saikhwan, P.; Chew, J. Y. M.; Paterson, W. R.; Wilson, D. I. Swelling and Its Suppression in the Cleaning of Polymer Fouling Layers. *Ind. Eng. Chem. Res.* **2007**, *46* (14), 4846–4855. <https://doi.org/10.1021/ie0615943>.
- [62] Deglmann, P.; Hellmund, M.; Hungenberg, K. D.; Nieken, U.; Schwede, C.; Zander, C. Side Reactions in Aqueous Phase Polymerization of N-Vinyl-Pyrrolidone as Possible Source for Fouling. *Macromol. React. Eng.* **2019**, *13* (5), 1–13. <https://doi.org/10.1002/mren.201900021>.
- [63] Cunningham, M. F.; O'Driscoll, K. F. Bulk Polymerization in Tubular Reactors I. Experimental Observations on Fouling. *Can. J. Chem. Eng.* **1991**, *69*, 630.
- [64] Buchelli, A.; Call, M. L.; Brown, A. L.; Bird, A.; Hearn, S.; Hannon, J. Modeling Fouling Effects in LDPE Tubular Polymerization Reactors. *Ind. Eng. Chem. Res.* **2005**, *44*, 1474.
- [65] Neßlinger, V.; Welzel, S.; Rieker, F.; Meinderink, D.; Nieken, U.; Grundmeier, G. Thin Organic-Inorganic Anti-Fouling Hybrid-Films for Microreactor Components. *Macromol. React. Eng.* **2022**, *2200043*, 1–16. <https://doi.org/10.1002/mren.202200043>.
- [66] Hohlen, A.; Augustin, W.; Scholl, S. Quantification of Polymer Fouling on Heat Transfer Surfaces During Synthesis. *Macromol. React. Eng.* **2020**, *14* (1). <https://doi.org/10.1002/mren.201900035>.
- [67] Hohlen, A.; Augustin, W.; Scholl, S. Investigation of Polymer Depositions During the Synthesis in a Heat Exchanger. *Chemie-Ingenieur-Technik* **2020**, *92* (5), 629–634. <https://doi.org/10.1002/cite.201900130>.
- [68] Gottschalk, N.; Kuschnerow, J. C.; Föste, H.; Augustin, W.; Scholl, S. Experimental Investigation on Fouling of a Polymer Dispersion on Modified Surfaces. *Chemie-Ingenieur-Technik* **2015**, *87* (5), 600–608. <https://doi.org/10.1002/cite.201400126>.





- [69] Chern, C. S.; Chen, Y. C. Stability of the Polymerizable Surfactant Stabilized Latex Particles during Semibatch Emulsion Polymerization. *Colloid Polym. Sci.* **1997**, *275*, 124–130.
- [70] Kemmere, M. F.; Meuldiek, J.; Drinkenburg, A. A. H.; German, A. L. Colloidal Stability of High-Solids Polystyrene and Polyvinyl Acetate Latices. *J. Appl. Polym. Sci.* **1999**, *74*, 1780–1791.
- [71] Lü, T.; Shan, G.; Shang, S. Stability of Two-Phase Polymerization of Acrylamide in Aqueous Poly(Ethylene Glycol) Solution. *J. Appl. Polym. Sci.* **2011**, *122*, 1121.
- [72] Böttcher, A.; Petri, J.; Langhoff, A.; Scholl, S.; Augustin, W.; Hohlen, A.; Johannsmann, D. Fouling Pathways in Emulsion Polymerization Differentiated with a Quartz Crystal Microbalance (QCM) Integrated into the Reactor Wall. *Macromol. React. Eng.* **2022**, *16* (2), 1–8. <https://doi.org/10.1002/mren.202100045>.
- [73] Madani, M. Belagsbildung in Chemischen Reaktoren Unter Berücksichtigung von Oberflächenaspekten. **2017**.
- [74] Bernstein, C. Methoden Zur Untersuchung Der Belagsbildung in Chemischen Reaktoren (Dissertation). **2017**.
- [75] Förster, J.; Tebrügge, J.; Osenberg, M.; Westerdick, S.; von Grotthuss, E.; Behrendt, F.; Vogt, M. A9.2 Fouling Detection in Polymerization Processes by Ultrasound Echo Measurements. In *SMSI 2021 - Sensors and Instrumentation*; AMA Service GmbH, Von-Münchhausen-Str. 49, 31515 Wunstorf, Germany, 2021; Vol. 48, pp 99–100. <https://doi.org/10.5162/SMSI2021/A9.2>.
- [76] Osenberg, M.; Förster, J.; Westerdick, S.; Tebrügge, J.; von Grotthuss, E.; Musch, T. Ultrasound Based Fouling Detection in Polymerization Processes Polymerization Process. In *Sensoren und Messsysteme*; 2022; Vol. 303, pp 272–274.
- [77] Tabrizi, F. F.; Fadae, M. M. Experimental Investigation of Continuous Conductivity Measurements during Emulsion Polymerizations Having Unstable/High-Fouling Reaction Mixture. *J. Appl. Polym. Sci.* **2017**, *134*, 44446.
- [78] Kiparissides, C.; MacGregor, J. F.; Hamielec, A. E. *Polymer Colloids II*; Plenum Press: New York, London, 1978.
- [79] Neßlinger, V.; Rust, S.; Atlanov, J.; Pauer, W.; Grundmeier, G. Monitoring Polymeric Fouling in a Continuous Reactor by Electrochemical Impedance Spectroscopy. *Chemie-Ingenieur-Technik* **2023**, No. 00, 1–10. <https://doi.org/10.1002/cite.202300032>.
- [80] Osenberg, M.; Forster, J.; Rust, S.; Fritsch, T.; Tebrugge, J.; Pauer, W.; Musch, T. Ultrasound Sensor for Process and Fouling Monitoring in Emulsion Polymerization Processes. *Proc. IEEE Sensors* **2022**, *2022-Octob*, 1–4. <https://doi.org/10.1109/SENSORS52175.2022.9967228>.
- [81] Jacob, L. I.; Pauer, W.; Schroeter, B. Influence of Redox Initiator Component Ratios on the Emulsion Copolymerisation of Vinyl Acetate and Neodecanoic Acid Vinyl Ester. *RSC Adv.* **2022**, *12* (22), 14197–14208. <https://doi.org/10.1039/d2ra01811j>.
- [82] Schroeter, B.; Bettermann, S.; Semken, H.; Melchin, T.; Weitzel, H. P.; Pauer, W. Kinetic Description of Ascorbic Acid Decomposition in Redox Initiator Systems for Polymerization Processes. *Ind. Eng. Chem. Res.* **2019**, *58* (29), 12939–12952. <https://doi.org/10.1021/acs.iecr.9b00710>.

- [83] Rust, S.; Pauer, W. Determination of Inline-Particle Sizes by Turbidity Measurement in High Solid Content Emulsion Polymerisations. *J. Polym. Res.* **2022**, *29* (7), 1–6. <https://doi.org/10.1007/s10965-022-03141-z>.
- [84] Rust, S.; Pauer, W. Formulation and Process Determined Fouling Prediction for the Continuous Emulsion Co Polymerisation of Vinyl Acetate. *J. Polym. Res.* **2023**, *30* (6), 1–11. <https://doi.org/10.1007/s10965-023-03588-8>.
- [85] Rust, S.; Osenberg, M.; Musch, T.; Pauer, W. Ultrasonic and Conversion - Based Inline Fouling Measurements for Continuous Emulsion Copolymerisation of Vinyl Acetate in a Tubular Reactor. *Sci. Rep.* **2024**, 1–12. <https://doi.org/10.1038/s41598-024-54321-4>.
- [86] Förster, J.; Fritsch, T.; Tebrügge, J.; Musch, T.; Osenberg, M.; Haspel, D.; Pauer, W.; Rust, S.; Klinkert, A.; Augustin, W.; Scholl, S.; Melchin, T.; Eckl, B. *Schlussbericht Zum Verbundprojekt: „KoPPonA 2.0“- Kontinuierliche Polymerisation in Modularen, Intelligenten, Gegen Belagsbildung Resistenten Reaktoren - Teilvorhaben: Verfahrensentwicklung Und Betriebliche Umsetzung Für Die Emulsionspolymerisation*; Hannover, 2023.
- [87] Baerns, M. *Technische Chemie*, 2nd editio.; Wiley VCH: Weinheim, 2021.
- [88] Levenspiel, O. *Tracer Technology*; Springer: New York Dordrecht Heidelberg London, 2012; Vol. 96.
- [89] Arian, E.; Rust, S.; Pauer, W. *ENPRO – „KoPPonA 2.0“ Kontinuierliche Polymerisation in Modularen, Intelligenten, Gegen Belagsbildung Resistenten Reaktoren 2. Zwischenbericht*; 2020.
- [90] Arian, E.; Pauer, W. *ENPRO – „KoPPonA 2.0“ Kontinuierliche Polymerisation in Modularen, Intelligenten, Gegen Belagsbildung Resistenten Reaktoren 1. Zwischenbericht*; 2020.
- [91] Brüggemann, O. Polyvinylalkohole; Böckler, F., Dill, B., Eisenbrand, G., Faupel, F., Fugmann, B., Gamse, T., Heretsch, P., Matissek, R., Pohnert, G., Rühling, A., Schmidt, S., Sprenger, G., Eds.; Thieme Gruppe PP - Stuttgart, 2009.
- [92] Rust, S. *Kontinuierliche Polymerisation in 3D-Gedruckten Reaktoren*, University of Hamburg, 2020.
- [93] Henk G. Merkus. *Particle Size Measurements*; Springer, 2009.
- [94] Elias, H.-G. Kohlenstoff-Ketten. In Makromoleküle Set. In *Makromoleküle*; 2002; p 207.
- [95] Hexion. VeoVa 10 Monomer <https://www.hexion.com/en-GB/product/veova-10-monomer>.
- [96] Bettermann, S. *3D Printing Technology Applications in the Digital Development and Intensification of Chemical Processes*, University of Hamburg, 2020.
- [97] Unfallversicherung, I. für A. der D. G. GESTIS-Stoffdatenbank <https://gestis.dguv.de/search>.

## 9. Appendix

### 9.1 Table of Chemicals

Table 1: Chemicals used and their classification according to GHS including hazard pictograms, safety and precautionary statements.<sup>[97]</sup>

<b>Chemical (CAS-number)</b>	<b>Hazard pictograms Signal word</b>	<b>H-phrases</b>	<b>P-phrases</b>
Acetone (67-64-1)	 Danger	225-319-336- EUH066	210-240- 305+351+338- 403+233
Ammonium iron(III) sulfate dodecahydrate (7783-83-7)	 Danger	318	280-305+351+338- 310
Ascorbic acid (50-81-7)	Not a hazardous substance according to Regulation (EG) No. 1272/2008		
Dimethylacetamide (127-19-5)	 Danger	312+332-319-360D	202-280- 302+352+312- 304+340+312- 305+351+338- 308+313
Methanol (67-56-1)	 Danger	225-331-311-301- 370	210-233-280- 302+352-304+340- 308+310-403+235
Mowiol 4-88 (9002-89-5)	Not a hazardous substance according to Regulation (EG) No. 1272/2008		

Potassium hydroxide (1310-58-3)	 Danger	290-302-314	234-260-280- 301+312- 303+361+353- 305+351+338
Sodium hydroxide (1310-73-2)	 Danger	290-314	280-301+330+331- 305+351+338- 308+310
<i>tert</i> -Butyl hydroperoxide (75-91-2)	 Danger	226-242-302-311- 330-314-317-341- 411	210-220-234-243- 264-273-280-284- 303+361+353- 305+351+338-310- 320-405-410- 411+235-420-501
Tetrahydrofuran (109-99-9)	 Danger	225-302-319-335- 351-EUH019	210-280- 301+312+330- 305+351+338- 370+378-403+235
Vinyl neodecanoate (26544-09-2)	 Warning	410	273-391-501
Vinyl acetate (108-05-4)	 Danger	225-332-335-351- 412	210-261-273- 304+340+312- 403+235
Water (7732-18-5)	Not a hazardous substance according to Regulation (EG) No. 1272/2008		

9.2 Supporting information “Formulation and process determined fouling prediction for the continuous emulsion co polymerisation of vinyl acetate”

Supplementary Information

Set-up number	Temperature [°C]	Emulsifier content [wt% based on monomer]	initiator content [wt% based on monomer]	Comonomer ratio $X_{VAc}$
01	30	8	1	0.9
02	40	8	1	0.9
03	50	8	1	0.9
04	20	8	1	0.9
05	20	8	0.1	0.9
06	20	8	2	0.9
07	20	5	1	0.9
08	20	15	1	0.9
09	20	8	1	1
10	20	8	1	0.8
11	20	8	0.3	0.9
12	20	8	0.5	0.9
13	20	8	0.8	0.9
14	5	8	1	0.9
15	10	8	1	0.9
16	20	12	1	0.9

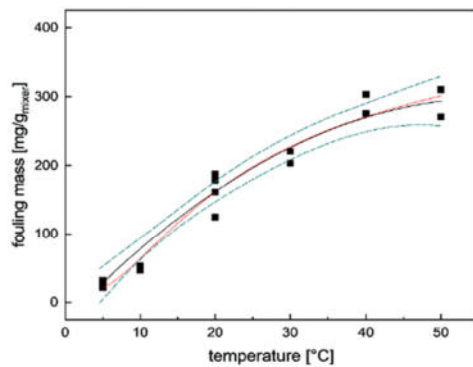


Fig. 9

Calculation of the fouling mass for the red point in Fig. 9 with the process conditions  $T = 50\text{ }^{\circ}\text{C}$ ,  $w_I = 1\text{ wt}\%$ ,  $w_E = 8\text{ wt}\%$ ,  $x_{VAc} = 0.9$ :

$$\begin{aligned}
 m_{\text{fouling}, t=120 \text{ min}, MV}(T = 50\text{ }^{\circ}\text{C}, w_I = 1\text{ wt}\%, w_E = 8\text{ wt}\%, x_{VAc} = 0.9) \\
 &= 326 \frac{\text{mg}}{\text{g}} \cdot \left( 0.902 \cdot e^{-\frac{173.6}{8.314T}} + 0.841 \right) \cdot \\
 &(\sqrt{w_I}) \cdot \left( \frac{1.70 \cdot (w_E - (-0.102))^{0.12} - 1.73}{0.665} \right) - 29.6 \frac{\text{mg}}{\text{g}} + 486.4 \cdot 0.9 - 467.2 \\
 &= 290.5 \text{ mg/g}_{\text{mixer}}
 \end{aligned}$$

Calculation of the conversion for the red point in Fig. 10 with the process conditions  
 $T = 20\text{ }^{\circ}\text{C}$ ,  $w_I = 1\text{ wt}\%$ ,  $w_E = 8\text{ wt}\%$ :

$$X(T = 20\text{ }^{\circ}\text{C}, w_I = 1\text{ wt}\%, w_E = 8\text{ wt}\%)_{t=3\bar{\tau}} = \left(0.902 \cdot e^{-\frac{173.6}{8.314T}} + 0.318\right) \cdot (\sqrt{1}) \cdot \left(\frac{1.71 \cdot (8 - 3.73)^{0.12} - 1.37}{0.665}\right) = 0.636$$

Raw data for modelling process

Table S1: Data from figure 5.

Conversion	Fouling mass [mg/g <sub>mixer</sub> ]
0.56765	124.9
0.63193	187.5
0.73739	223.1
0.74496	185.7
0.56765	161.2
0.58655	178.1
0.46597	120.6
0.37479	96
1.01092	232.1
0.5958	227.7
0.24454	33.4
0.22647	7.6
0.65798	135.1
0.66933	173.5
0.83025	220.5
0.74664	203.2
0.85	275.2
0.81639	302.97
0.91134	309.95
0.324	94
0.445	105.8
0.495	87.8
0.354	113.7
0.381	126
0.632	197.2
0.737	197.7

Table S2: Data from figure 6.

Temperature [°C]	Conversion
20	0.56765
20	0.63193
20	0.73739
20	0.74496
20	0.56765
20	0.58655
30	0.83025
30	0.74664
40	0.85
40	0.81639
50	0.91134
50	0.92
5	0.35378
10	0.38067

Table S3: Data from figure 7.

Emulsifier content [wt%]	Conversion
8	0.58403
8	0.63193
8	0.73739
8	0.74496
8	0.56765
8	0.73193
5	0.41134
5	0.37479
15	0.82311
15	1
12	0.86311
12	0.83403

Table S4: Data from figure 8.

Initiator content [wt%]	Conversion
1	0.56765
1	0.63193
1	0.73739
1	0.74496
1	0.56765
1	0.58655
0.1	0.24454
0.1	0.22647
2	0.65798
2	0.66933
0.3	0.26303
0.3	0.34664
0.5	0.27227
0.5	0.44538
0.8	0.45882
0.8	0.72227

Table S5: Data from figure 9.

Proportion vinyl acetate	Fouling mass [mg/g <sub>mixer</sub> ]
0.9	124.9
0.9	187.5
0.9	223.1
0.9	185.7
0.9	161.2
0.9	178.1
1	211.7
1	193.9
0.8	103
0.8	108.1



### 9.3 Supporting information “Ultrasonic and conversion-based inline fouling measurements for continuous emulsion copolymerisation of vinyl acetate”

Supplementary information for the publication “Ultrasonic and conversion-based inline fouling measurements for continuous emulsion copolymerisation of vinyl acetate in a tubular reactor”

Author information

Sören Rust<sup>1</sup>, Marco Osenberg<sup>2</sup>, Thomas Musch<sup>2</sup>, Werner Pauer<sup>1</sup>

Corresponding author

Werner Pauer, werner.pauer@chemie.uni-hamburg.de

Affiliations

<sup>1</sup> Institute for Technical and Macromolecular Chemistry, University of Hamburg, Bundesstraße 45, 20146 Hamburg, Germany

<sup>2</sup> Ruhr-University Bochum, Chair of Electronic Circuits, Universitätsstraße 150, 44801 Bochum, Germany

Raw data Fig. 4+5

experiment	emulsion					deposit			deposit reactor inlet	
	molecular weight	P-SR-455E	P-SR-456E	P-SR-457E	P-SR-458E	P-SR-459E	P-SR-456B Belag	P-SR-457B Belag	P-SR-458B Belag	P-SR-457A Anfang
3.89E+02	0.00E+00	0.00E+00	0.00E+00	0.00E+00	0.00E+00	0.00E+00	0.00E+00	0.00E+00	0.00E+00	0.00E+00
3.97E+02	0.00E+00	1.87E-03	0.00E+00	3.74E-06	0.00E+00	0.00E+00	0.00E+00	0.00E+00	0.00E+00	8.26E-04
4.05E+02	3.77E-03	2.35E-02	0.00E+00	4.96E-04	0.00E+00	0.00E+00	0.00E+00	0.00E+00	0.00E+00	1.12E-04
4.13E+02	1.02E-03	2.38E-02	9.93E-05	2.04E-02	0.00E+00	0.00E+00	0.00E+00	0.00E+00	0.00E+00	1.44E-03
4.21E+02	4.54E-05	3.04E-02	1.62E-03	1.59E-02	0.00E+00	0.00E+00	0.00E+00	0.00E+00	0.00E+00	3.90E-04
4.30E+02	1.22E-03	2.10E-02	0.00E+00	2.91E-02	0.00E+00	0.00E+00	0.00E+00	0.00E+00	0.00E+00	6.20E-03
4.39E+02	7.03E-03	2.35E-02	2.54E-05	1.46E-02	0.00E+00	0.00E+00	0.00E+00	0.00E+00	0.00E+00	1.24E-02
4.48E+02	4.10E-03	2.78E-02	4.93E-04	3.27E-02	0.00E+00	0.00E+00	0.00E+00	0.00E+00	0.00E+00	1.45E-02
4.57E+02	7.88E-03	3.55E-02	2.62E-04	2.81E-02	0.00E+00	0.00E+00	0.00E+00	0.00E+00	0.00E+00	2.98E-02
4.66E+02	5.61E-03	4.74E-02	1.50E-04	3.78E-02	2.41E-04	0.00E+00	0.00E+00	0.00E+00	0.00E+00	3.38E-02
4.76E+02	2.65E-03	4.35E-02	3.60E-03	4.67E-02	4.82E-03	0.00E+00	0.00E+00	0.00E+00	0.00E+00	3.39E-02
4.86E+02	8.52E-03	4.55E-02	5.97E-03	3.71E-02	5.39E-03	0.00E+00	0.00E+00	0.00E+00	0.00E+00	3.51E-02
4.96E+02	8.08E-03	4.91E-02	1.55E-03	3.09E-02	1.34E-04	0.00E+00	0.00E+00	0.00E+00	0.00E+00	4.78E-02
5.06E+02	7.22E-03	3.52E-02	4.31E-03	3.72E-02	3.49E-03	0.00E+00	0.00E+00	0.00E+00	0.00E+00	5.40E-02
5.16E+02	6.76E-03	4.47E-02	9.75E-03	3.24E-02	1.22E-02	0.00E+00	0.00E+00	0.00E+00	0.00E+00	6.40E-02
5.27E+02	9.08E-03	4.36E-02	4.32E-03	3.25E-02	4.91E-03	0.00E+00	0.00E+00	0.00E+00	0.00E+00	5.89E-02
5.37E+02	4.38E-03	3.83E-02	1.23E-04	2.84E-02	6.56E-03	0.00E+00	0.00E+00	0.00E+00	0.00E+00	5.83E-02
5.48E+02	1.75E-03	4.42E-02	4.66E-03	4.20E-02	2.05E-04	0.00E+00	0.00E+00	0.00E+00	0.00E+00	5.74E-02
5.59E+02	6.08E-03	4.20E-02	0.00E+00	3.87E-02	1.52E-03	0.00E+00	0.00E+00	0.00E+00	0.00E+00	6.19E-02
5.71E+02	4.11E-03	4.77E-02	5.60E-05	3.49E-02	0.00E+00	0.00E+00	0.00E+00	0.00E+00	0.00E+00	7.46E-02
5.83E+02	2.99E-03	2.51E-02	2.99E-03	3.15E-02	0.00E+00	0.00E+00	0.00E+00	0.00E+00	0.00E+00	5.99E-02
5.94E+02	3.94E-03	4.35E-02	3.48E-05	2.69E-02	0.00E+00	0.00E+00	0.00E+00	0.00E+00	0.00E+00	6.74E-02
6.07E+02	4.39E-03	4.28E-02	2.55E-03	3.49E-02	8.21E-05	0.00E+00	0.00E+00	0.00E+00	0.00E+00	8.93E-02
6.19E+02	5.96E-03	3.15E-02	2.72E-05	2.94E-02	4.23E-03	0.00E+00	0.00E+00	0.00E+00	0.00E+00	8.38E-02
6.32E+02	3.52E-03	4.44E-02	3.15E-03	3.95E-02	0.00E+00	0.00E+00	0.00E+00	0.00E+00	0.00E+00	6.97E-02
6.45E+02	1.89E-03	3.58E-02	4.15E-06	3.76E-02	6.29E-05	0.00E+00	0.00E+00	0.00E+00	0.00E+00	8.76E-02
6.58E+02	2.20E-03	2.82E-02	1.14E-03	2.74E-02	5.42E-03	0.00E+00	0.00E+00	0.00E+00	0.00E+00	8.31E-02
6.71E+02	2.31E-03	4.00E-02	1.45E-06	3.86E-02	1.73E-02	0.00E+00	0.00E+00	0.00E+00	0.00E+00	8.84E-02
6.85E+02	3.76E-04	5.27E-02	3.55E-03	3.47E-02	1.96E-06	0.00E+00	0.00E+00	0.00E+00	0.00E+00	9.31E-02
6.99E+02	2.66E-03	5.21E-02	6.99E-03	2.78E-02	4.21E-04	0.00E+00	0.00E+00	0.00E+00	0.00E+00	8.36E-02
7.13E+02	5.98E-03	4.08E-02	6.07E-05	4.61E-02	7.03E-08	0.00E+00	0.00E+00	0.00E+00	0.00E+00	7.31E-02
7.28E+02	6.05E-03	3.67E-02	4.66E-03	3.72E-02	1.92E-05	0.00E+00	0.00E+00	0.00E+00	0.00E+00	8.26E-02
7.43E+02	8.99E-03	3.63E-02	1.41E-02	3.44E-02	9.59E-08	0.00E+00	0.00E+00	0.00E+00	0.00E+00	7.79E-02
7.58E+02	9.41E-03	3.66E-02	5.19E-03	3.03E-02	1.50E-02	0.00E+00	0.00E+00	0.00E+00	0.00E+00	7.67E-02
7.73E+02	8.85E-03	4.84E-02	6.36E-03	3.97E-02	1.28E-02	0.00E+00	0.00E+00	0.00E+00	0.00E+00	7.79E-02
7.89E+02	1.86E-02	5.52E-02	8.47E-03	4.37E-02	1.56E-04	0.00E+00	0.00E+00	0.00E+00	0.00E+00	8.39E-02
8.05E+02	1.55E-02	5.10E-02	9.32E-03	4.92E-02	1.85E-02	0.00E+00	0.00E+00	0.00E+00	0.00E+00	1.03E-01
8.22E+02	1.33E-02	4.40E-02	8.60E-03	4.15E-02	2.23E-02	0.00E+00	0.00E+00	0.00E+00	0.00E+00	7.89E-02
8.38E+02	8.88E-03	3.49E-02	1.14E-02	4.41E-02	1.69E-03	0.00E+00	0.00E+00	0.00E+00	0.00E+00	8.22E-02
8.56E+02	1.56E-02	4.10E-02	1.74E-02	5.37E-02	2.67E-02	0.00E+00	0.00E+00	0.00E+00	0.00E+00	8.87E-02
8.73E+02	1.24E-02	6.32E-02	8.98E-03	4.25E-02	1.51E-02	0.00E+00	0.00E+00	0.00E+00	0.00E+00	9.81E-02













6.28E+06	0.00E+00	0.00E+00	0.00E+00	0.00E+00	0.00E+00	0.00E+00	0.00E+00	0.00E+00	5.26E-03
6.41E+06	0.00E+00	0.00E+00	0.00E+00	0.00E+00	0.00E+00	8.31E-03	0.00E+00	0.00E+00	1.21E-02
6.54E+06	0.00E+00	0.00E+00	0.00E+00	0.00E+00	0.00E+00	7.32E-03	0.00E+00	0.00E+00	7.12E-04
6.68E+06	0.00E+00	0.00E+00	0.00E+00	0.00E+00	0.00E+00	0.00E+00	0.00E+00	0.00E+00	0.00E+00
6.81E+06	0.00E+00	0.00E+00	0.00E+00	0.00E+00	0.00E+00	0.00E+00	0.00E+00	0.00E+00	0.00E+00
6.95E+06	0.00E+00	0.00E+00	0.00E+00	0.00E+00	0.00E+00	0.00E+00	0.00E+00	0.00E+00	0.00E+00
7.09E+06	0.00E+00	0.00E+00	0.00E+00	0.00E+00	0.00E+00	0.00E+00	0.00E+00	0.00E+00	9.09E-03
7.24E+06	0.00E+00	0.00E+00	0.00E+00	0.00E+00	0.00E+00	0.00E+00	0.00E+00	0.00E+00	6.68E-04
7.39E+06	0.00E+00	0.00E+00	0.00E+00	0.00E+00	0.00E+00	0.00E+00	0.00E+00	0.00E+00	0.00E+00
7.54E+06	0.00E+00	0.00E+00	0.00E+00	0.00E+00	0.00E+00	0.00E+00	0.00E+00	0.00E+00	1.63E-02
7.69E+06	0.00E+00	0.00E+00	0.00E+00	0.00E+00	0.00E+00	0.00E+00	0.00E+00	0.00E+00	1.98E-02
7.85E+06	1.64E-04	0.00E+00	0.00E+00	0.00E+00	0.00E+00	0.00E+00	0.00E+00	0.00E+00	7.41E-03
8.01E+06	6.49E-04	0.00E+00	0.00E+00	0.00E+00	0.00E+00	0.00E+00	0.00E+00	0.00E+00	5.10E-04
8.17E+06	0.00E+00	0.00E+00	0.00E+00	0.00E+00	0.00E+00	0.00E+00	0.00E+00	0.00E+00	0.00E+00
8.34E+06	0.00E+00	0.00E+00	0.00E+00	0.00E+00	0.00E+00	0.00E+00	0.00E+00	0.00E+00	0.00E+00
8.51E+06	0.00E+00	0.00E+00	0.00E+00	0.00E+00	0.00E+00	3.86E-03	0.00E+00	0.00E+00	0.00E+00
8.68E+06	2.28E-04	0.00E+00	0.00E+00	0.00E+00	0.00E+00	4.03E-03	0.00E+00	0.00E+00	5.93E-03
8.86E+06	9.58E-04	0.00E+00	0.00E+00	0.00E+00	0.00E+00	0.00E+00	0.00E+00	0.00E+00	1.84E-02
9.04E+06	0.00E+00	0.00E+00	2.65E-03	0.00E+00	0.00E+00	0.00E+00	0.00E+00	0.00E+00	1.21E-02
9.23E+06	0.00E+00	0.00E+00	5.10E-04	0.00E+00	0.00E+00	0.00E+00	0.00E+00	0.00E+00	9.21E-03
9.42E+06	0.00E+00	0.00E+00	0.00E+00	0.00E+00	0.00E+00	0.00E+00	0.00E+00	0.00E+00	3.13E-03
9.61E+06	0.00E+00	0.00E+00	0.00E+00	0.00E+00	0.00E+00	6.38E-03	0.00E+00	0.00E+00	1.32E-02
9.80E+06	0.00E+00	0.00E+00	0.00E+00	0.00E+00	0.00E+00	7.17E-03	0.00E+00	0.00E+00	5.38E-03
1.00E+07	0.00E+00	0.00E+00	0.00E+00	0.00E+00	1.36E-02	0.00E+00	0.00E+00	0.00E+00	4.61E-04
1.02E+07	1.08E-04	0.00E+00	0.00E+00	0.00E+00	2.15E-03	0.00E+00	0.00E+00	0.00E+00	0.00E+00
1.04E+07	5.00E-04	0.00E+00	0.00E+00	0.00E+00	6.68E-03	0.00E+00	0.00E+00	0.00E+00	2.03E-02
1.06E+07	0.00E+00	0.00E+00	0.00E+00	0.00E+00	1.10E-03	0.00E+00	0.00E+00	0.00E+00	1.29E-02
1.08E+07	1.02E-04	0.00E+00	0.00E+00	0.00E+00	0.00E+00	6.82E-03	0.00E+00	0.00E+00	2.32E-02
1.11E+07	4.94E-04	0.00E+00	0.00E+00	0.00E+00	0.00E+00	8.25E-03	0.00E+00	0.00E+00	2.21E-02
1.13E+07	2.04E-04	0.00E+00	0.00E+00	0.00E+00	0.00E+00	0.00E+00	0.00E+00	0.00E+00	1.13E-02
1.15E+07	1.23E-03	0.00E+00	0.00E+00	0.00E+00	0.00E+00	0.00E+00	0.00E+00	0.00E+00	1.22E-03
1.18E+07	1.08E-03	0.00E+00	0.00E+00	0.00E+00	0.00E+00	2.96E-04	0.00E+00	0.00E+00	4.05E-03
1.20E+07	0.00E+00	0.00E+00	4.18E-03	0.00E+00	0.00E+00	3.76E-04	0.00E+00	0.00E+00	5.91E-04
1.22E+07	1.30E-04	0.00E+00	1.02E-03	0.00E+00	6.78E-04	0.00E+00	0.00E+00	0.00E+00	1.51E-03
1.25E+07	6.79E-04	0.00E+00	6.96E-06	0.00E+00	1.30E-04	0.00E+00	0.00E+00	0.00E+00	7.30E-04
1.28E+07	7.63E-05	0.00E+00	1.75E-06	0.00E+00	0.00E+00	1.79E-02	0.00E+00	0.00E+00	1.29E-02
1.30E+07	6.80E-04	0.00E+00	0.00E+00	0.00E+00	0.00E+00	2.67E-02	0.00E+00	0.00E+00	1.44E-02
1.33E+07	1.85E-03	0.00E+00	0.00E+00	0.00E+00	1.34E-02	3.78E-03	7.03E-04	0.00E+00	1.69E-02
1.36E+07	2.99E-03	0.00E+00	0.00E+00	0.00E+00	2.74E-03	0.00E+00	2.34E-03	0.00E+00	6.62E-03
1.38E+07	5.51E-03	0.00E+00	0.00E+00	0.00E+00	0.00E+00	0.00E+00	0.00E+00	0.00E+00	1.56E-02
1.41E+07	4.54E-03	4.74E-03	2.23E-03	0.00E+00	0.00E+00	4.41E-03	0.00E+00	0.00E+00	3.00E-02
1.44E+07	2.74E-03	6.55E-04	4.09E-03	0.00E+00	1.10E-03	9.28E-03	0.00E+00	0.00E+00	1.10E-02
1.47E+07	0.00E+00	0.00E+00	9.70E-04	0.00E+00	2.41E-04	4.33E-03	0.00E+00	0.00E+00	1.11E-03
1.50E+07	8.69E-05	0.00E+00	0.00E+00	0.00E+00	0.00E+00	0.00E+00	0.00E+00	0.00E+00	7.41E-04
1.53E+07	1.61E-03	0.00E+00	2.51E-03	0.00E+00	0.00E+00	1.57E-04	2.16E-04	0.00E+00	1.40E-03
1.56E+07	8.26E-03	0.00E+00	5.08E-03	0.00E+00	4.34E-03	6.42E-03	7.73E-04	0.00E+00	4.03E-03
1.59E+07	9.98E-03	0.00E+00	6.25E-03	0.00E+00	1.02E-03	9.37E-03	0.00E+00	0.00E+00	1.50E-02
1.63E+07	8.47E-04	0.00E+00	1.49E-03	0.00E+00	0.00E+00	5.49E-03	5.73E-04	0.00E+00	1.16E-02
1.66E+07	5.88E-03	0.00E+00	9.67E-04	3.56E-04	3.72E-04	8.53E-03	2.12E-03	0.00E+00	1.74E-03
1.69E+07	2.83E-03	0.00E+00	2.98E-04	3.63E-04	9.11E-05	0.00E+00	0.00E+00	0.00E+00	6.33E-03
1.73E+07	1.64E-03	0.00E+00	1.61E-03	0.00E+00	5.19E-03	0.00E+00	1.53E-03	1.17E-03	1.16E-02



Raw data Fig. 6

name	runtime	Fouling mass	runtime	Fouling mass	runtime	Fouling mass
unit	min	mg/g	min	mg/g	min	mg/g
comment	-	5 °C	-	20 °C	-	40°C
	30		60	51.5	30	93
	30		30	16	30	78
	40		60	24.2	45	145
	40		120	98.5	45	133
	50		90	88.9	60	173
	60	19.5569	30	19.9	60	149
	60	14.10725	30	3.99	75	179
	75	16.5422	90	87.6	75	201
	75	19.50279	30	28.2	90	256
	90	14.09179	45	20.9	90	217
	90	12.10518	45	47.7	120	303
	120		60	65.8	120	310
	120	16.88232	60	48.9		
	120	19.28635	30	18.6		
	150	17.28428	45	27.2		
	150	26.14286	20	7.85		
	180	17.83311	20	9.74		
	180	20.3299	30	12.41438		
			30	18.98488		
			40	20.52315		
			40	21.23431		
			50	21.57443		
			60	40.5052		
			60	30.6108		
			75	42.15942		
			75	42.40678		
			90	75.93952		
			90	71.4252		
			120	103.65157		
			120	113.26769		
			120	116.81576		
			150	175.58695		
			150	156.58661		
			180	186.48625		
			180	186.16932		

Raw data Fig. 7

Name	mixing element	fouling mass	Measurement error	fouling mass	Measurement error
unit	-	mg/g	mg/g	mg/g	mg/g
comment	-	local, 20 °C		integral, 20 °C	
	1	203.16109	23.94982	188.53156	21.21738
	2	162.16216	32.2428	188.53156	21.21738
	3	154.35435	16.58354	188.53156	21.21738
	4	173.21321	22.57044	188.53156	21.21738
	5	191.23123	29.66164	188.53156	21.21738
	6	214.65465	25.89863	188.53156	21.21738
	7	220.94421	32.64783	188.53156	21.21738

Raw data Fig. 8

name	runtime	Fouling mass	runtime	Fouling mass
unit	min	mg/g	min	mg/g
comment		Mixing element 7		Reactor average
	60	86.7	60	51.5
	30	62.7	30	16
	60	33.5	60	24.2
	120	186.8	120	98.5
	90	170.8	90	88.9
	60	165.7	30	19.9
	30	48.1	30	3.99
	30	34.3	90	87.6
	90	163.9	30	28.2
	30	25.8	45	20.9
	45	77.3	45	47.7
	45	137.3	60	65.8
	60	149.3	60	48.9
	60	103.9	30	18.6
	30	55.8	45	27.2
	45	56.7	20	7.85
	20	10.3	20	9.74
	20	14.6	30	12.41438
	150	188.4	30	18.98488
	150	165.3	40	20.52315
	180	192.3	40	21.23431
	180	182	50	21.57443
	120	174.4	60	40.5052
			60	30.6108
			75	42.15942
			75	42.40678
			90	75.93952
			90	71.4252
			120	103.65157
			120	113.26769
			120	116.81576
			150	175.58695
			150	156.58661
			180	186.48625
			180	186.16932

Raw data Fig. 9

name	Decrease in reaction volume	Decrease in conversion
unit	-	-
	0.29052	0.32967
	0.14072	0.14706
	0.48191	0.52326
	0.4187	0.5
	0.44386	0.38824
	0.10827	0.07692
	0.08672	0.14737
	0.42438	0.39726
	0.09831	0.0274
	0.23298	0.10588
	0.2748	0.20732
	0.36789	0.32558
	0.30287	0.3
	0.11343	0.04819
	0.21978	0.275
	0.03933	0.07407

Raw data Fig. 10

name	Fouling mass	Fouling mass	Fouling mass	Fouling mass
unit	mg/g	g	mg/g	g
comment	Average reactor (a)	Measurement cell	Static mixer 7 (b)	Measurement cell
	51.5	1.008	34.2	0.671
	24.2	0.79	33.8	0.788
	98.5	1.11412	47.97	0.859
	88.9	1.113	56.2	0.623
	19.9	0.86	86.4	1.007
	3.99	0.672	103.9	0.935
	28.2	0.426	105.7	0.934
	20.9	1	137.7	0.979
	47.7	0.98	148.3	1.039
	65.8	1.0339	151.5	1.029
	48.9	0.936	166.1	1.185
	18.6	0.623	170.7	1.112
	27.2	0.999	187.2	1.113
	7.85	0.141		
	9.74	0.206		

Raw data Fig. 12

name	$\Delta$ ASV	Fouling mass
unit	m/s	g
comment		Measurement cell
	125	1.008
	6	0.152
	120	1.1142
	170	1.113
	150	1.185
	120	0.86
	78	0.672
	130	1.0003
	120	0.98
	155	1.0339
	125	0.936
	85	0.625
	140	0.999
	20	0.141
	35	0.206

Raw data Fig. 11+13

time	Fig. 11		Fig. 13	
	sound velocity	fouling mass	runtime	ASV
min	m/s	mg/g	min	m/s
		static mixer 7		
0	1309.2	0	-20	1217.2
0.32032	1311.2		-19.5	1217
0.63738	1313.5		-19	1218.7
0.95007	1312.9		-18.5	1220.8
1.2631	1316.7		-18	1219.5
1.5744	1314.3		-17.5	1218.6
1.8826	1310.8		-17	1218.4
2.1933	1311.4		-16.5	1218.2
2.5084	1308		-16	1218.7
2.8211	1312		-15.5	1218.8
3.1326	1312.4		-15	1219.6
3.4405	1317.5		-14.5	1217
3.7518	1318.7		-14	1218.7
4.0672	1323.1		-13.5	1218.4
4.3958	1325.1		-13	1218.2
4.7612	1326.6		-12.5	1218.7
5.1139	1321.5		-12	1218.8

5.4635	1327.6		-11.5	1219.6
5.7874	1329.3			
6.1005	1333.3		0.167	1369.013333
6.4111	1331.3		0.469	1370.126667
6.7252	1327.1		0.776	1369.26
7.0374	1328.3		1.089	1367.926667
7.3469	1326		1.391	1366.613333
7.6573	1321.6		1.694	1364.94
7.9675	1321.6		2.008	1364.36
8.2833	1320.4		2.316	1360.6
8.596	1316.4		2.62	1364.08
8.9246	1313.6		2.925	1366.473333
9.2374	1313.5		3.233	1366.5
9.5502	1314.6		3.536	1366.34
9.8805	1314.3		3.842	1363.16
10.243	1315.7		4.148	1362.933333
10.614	1313		4.461	1366.106667
10.961	1312.8		4.759	1367.193333
11.31	1309.2		5.066	1366.28
11.635	1308.1		5.375	1368.386667
11.949	1305.9		5.676	1368.013333
12.262	1307.3		5.983	1366.533333
12.591	1301.7		6.292	1367.873333
12.919	1305.8		6.592	1365.64
13.234	1299.7		6.898	1365.666667
13.561	1307		7.197	1361.293333
13.887	1302.1		7.508	1359.833333
14.206	1295.2		7.839	1360.88
14.53	1292.6		8.156	1357.906667
14.843	1298.3		8.477	1358.466667
15.16	1299.2		8.808	1358.933333
15.485	1297		9.156	1354.813333
15.813	1296		9.486	1354.646667
16.127	1292.8		9.8	1351.26
16.457	1288.8		10.108	1348.253333
16.784	1288.5		10.412	1346.293333
17.117	1289.4		10.717	1343.346667
17.449	1289.3		11.024	1341.186667
17.768	1286.7		11.328	1342.513333
18.092	1285.7		11.633	1341.913333
18.419	1292.5		11.933	1344.32
18.735	1286.5		12.235	1343.726667
19.059	1289.2		12.533	1343.406667
19.375	1284.5		12.841	1344.573333
19.701	1287.1	10.3	13.149	1344.12
20.019	1283.6	14.6	13.446	1342.546667
20.343	1283.8		13.748	1345.24
20.659	1283.9		14.05	1345.16
20.985	1284.5		14.358	1346.38
21.3	1284.3		14.659	1346.193333
21.627	1286.3		14.964	1346.08
21.942	1290.6		15.262	1346.84
22.268	1289.5		15.572	1345.22
22.595	1288.6		15.869	1344.66
22.913	1286.9		16.174	1345.533333
23.239	1285.9		16.471	1344.68
23.552	1285.4		16.781	1345.553333
23.867	1286.4		17.079	1346.8
24.193	1285.5		17.379	1347.553333
24.509	1287.5		17.683	1348.36
24.82	1288.5		17.984	1348.793333
25.131	1286.8		18.286	1348.686667
25.443	1290.4		18.6	1348.933333
25.756	1287.4		18.906	1347.993333
26.067	1291.4		19.206	1346.906667
26.379	1287.7		19.519	1347.74
26.687	1293.3		19.825	1347.78
27.001	1297.3		20.124	1349.26
27.311	1295.9		20.433	1350.206667
27.625	1294.1		20.734	1350.413333
27.937	1292.7		21.034	1350.96
28.247	1299.4		21.333	1349.5
28.556	1298.7		21.64	1347.966667

28.869	1301.5		21.935	1348.013333
29.183	1298.6		22.23	1347.486667
29.502	1302.9		22.525	1348.026667
29.823	1298.8	55.8	22.831	1347.88
30.137	1305.2	25.8	23.129	1348.473333
30.465	1298.3	34.3	23.422	1348.593333
30.78	1308.1	48.1	23.717	1350.126667
31.088	1306.4	62.7	24.024	1349.78
31.399	1312.7		24.321	1350.106667
31.711	1306.6		24.628	1350.093333
32.025	1305.6		24.926	1350.473333
32.338	1307.6		25.231	1350.333333
32.648	1304.9		25.527	1350.326667
32.976	1311.3		25.824	1352.006667
33.287	1309.6		26.124	1354.586667
33.6	1307.8		26.425	1355.313333
33.911	1310.1		26.722	1356.926667
34.225	1313		27.016	1356.246667
34.538	1314.2		27.315	1356.44
34.846	1308.9		27.617	1356.393333
35.158	1318.3		27.914	1358.106667
35.472	1316.1		28.223	1359.773333
35.799	1319.6		28.52	1362.84
36.112	1314.1		28.826	1364.38
36.432	1317.2		29.122	1365.173333
36.753	1318.5		29.418	1367.16
37.082	1323.6		29.723	1369.193333
37.403	1324.7		30.036	1371.533333
37.724	1323.4		30.333	1370.946667
38.04	1324.9		30.628	1367.193333
38.365	1327.9		30.933	1362.66
38.678	1329.4		31.229	1353.88
39.006	1332.4		31.525	1346.173333
39.328	1329.2		31.825	1338.946667
39.649	1330		32.127	1332.226667
39.972	1334.4		32.422	1324.433333
40.291	1336.2		32.718	1318.9
40.608	1330.3		33.022	1316.273333
40.93	1333.6		33.319	1317.253333
41.248	1332.3		33.616	1317.586667
41.574	1335.4		33.908	1315.16
41.886	1335.4		34.204	1313.066667
42.2	1334.8		34.509	1311.153333
42.513	1339.1		34.804	1311.54
42.823	1338.7		35.1	1313.86
43.142	1333.3		35.4	1317.053333
43.462	1332		35.702	1323.753333
43.777	1339.1		35.998	1330.153333
44.104	1338.3		36.299	1335.553333
44.433	1340.4		36.6	1340.066667
44.759	1340.2	77.3	36.897	1344.02
45.08	1341.9	137.3	37.191	1345.013333
45.409	1345.2	56.7	37.485	1342.273333
45.722	1346.6		37.778	1336.74
46.032	1350.1		38.082	1332.1
46.343	1349.9		38.379	1328.226667
46.67	1350.8		38.676	1323.986667
46.982	1352.7		38.981	1319.713333
47.294	1350.6		39.278	1315.433333
47.608	1351.5		39.575	1311.24
47.921	1356.5		39.882	1307.333333
48.249	1353.6		40.176	1303.586667
48.563	1357.5		40.473	1300.246667
48.869	1358.8		40.781	1296.94
49.181	1353.9		41.078	1293.546667
49.495	1359.7		41.377	1290.246667
49.808	1353.7		41.679	1286.92
50.121	1356.1		41.983	1283.753333
50.429	1352.9		42.283	1280.573333
50.742	1359.2		42.577	1277.713333
51.051	1359		42.871	1275.033333
51.367	1360.4		43.167	1272.353333
51.679	1359.2		43.475	1269.66

52.006	1365.7		43.772	1266.98
52.321	1360.9		44.075	1264.3
52.65	1362.5		44.378	1261.3
52.963	1362.4		44.683	1258.74
53.284	1364.1		44.979	1256.133333
53.605	1366.1		45.282	1253.666667
53.932	1363.9		45.585	1251.286667
54.246	1363.8		45.881	1249.006667
54.559	1371.3		46.193	1246.933333
54.867	1372.7		46.517	1245.026667
55.176	1371.2		46.868	1243.393333
55.491	1367		47.18	1241.72
55.805	1373.9		47.49	1240.026667
56.126	1371.1		47.787	1238.426667
56.442	1369.1		48.087	1236.88
56.755	1371.2		48.392	1235.406667
57.067	1368.2		48.7	1234.02
57.379	1368.8		48.998	1233.246667
57.693	1372.3		49.307	1231.873333
58.004	1370		49.604	1230.56
58.313	1370.2		49.908	1229.353333
58.625	1367.6		50.205	1228.206667
58.936	1366.3		50.515	1227.113333
59.251	1372.8		50.813	1226.053333
59.563	1370.1	86.7	51.112	1224.84
59.872	1372.6	33.5	51.417	1223.66
60.182	1377.6	165.7	51.711	1222.526667
60.498	1375.2	149.3	52.01	1221.5
60.808	1379.3	103.9	52.313	1220.66
61.133	1378.3		52.623	1220
61.451	1378.9		52.921	1219.5
61.764	1377.3		53.226	1219.14
62.09	1381		53.525	1218.646667
62.405	1386.2		53.833	1218.533333
62.715	1379.1		54.129	1218.42
63.035	1382.6		54.435	1218.32
63.355	1381.3		54.737	1218.393333
63.666	1377.6		55.029	1218.62
63.978	1378.7		55.329	1218.801786
64.292	1375.2		55.634	1218.983571
64.756	1377		55.934	1219.165357
65.229	1375.3		56.235	1219.347143
65.6	1380.4		56.549	1219.528929
65.98	1378.6		56.845	1219.710714
66.308	1380.9		57.149	1219.8925
66.621	1380.9			
66.929	1380.1			
67.241	1383.3			
67.553	1383.2			
67.869	1381.7			
68.181	1387.1			
68.492	1386.5			
68.801	1388.2			
69.112	1386.6			
69.425	1389.2			
69.738	1388.1			
70.047	1388			
70.359	1385			
70.67	1393			
70.983	1387.1			
71.297	1386.8			
71.605	1384.2			
71.916	1384.7			
72.228	1387.2			
72.542	1390.8			
72.855	1391.5			
73.163	1385.2			
73.475	1385.6			
73.788	1393.1			
74.102	1388.9			
74.424	1390			
74.726	1392.1			
75.05	1389.8			

75.364	1397.3			
75.679	1389.4			
75.991	1399.2			
76.301	1396.5			
76.613	1400			
76.921	1397.2			
77.233	1405.6			
77.544	1399.3			
77.859	1396.4			
78.182	1404.6			
78.501	1403.4			
78.825	1401.4			
79.143	1397.4			
79.455	1400.4			
79.784	1399.5			
80.107	1409.2			
80.425	1399			
80.738	1407.1			
81.051	1400.2			
81.375	1401.9			
81.688	1404.9			
81.999	1401.4			
82.311	1409.3			
82.626	1402.9			
82.944	1404.5			
83.268	1406.1			
83.581	1404.8			
83.889	1407.4			
84.199	1401.6			
84.511	1407.6			
84.825	1407.1			
85.139	1410.2			
85.467	1412.1			
85.797	1408.7			
86.11	1409.5			
86.421	1410.2			
86.733	1404.2			
87.058	1412.3			
87.371	1410			
87.683	1407.1			
87.994	1410.3			
88.309	1411.5			
88.622	1410			
88.929	1412.3			
89.245	1420.2			
89.567	1412.3			
89.884	1421.2	170.8		
90.199	1408.6	163.9		
90.523	1415.4			
90.837	1414.3			
91.151	1417.3			
91.476	1415.4			
91.792	1411			
92.105	1419.8			
92.434	1420.1			
92.759	1416.8			
93.078	1417.1			
93.395	1419.7			
93.715	1418.7			
94.027	1413.4			
94.338	1411.1			
94.66	1415.7			
94.979	1417.7			
95.302	1416.7			
95.622	1419.3			
95.937	1422.4			
96.246	1418.3			
96.559	1418.2			
96.885	1418.4			
97.215	1416.8			
97.529	1413.6			
97.843	1416.3			
98.161	1420.7			

---

98.483	1422.2			
98.801	1418.7			
99.119	1422.7			
99.439	1423.4			
99.766	1421.9			
100.08	1420.5			
100.41	1417.5			
100.73	1411.7			
101.05	1418.9			
101.37	1422.2			
101.69	1414.4			
102.01	1419.3			
102.33	1418.6			
102.65	1410.9			
102.97	1414.5			
103.29	1418.3			
103.6	1420.7			
103.92	1417.8			
104.29	1423.3			
104.67	1420.6			
105.03	1413.6			
105.42	1425.6			
105.75	1425.3			
106.06	1428.6			
106.38	1427.1			
106.7	1427.6			
107.01	1428.9			
107.33	1430.8			
107.65	1423.5			
107.96	1423			
108.27	1422.6			
108.59	1431.6			
108.91	1428.2			
109.23	1423.7			
109.54	1429.1			
109.85	1437.5			
110.17	1427.2			
110.51	1430.1			
110.83	1431.3			
111.15	1424.1			
111.46	1426.5			
111.78	1437.6			
112.1	1433.9			
112.42	1430			
112.73	1432.8			
113.05	1423			
113.37	1431.6			
113.68	1432.3			
113.99	1425.3			
114.3	1427.9			
114.62	1429.9			
114.94	1428.4			
115.26	1424.8			
115.58	1432.3			
115.9	1429.9			
116.21	1432.2			
116.52	1426.4			
116.83	1428.5			
117.15	1427.6			
117.46	1428			
117.77	1429.9			
118.09	1430.5			
118.41	1430.6			
118.72	1429.2			
119.04	1429.9			
119.35	1430.4			
119.66	1426.8			
119.98	1430.8	186.8		

---



## 10. Acknowledgement

First of all, I would like to thank Dr. Werner Pauer and Prof. Gerrit Luinstra for supervising and assigning this interesting topic as well as evaluating this dissertation.

I would also like to thank Dr. Werner Pauer, Dr. Christoph Wutz and Prof. Volkmar Vill for chairing the examination committee.

I would like to thank all members of the KoPPonA 2.0 project for the pleasant co-operation and the helpful feedback & discussions. Especially to Mrs. Vanessa Neßlinger and Mr. Marco Osenberg for a great collaboration and joint publications.

I would also like to thank Mrs Susanne Grieser, Mr. Stefan Bleck and Mr Michael Gröger for many analytical measurements and the discussion of associated questions.

I would also like to thank my former student assistants Mrs Wiebke Kahns, Mrs Julia Eichbaum and Mr Matthias Günther for their active support performing polymerisation, analysing samples and most of all helping while cleaning the fouling.

I would also like to thank Mrs Wiebke Kahns, Mrs. Elli Richter and Mrs. Ira Wirth for their continued cooperation during their bachelor's theses. Moreover, I would like to thank Mr. Jonas Fechner for the cooperation during his master's thesis.

I would also like to thank my interns Mrs Larissa Großmann and Mrs Julia Eichbaum for their excellent cooperation during the internship.

I would like to thank the entire working groups Pauer and Luinstra for the nice and humorous interaction with each other, great times, and the many discussions on a professional and personal level.

Special thanks go to my family and friends, who have always supported me unconditionally in all situations.

## 11. Declaration on oath

I hereby declare on oath, that I have written the present dissertation on my own and have not used other than the acknowledged resources and aids. The submitted written version corresponds to the version on the electronic storage medium. I hereby declare that I have not previously applied or pursued for a doctorate (Ph.D. studies).

A handwritten signature in black ink, appearing to read 'J. Kuhl', is written in a cursive style.

Hamburg, March 22, 2024